FOSSIL ENERGY

DOE/BC/14662-7
(DE92001048)

QUANTITATION OF MICROBIAL PRODUCTS AND THEIR EFFECTIVENESS IN ENHANCED OIL RECOVERY

ANNUAL REPORT

By
Michael J. McInerney
Roy M. Knapp

June 1992

Performed Under Contract No. DE-AC22-90BC14662

University of Oklahoma
Norman, Oklahoma

National Petroleum Technology Office
U. S. DEPARTMENT OF ENERGY
Tulsa, Oklahoma

DISCLAIMER

This report was prepared as an account of work sponsored by an agency of the United States Government. Neither the United States Government nor any agency thereof, nor any of their employees, makes any warranty, express or implied, or assumes any legal liability or responsibility for the accuracy, completeness, or usefulness of any information, apparatus, product, or process disclosed, or represents that its use would not infringe privately owned rights. Reference herein to any specific commercial product, process, or service by trade name, trademark, manufacturer, or otherwise does not necessarily constitute or imply its endorsement, recommendation, or favoring by the United States Government or any agency thereof. The views and opinions of authors expressed herein do not necessarily state or reflect those of the United States Government or any agency thereof.

This report has been reproduced directly from the best available copy.

Available to DOE and DOE contractors from the Office of Scientific and Technical Information, P.O. Box 62, Oak Ridge, TN 37831; prices available from (615)576-8401, FTS 626-8401.

Available to the public from the National Technical Information Service, U.S. Department of Commerce, 5285 Port Royal Rd., Springfield, VA 22161.

DOE/BC/14662-7
Distribution Category UC-122

QUANTITATION OF MICROBIAL PRODUCTS AND THEIR EFFECTIVENESS IN ENHANCED OIL RECOVERY

Annual Report

By
Michael J. McInerney
Roy M. Knapp

June 1992

Work Performed Under Contract No. AC22-90BC14662

Prepared for
U.S. Department of Energy
Assistant Secretary for Fossil Energy

E.B. Nuckols, Project Manager
Metairie Site Office
900 Commerce Road, East
New Orleans, LA 70123

Prepared by
University of Oklahoma
Department of Botany and Microbiology and
Department of Petroleum and Geological Engineering
770 Van Vleet Oval, Room 135
Norman, Oklahoma 73019-0245

TABLE OF CONTENTS

LIST OF TABLES v

LIST OF FIGURES vii

1. EXECUTIVE SUMMARY 1

2. INTRODUCTION 5

   2.1 Overview of MEOR 5
   2.2 Project Objectives 7
   References 8

3. QUANTITATION OF METABOLITES BY SELECTED STRAINS 11

   3.1 Introduction 11
   3.2 Materials and Methods 19
   3.3 Results 23
   3.4 Discussion 36
   References 47

4. BACTERIAL TRANSPORT AND ACTIVITY IN UNCONSOLIDATED POROUS MATERIALS 50

   4.1 Introduction 50
   4.2 Materials and Methods 53
   4.3 Results 61
   4.4 Discussion 81
   References 94

5. MATHEMATICAL MODELING OF MEOR PROCESSES 98

   5.1 Introduction 98
   5.2 Microbial Activities 99
   5.3 Assumptions 100
   5.4 Model Equations 100
   5.5 Simplification and Specification 106
   5.6 Numerical Solutions 111
   5.7 Model Validation 115
   5.8 Discussion 134
   References 135

6. ACCOMPLISHMENTS 137

LIST OF TABLES

TABLE		PAGE
3.1	Effect of external electron acceptors on the growth of the halophilic strains	30
3.2	Effect of gas phase on the growth of the halophilic strains	31
3.3	Substrate utilization by the halophilic strains	33
3.4	Glucose fermentation products of the anaerobic halophiles isolated from SEVVSU brines	35
3.5	Differences between anaerobic halophilic bacteria	37
3.6	Comparison of substrate utilization by various fermentative haloanaerobes	40
4.1	Characteristics of the *E. coli* strains used	54
4.2	Characteristics of the porous media used	57
5.1	Static, unconsolidated core process	108
5.2	Specified model equations for the initial injection period	110
5.3	Model equations for incubation period	112
5.4	Model equations for post injection period	113
5.5	Kinetic parameters for static unconsolidated core systems	117
5.6	Initial data for MEOR process in Core #6	124
5.7	Injection data for MEOR process in Core #6	125
5.8	Incubation data for MEOR process in Core #6	126

LIST OF FIGURES

FIGURE PAGE

3.1 Effect of NaCl concentration on the growth of strain VS-732 24
3.2 Effect of NaCl concentration on the growth of strain VS-751 25
3.3 Effect of NaCl concentration on the growth of strain VS-752 26
3.4 Effect of NaCl concentration on the growth of strain VS-511 27
3.5 Effect of NaCl concentration on the growth of strain TTL-30 29
4.1A Growth of *E. coli* RW262 in GNM-saturated, sand-packed cores and liquid cultures 63
4.1B Metabolism of strain RW262 with time in nutrient-saturated, sand-packed cores 64
4.2A Growth of strain RW262 in different sections of GNM-saturated, 10-cm-long plastic cores with time . . . 66
4.2B Galactose consumption by strain RW262 in different sections of GNM-saturated, 10-cm-long plastic cores with time 68
4.2C Acetate production by strain RW262 in different sections of GNM-saturated, 10-cm-long plastic cores with time . . 69
4.3 Cell concentration and galactose consumption by strain RW262 in different sections of plastic cores with lower galctose concentration at 11.5 h of incubation 70
4.4 Transport of strain RW262 through 10-cm-long plastic cores without galactose added 72
4.5A Growth and transport of the chemotactic strain RP437 through MGM-saturated, 10-cm-long plastic cores . 74
4.5B Growth and transport of the non-chemotactic strain RP5232 through MGM-saturated, 10-cm-long plastic cores . 75
4.6 Growth and transport of the non-motile strain RP2912 through MGM-saturated, 10-cm-long cores 77
4.7A Mechanisms of penetration through sand-packed cores by chemotactic and nonchemotactic strains of *E. coli* . . 79
4.7B Mechanisms of penetration through sand-packed cores by motile and nonmotile strains of *E. coli* 80
5.1 Consumption of galactose during batch fermentation . . . 118
5.2 Consumption of nitrate during batch fermentation 119
5.3 Growth of biomass during batch fermentation 120
5.4 Production of acetate during batch fermentation 121
5.5 Production of CO_2 during batch fermentation 122
5.6 Production of CO_2 during MEOR processes in Core #6 . . . 127
5.7 Production of N_2 during MEOR processes in Core #6 . . . 128
5.8 Cumulative production of total gases (CO_2 and N_2) during MEOR processes in Core #6 129
5.9 Production of acetate during MEOR processes in Core #6 130

LIST OF FIGURES (con't.)

FIGURE PAGE

5.10 Consumption of glucose during MEOR processes in Core #6 131
5.11 Consumption of nitrate during MEOR processes in Core #6 132
5.12 Consumption of ammonium during MEOR processes in Core #6 133

1. EXECUTIVE SUMMARY

The overall goal of this project is to obtain quantitative information on the amount and rate of microbial growth and product formation, to correlate microbial activity to oil recovery, and to develop mathematical models that predict microbial activity and oil recovery in porous media. During the first phase of this work, the metabolism and nutritional features of halophilic bacteria indigenous to a reservoir selected for a field trial of a microbial selective plugging process were characterized. Also, simple porous systems were designed and used to obtain statistically reliable data on the in situ rates of microbial growth, substrate consumption, and product formation required to test the mathematical predictions of these primary dependent variables.

Information on the metabolism and nutritional features of indigenous microbial populations is necessary to develop successful in situ microbially enhanced oil recovery processes. Five bacteria were isolated and characterized from brine samples obtained from the Southeast Vassar Vertz Sand Unit, Payne County, Okla. All of the isolates were strictly anaerobic and obligately halophilic, requiring a minimum of 6 to 9% (wt/vol) NaCl for growth in a complex medium. All of the strains were gram-negative, catalase negative, non-sporing rods that were inhibited by chloroamphenicol, tetracycline, and penicillin, but not cyclohexamide or azide, indicating that these strains are eubacteria and not archaebacteria. All of the isolates used carbohydrates, but with two exceptions did not use amino acids or several of the tested

aromatic compounds as energy sources. VS-752 and TTL-30 both used pyrogallic acid. Glucose was fermented to H_2, CO_2, ethanol, and acetate by all the strains. Formate was an additional product from glucose in the case of VS-732 and VS-751. The change in the gas phase from N_2/CO_2 to H_2/CO_2 stimulated the growth of strains VS-732 and VS-511, but completely inhibited the growth of strain TTL-30. The presence of a carbon monoxide gas phase at the various concentrations tested was inhibitory to all the strains. Methane was not produced by any of the strains. These studies show that the brines of a hypersaline oil reservoir contain numerous anaerobic bacteria that use a variety of fermentable carbohydrates and produce useful products such as acids, solvents, and gases.

Statistically reliable data on the in situ rates of growth, substrate consumption, and product formation are required to test the validity of the mathematical models developed for microbially enhanced oil recovery processes. To follow the kinetics of microbial growth and metabolism in situ, a simple porous core system that could be easily replicated and aseptically divided into sections at different times was developed. This core system was used to study the kinetics of growth and the mode of penetration of strains of *Escherichia coli* through anaerobic, nutrient-saturated, Ottawa sandpacks (permeability of 7.0 μm^2 and a porosity of 37%) under static conditions. *E. coli* was used in these initial experiments since its metabolism and growth kinetics are well described and many mutants which lack biological functions important for growth and penetration in porous media are available.

The in situ rate of growth of a wild type, motile strain RW262 was two times slower inside of cores compared with that in liquid cultures. The metabolism of galactose by strain RW262 was not altered inside cores as acetate was the only liquid product detected either inside of the cores or in liquid cultures. Without applied advective force, the chemotactic, motile strain RW262 grew exponentially and moved through cores at a rate of about 0.1 m/d. The cell population moved through cores in a band-like fashion as the front of the moving cells consisted of high cell concentrations (greater than 10^5 cells/ml). Until the breakthrough of the cells occurred, galactose consumption and acetate production were observed only in the front sections of the core, showing that the cell propagation preceded the complete depletion of the substrate or the accumulation of large amounts of products. A motile, nonchemotactic mutant of *E. coli* penetrated cores faster than did the chemotactic parental strain which could be explained based on differences in their mode of growth inside the cores. The chemotactic strain RP437 grew and moved through cores in a band-like fashion. In contrast, cells of the nonchemotactic strain moved through cores in a diffuse manner as the front of the moving cells consisted of low cell concentrations ($\leq 10^3$ cells/ml), and the appearance of nonchemotactic mutant cells in a section of the core was not necessarily followed by an increase in cell concentration in that section with time. The propagation of the nonmotile strain RP2912 seemed to require a critical cell density in a section of the core before cells were detected in the next section. This

suggested that the transport of nonmotile cells through porous material may have occurred by a physical displacement process where some of the progeny cells were forced into the less populated regions of the core.

A three-phase, multispecies, one-dimensional model was developed to simulate bacterial transport, growth, and metabolism involved in a microbially enhanced oil recovery process and to predict the change in permeability as a result of in situ microbial activity in porous media. Convection-dispersion equations and microbial growth kinetics were incorporated into the model to characterize and quantify biomass production, product formation, and nutrient utilization during the MEOR process. Permeability reduction by the MEOR process was assumed to be due to pore plugging by the retention and growth of bacterial cells. The model was applied to static, unconsolidated sandpacks and sandstone core-flood experiments to simulate microbial movement, metabolite production, and nutrient consumption coupled to microbial growth and to predict the net permeability reduction. Comparison between numerical solutions and experimental results indicated that the model simulated the essential microbial kinetics of these laboratory experiments and can be extended to provide numerical predictions for the purposes of design and evaluation of MEOR field projects.

2. INTRODUCTION

2.1 Overview of Microbially Enhanced Oil Recovery

MEOR processes can be grouped into three main categories depending on the type of production problem to be treated, whether the process is localized in the well bore or the near well bore environment, or whether the process is reservoir-wide (Knapp et al., 1990). Most of the microbial field trials can be classified as well bore clean-out or well stimulations where the purpose of the treatment is to increase the production of oil from an individual well (Hitzman, 1983, 1988; Lazar, 1991). Well bore clean-out processes generally involve the use of hydrocarbon or scale-removing bacteria to remove deposits from the tubing, rods, or other surfaces in the well itself. At least two commercial processes are available (Pelger, 1991; Oppenheimer and Heibert, 1989).

In well stimulation processes, a well close to its economic limit is injected with a mixed anaerobic culture and an aqueous solution of a fermentable carbohydrate, usually molasses. The well is closed for a period of time before fluid is allowed to flow. The increased oil production is likely due to the generation of gases, solvents, and surfactants in the vicinity of the well bore to remove entrapped particulate material and alter the wettability of the rock. Recently, Sheehy (1990) developed a well stimulation process that relies on the stimulation of indigenous bacteria with inorganic nutrients rather than using injected bacteria and a carbohydrate-based nutrient. This is one of the few processes

where appropriate controls have been conducted to demonstrate the feasibility of the process. After the treatment, oil production from the well increased 40% over the control levels and was maintained for more than a year. Another type of well stimulation method involves the use of ultramicrobacteria to plug selectively thief zones and reduce coning in heavy oil production (Lappin-Scott et al., 1988).

Microbially enhanced waterflooding processes are displacement processes that are done late in the life of a waterflood. Nutrients with or without a bacterial inoculum are injected into the formation in order to stimulate microbial activity throughout the reservoir to mobilize residual oil, or to alter the flow paths of the waterflood. The number of reported field trials of this type of MEOR process is much fewer than individual well treatment processes described above. However, several of these projects have been well documented and from this information it is clear that additional oil has been recovered (Yarbrough and Coty, 1983; Lazar et al., 1990; Wagner, 1991; Bryant and Burchfield, 1991). Analysis of two of these studies suggests that about one barrel of oil was recovered for every gallon of molasses used (Lazar et al., 1991; Bryant and Burchfield, 1991), which would indicate that microbially enhanced waterflooding is economically feasible.

This brief survey of ongoing MEOR field trial shows that the potential for microbial processes to stimulate and enhance the recovery of oil is large. These processes may be the only economically viable EOR process in the near future. However, the

lack of information on the effectiveness of MEOR has limited its use to marginal reservoirs where the financial loss which would be small should the project be unsuccessful. As is the case with other EOR processes, unpredictable technical performance has imposed an unacceptable risk which has restricted the general application of MEOR.

2.2 Project Objectives

There is a great potential for the use of microorganisms to enhance oil recovery. However, microbially enhanced oil recovery (MEOR) processes have not been widely applied because of the same problem that limits the general application of any enhanced oil recovery (EOR) process. The unpredictable technical performance of MEOR or any EOR process creates an unacceptable risk that limits the widespread application of these processes. For most EOR processes, the lack of predictability stems from an inadequate knowledge of the reservoir, rock-fluid interactions, and the basic mechanisms by which EOR processes mobilize and displace oil. In addition to these problems, little information is available on the amount(s) of microbial cells and products needed to recover additional oil and the rates at which these processes occur. Thus, it is not possible to determine whether a MEOR process will be economically beneficial. The main goal of this project is to develop quantitative relationships that correlate the amount of microbial growth and product formation to the amount of oil recovered. This information can then be used to make more accurate

predictions concerning the amount of oil likely to be recovered when implementing a MEOR process.

The initial stages of the project have focused on understanding the metabolism of halophilic bacterial strains which were isolated from brines taken from a hypersaline oil reservoir where a microbial selective plugging field project is currently underway. The nutrition, substrate utilization pattern, and fermentation products from carbohydrates of five of these isolates was determined. Next, studies were conducted to determine the mechansims by which bacteria pentetrate porous materials and to obtain kinetic and stoichiometric information on the in situ growth and metabolism of bacteria in porous media. The final part of the work was the development of a mathematical model to predict oil recovery and permeability modification from the in situ microbial activities. The model was verified by comparing simulator predictions with actual experimental data. Initial studies suggest that the model does stimulate the essential kinetics of microbial growth and metabolism. The following chapters describe these three aspects of the work in greater detail.

REFERENCES

Bryant, R. S. and T. E. Burchfield. 1991. Microbial enhanced waterflooding: a pilot study, pp. 399-420. In E. C. Donaldson (ed.), Microbial enhancement of oil recovery-recent advances. Elsevier Science Publishers, Amsterdam.

Hitzman, D. O. 1983. Petroleum microbiology and the history of its role in enhanced oil recovery, pp.162-218. In: E. C. Donaldson and J. B. Clark (eds.), Proceeding of the International Conference on Microbial Enhancement of Oil Recovery. Technology Transfer Branch, U. S. Department of Energy, Bartlesville, OK.

Hitzman, D. O. 1988. Review of microbial enhanced oil recovery field tests, pp. VI, 1-41. In: T. E. Burchfield and R. S. Bryant (eds.), Proceedings of the Symposium on Applications of Microorganisms to Petroleum Technology. National Technical Information Service, Springfield, Virginia.

Knapp, R. M., J. L. Chisholm and M. J. McInerney. 1990. Microbially enhanced oil recovery, pp. 229-234. Proceedings of the SPE/UH emerging technologies conference. Institute for improved oil recovery, University of Houston, Houston, Texas.

Lappin-Scott, H. M., F. Cusack and J. Costerton. 1988. Nutrient resuscitation and growth of starved cells in sandstone cores: a novel approach to enhanced oil recovery. Appl. Environ. Microbiol. 54: 1373-1382.

Lazar, I., S. Dorota, M. Stefanescu, L. Sandulescu, P. Constantinescu, C. Morosanu, N. Botea and O. Iliescu. 1991. Preliminary results of some recent MEOR field trials in Romania, pp. 365-386. In E. C. Donaldson (ed.), Microbial enhancement of oil recovery-recent advances. Elsevier Science Publishers, Amsterdam.

Oppenheimer, C. H. and F. Hiebert. 1989. Microbial techniques for paraffin reduction in producing oil wells. Final Report. DOE contract No. FG19086BC 14014, DOE/BC/14014-9, (DE 89000741).

Pelger, J. W. 1991. Microbial enhanced oil recovery treatments and well bore stimulation using microorganisms to control paraffin, emulsion, corrosion, and scale formation, pp. 451-466. In E. C. Donaldson (ed.), Microbial enhancement of oil recovery-recent advances. Elsevier Science Publishers, Amsterdam.

Sheehy, A. J. 1990. Field studies of microbial EOR. Paper SPE/DOE 20254 presented at the SPE/DOE Seventh Symposium on Enhanced Oil Recovery, Tulsa, Okla. Society of Petroleum

Engineers, Dallas, Texas.

Wagner, M. 1991. Microbial enhancement of oil recovery from carbonate reservoirs with complex formation characteristics, pp. 387-398. In E. C. Donaldson (ed.), Microbial enhancement of oil recovery-recent advances. Elsevier Science Publishers, Amsterdam.

Yarbrough, H. F. and V. F. Coty. 1983. Microbially enhanced oil recovery from the Upper Cretaceous Nacatoch Formation, Union County Arkansas, pp. 149-153. In: E. C. Donaldson and J. B. Clark (eds)., Proceeding of the International Conference on Microbial Enhancement of Oil Recovery. Technology Transfer Branch, U. S. Department of Energy, Bartlesville, OK.

3. QUANTITATION OF METABOLITES BY SELECTED STRAINS

3.1 Introduction

3.1.1 MEOR in hypersaline petroleum reservoirs. Most mid-continent United States petroleum reservoirs brines have NaCl concentrations of over 10% (wt/vol) (Udegbunam et al., 1991). Thus, tolerance to NaCl is an important characteristic needed for microorganisms to be useful for MEOR. A major obstacle for the application of MEOR has been the inability of microorganisms to survive and be active at high salt concentrations. There have been reports where levels of NaCl above 1% (wt/vol) have inhibited the ability of bacteria to grow in sandstones (Smith and Collins, 1985), and salt concentrations above 3% have been cited as the cause for failure of some MEOR studies (Grula et al., 1985). Bacteria capable of producing useful oil recovery products such as surfactants and polymers have been grown in media with NaCl concentrations of up to 8% NaCl (Javaheri et al., 1985; Pfiffner et al., 1986) and have been shown to selectively plug sandstones and recover additional oil (Raiders et al., 1989). It would be, however, preferable to have organisms that produce useful products at a higher and wider range of salt concentrations.

Bacteria capable of growing at NaCl concentrations of up to 32% have been described (Kushner, 1978). Halophilic and halotolerant bacteria have been isolated from a variety of hypersaline environments and have been studied in great detail (Rodrigues-Valera, 1988). These organisms, however, may not be applicable for MEOR since the vast majority of these are aerobes.

The organisms have to be either facultative or obligately anaerobic to be useful in MEOR, since oil reservoirs are predominantly anoxic. Little is known about the physiology of strictly anaerobic, obligately halophilic fermentative bacteria. Most of the haloanaerobes described to date have been isolated from either the Dead Sea or hypersaline salt lakes (Oren, 1988). There has been only one report of the isolation of a fermentative haloanaerobe from oil brines (Gevertz et al., 1991), although their isolation from oil-water injection filters have been reported (Rengpipet et al., 1988). Methanogenic (Gevertz et al., 1991; Belyaev et al., 1990) and sulfate-reducing bacteria have been isolated from oil field brines. The organism studied by Gervertz et al. (1991) is an obligate anaerobe with an optimal salt requirement of 2.5% NaCl and a low salt tolerance range (2.5%-10% NaCl). There is not any information on the occurrance of fermentative haloanaerobes in oil brines with NaCl concentrations above 10%. Thus, it is not known if MEOR will be effective in highly saline reservoirs where salt concentrations may exceed 10% NaCl.

Most petroleum reservoirs have environmental conditions that would severely limit the growth of most known microbial species. Since only a few of the environmental conditions of the reservoir can be changed, suitable microorganisms must be selected which can grow in the environment of the reservoir. It is likely that the microorganisms with the desired characteristics for MEOR, are present in the reservoir (McInerney and Westlake, 1990). Efforts

should be directed toward the isolation of haloanaerobes from hypersaline oil brines with a wide range of salt tolerance, and the capability of producing oil releasing metabolites. Studies on the physiology and metabolism of these microorganisms will provide valuable information on the diversity of microorganisms in hypersaline anaerobic ecosystems, and also prove helpful in MEOR pilot studies in hypersaline petroleum reservoirs.

3.1.2 Fermentative haloanaerobic bacteria. Although anaerobic halophilic bacteria have long been reported in hypersaline anaerobic sediments (Elazari-Volcani, 1943), very few have been isolated and studied in detail. Three genera have been described to date: *Halobacteroides* which includes *Halobacteroides halobius* (Oren et al., 1984), and *Halobacteroides acetoethylicus* (Rengpipet et al., 1988); *Haloanaerobium* which includes *Haloanaerobium prevalans* (Zeikus et al., 1983); and *Sporohalobacter* which includes *Sporohalobacter lortetii* (formerly *Clostridium lortetii*) (Oren et al., 1987), and *Sporohalobacter marismortui* (Oren et al., 1987). The genera *Halobacteroides* and *Haloanaerobium* are included under the family *Haloanaerobiaceae* (Oren et al., 1984). Recently Hirotaka et al., (1989) isolated four strictly anaerobic, chemoorganotrophic, halophilic eubacteria including one alkalophile. The taxonomic status of these isolates is still not clear.

Haloanaerobium prevalens (Zeikus et al., 1983) was isolated from the bottom sediments and anoxic waters of the Great Salt Lake, Utah. The bacterium is a gram-negative, straight rod with

dimensions of 0.5 by 1.5 μm, and forms white to translucent and glistening colonies (0.5 to 2.9 mm diameter) on complex mineral salts medium containing 12.5% NaCl. Cells are not motile and do not form spores. It is an obligate anaerobe, and is capable of growing at salt concentrations ranging between 5 to 25%, with optimum growth occuring at 12.5% NaCl. The temperature range for growth is between 15 to 45°C, with optimum growth occuring at 37°C. The pH range for growth is between 6.0 and 8.0, with optimum growth at pH 7.0 to 7.4. The doubling time of the bacterium is about four hours. Fructose, glucose, mannose, pectin, and N-acetyl glucosamine support growth. Cellobiose, galactose, lactose, pyruvate, chitin, starch or methionine do not support growth. The organism is catalase and oxidase negative and does not reduce nitrate to nitrite. Fermentation products from glucose include acetate, butyrate, CO_2 and H_2. The organism also produces methylmercaptin during the degradation of methionine. The organism is found in high numbers (10^8 cells/ml), and is believed to be functioning as a hydrolytic-bacterium producing substrates for sulfate-reducing and methanogenic bacteria.

Halobacteroides halobius (Oren et al., 1984) was isolated from an enrichment culture containing Dead Sea water (80%), pyruvate, sulfate, yeast extract, ascorbate, and thioglycollate, and dead sea sediment collected from a depth of 60m. The bacterium is a gram-negative long flexible rod with a mean size of 0.5 by 10-20 μm, and forms grey, circular colonies (1-2 mm diameter) with glossy surface on complex medium. Cells are motile by means of

peritrichous flagella and do not form endospores. The organism is an obligate anaerobe with a high salt requirement. The salt concentration range for growth is between 7 and 19%, with an optimum of 10 to 15%. The organism tolerates magnesium concentrations up to 1 M, with some growth occuring up to 1.5 M in the presence of 1.5 M NaCl. The optimum temperature for growth is between 37 to 42°C. The minimum doubling time is 55 min, at 41°C in the presence of 1.5 M NaCl. Glucose, fructose, sucrose, galactose, mannose, maltose, raffinose, pyruvate, and starch support growth. Arabinose, sorbose, rhamnose, fucose, ribose, xylose, melibiose, melizitose, lactose, cellobiose, ascorbate, gluconate, mannitol, sorbitol, ethylene glycol, glycerol, acetate, fumarate, glycine, alanine, lysine, and arganine do not support growth. Biotin and p-aminobenzoic acid are required for growth. The strain is oxidase and catalase negative, does not produce indole from tryptophan, does not reduce nitrate to nitrite, and does not contain cytochromes. Ethanol, acetate CO_2 and H_2 are the products of glucose fermentation.

Clostridium lortetii (Oren, 1983), which was later renamed *Sporohalobacter lortetii* (Oren et al., 1987), was also isolated from the Dead Sea sediment using an enrichment method similar to that used for the isolation of *H. halobius*, except pyruvate was replaced with sodium lactate. The organism is a gram-negative, rod-shaped bacterium with a mean cell size of 0.5-0.6 by 5-10 μm, and forms grey translucent colonies (0.5-1 mm diameter) with glossy surface on complex medium. Growing cells are motile by means of

peritrichous flagella, but motility is lost in older cultures. Round terminal endospores are formed, with gas vacuoles attached to them. The organism is an obligate anaerobe and requires high salt concentrations for growth. The salt concentration range for growth is between 4 and 15% NaCl with optimal growth occuring at 8% NaCl (at 30°C) and 10% NaCl (at 45°C). Divalent cation concentrations of above 20 mM are required for optimal growth, and magnesium concentrations of up to 0.5 M in addition to 1.8 M NaCl are tolerated. The optimum growth temperature is between 37 and 45°C, with no growth occurring above 55°C. The organism grows well in medium containing glutamic acid, yeast extract, beef extract or casamino acids. Fermentation products include acetate, propionate, isobutyrate, n-butyrate, isovalerate and H_2. Acetate and butyrate are the only fermentation products in medium containing glutamic acid and yeast extract. Glucose is used, but only in older cultures, after other more suitable substrates are utilized. Fructose, maltose, glucose, sucrose, and starch stimulate growth but not cellobiose, galactose, lactose or mannose. The organism is catalase and oxidase negative and does not contain cytochromes. The organism does not hydrolyze gelatin but produces indole from tryptophan.

Sporohalobacter marismortui (Oren et al., 1987) is a rod-shaped bacterium, occasionally producing terminal endospores, but without gas vacuoles. The generation time in medium containing between 3.0 to 12% NaCl and 36- 45°C is as short as 40 min. Glucose, fructose, sucrose and starch are able to serve as carbon

and energy sources.

Halobacteroides acetoethylicus (Rengpipat et al., 1988) was isolated from deep subsurface gas-bearing sandstones and brine waters associated with injection water filter on an offshore oil rig in the Gulf of Mexico. The organism is a gram-negative, rod-shaped bacterium, with dimensions of 0.4-0.6 by 1-1.5 μm, and forms raised circular, white to translucent colonies (1-1.5 mm in diameter) on complex medium. Cells are motile by means of peritrichous flagella and are non-sporeforming. It is an obligate anaerobe and grows best in moderate salt concentrations. The optimal NaCl requirement for growth is 10%, with no growth occurring below 5% and above 22% NaCl. The optimum temperature for growth is 34°C, with growth occurring over a range of 15-45°C. The optimum pH for growth is 6.3-7.4, with no growth occurring below 5.4 and above 8.0. The doubling time of the bacterium is between 7.8 to 9.5 h. Glucose, cellobiose, fructose, lactose, mannose, N-acetyl glucosamine, pyruvate, sucrose, whey and xylose are fermented. Chitin, galactose, glutamine, glycerol, lactate, methionine, pectin, or starch are not fermented. The organism is catalase and oxidase negative. The glucose fermentation products include acetate, ethanol CO_2 and H_2.

Recently Hirotaka et al. (1989) reported the isolation of four strictly anaerobic halophiles from the aerobic subsurface sediments of hypersaline environments in California and Nevada. Three of the halophiles (Strains SS-11, SS-15 and SS-21) were isolated from the 0-10 cm depth of surface sediment of hypersaline muds of Salton

Sea, California using a screening medium containing trypticase, yeast extract, glucose and 15% NaCl. Strain M-20 was isolated from the subsurface sediments of Big Soda Lake, Nevada, using similar medium except for pH and NaCl concentration which were 10.0 and 20%, respectively. All four strains are gram-negative, non-sporeforming, strictly anaerobic rods exhibiting motility by means of peritrichous flagella. Cells of strains SS-11, and SS-15 are straight rods, occurring singly or in pairs, with dimensions 1.0-1.3 by 2.5-3.5 μm and 0.6-0.8 by 3.0-8.0 μm, respectively. Cells of strain SS-21 are straight or slightly curved rods, occurring singly, in pairs or as long chains, with cell dimensions of 0.5-0.7 by 2.5-4.0 μm. Strain M-20 cells are small rods measuring 0.5-0.7 by 0.9-2.2 μm. Cell membranes of all the strains contain fatty acid glycerol esters. The optimum temperature for growth of the strains is between 37°C and 45°C, with no growth occurring above 50-55°C. The optimum NaCl concentration range for growth of strains SS-11, SS-15, and M-20 is between 5 and 10%, and that for strains SS-21 is between 12 and 20%. The pH range for strains SS-11, SS-15 and SS-21, is between 6.5 and 8.5-9.5, and that for strain M-20 is between 7.0 to 10.0 (optimum pH between 8.5 to 9.5).

The glucose fermentation products of strains SS-11, SS-15, and M-20 include acetate, propionate, n-butyrate, hydrogen, and carbon dioxide. Strain M-20 produces lactate in addition to the above fermentation products. The glucose fermentation products of strain SS-21 are ethanol, acetate, lactate, pyruvate, hydrogen and carbon

dioxide. Glucose, dextran and soluble starch stimulates growth of all the strains. Sorbose, rhamnose, sorbitol, alanine, arganine, acetate, lactate, fumarate, and succinate are not fermented by any of the four strains.

3.1.3 Objectives. The Department of Botany and Microbiology and the School of Petroleum and Geological Engineering at the University of Oklahoma has been involved in a joint research program to investigate the use of non-pathogenic microorganisms to enhance oil recovery. This research has mainly focused on the use of indigenous microorganisms and their metabolic products to improve volumetric sweep efficiency. A procedure involving the addition of nutrients to stimulate the growth of indigenous microorganisms in high permeable zones of the reservoir is being carried out in a section of the South East Vassar Vertz Sand Unit (SEVVSU), Payne County, Oklahoma, which is a hypersaline petroleum reservoir (Knapp et al., 1989). Part of the scope of this contract is to characterize the physiology of bacteria isolated from this reservoir and to determine the kinds and amounts of metabolites that are produced by these bacteria. Here, we report the cellular, growth, and metabolic characteristics of five bacteria isolated from the Southeast Vassar-Vertz reservoir.

3.2 Materials and Methods

3.2.1 Isolation and culture methods. Several anaerobic halophilic bacteria were isolated from the brines (Bhupathiraju et al, 1991). Seven anaerobic heterotrophic halophiles and thirty

anaerobic nitrate-using halophiles were isolated. Of these, four anaerobic heterotrophic halophilic strains designated VS-732, VS-751, VS-752, VS-511, and one molasses-using halophilic strain designated TTL-30 were selected for further studies. Molasses nitrate medium with 15% NaCl (Knapp et al., 1989) was modified by reducing the NaCl concentration to 12%, deleting molasses, including glucose (0.5%, wt/vol), casamino acids (0.1%, wt/vol) and yeast extract (0.1%,wt/vol), and a gas phase of 80% N_2:20% CO_2 to grow and maintain all the isolates. Tests to determine the optimal temperature range of the isolates were done using this medium and incubating them at various temperatures. The optimal salt requirement was determined by changing the salt content of the medium as indicated. For experiments requiring a medium prepared without CO_2, bicarbonate was replaced with PIPES (piperazine-N,N'-bis[2-ethanesulfonic acid]) dipotassium salt (1.5 g/l). Vitamins (Balch and Wolfe, 1976) were added to culture medium whenever complex medium was not used. Cultures were routinely checked under phase contrast microscope to insure purity.

3.2.2 Metabolic characteristics. All experiments were done in duplicates and the results reported as mean values. The ability of the isolated strains to utilize different substrates were tested by replacing yeast extract, casamino acids, and glucose with the test compound, at 10 mM (unless otherwise indicated) and comparing the growth (A_{660}) and the amount of acetate produced, with that obtained in uninoculated control tubes containing the respective substrate. The ability of the isolates to utilize amino acid

mixtures was also tested. The amino acid combinations tested included the following: alanine-glycine, leucine-proline, isoleucine-tryotophan, valine-ornithine, phenylalanine-leucine and histidine-sarcosine. The effect of the gas phase on the growth of the isolates was tested by changing the gas phase from 80% N_2:20% CO_2 to 80% H_2:20% CO_2. The ability to use carbon monoxide was determined using different gas phase concentrations (100%CO, 75%CO:25%N_2, 50%CO: 50%N_2, 25%CO:75%N_2). The effect of external electron acceptors on the growth of the isolates was tested in medium with glucose as an electron donor. Compounds tested as electron acceptors included elemental sulfur, sodium sulfate, sodium thiosulfate, sodium sulfite, sodium nitrate, and sodium nitrite at a concentration of 0.3% (wt/vol).

3.2.3 Miscellaneous Tests. Gram staining was performed using both heat-fixed smears and smears fixed with acetic acid (Dussault, 1955). Antibiotic susceptibility tests were performed by adding various filter-sterilized antibiotics to the growth medium. Antibiotics tested included chloramphenicol, tetracycline, penicillin, cyclohexamide, each at 10 μg/ml. The effect of sodium azide on growth, at 50 μg/ml was also tested. Susceptibility to the above inhibitors was determined by comparision of growth in medium containing the inhibitor to controls that lacked it.

3.2.4 Analytical Techniques. Growth was followed by measuring the increase in absorbance at 660 nm using a Bausch and Lomb Spectronic 21 Spectrophotometer. Microscopic examinations were performed using an Olympus Photomicrographic System Model

DM-10AD phase contrast microscope. Glucose was measured colorimetrically by the glucose oxidase method (Sigma Chemical Co., St Louis, MO.) using a Beckman DU 64 Spectrophotometer. Volatile fatty acids and alcohols were analyzed with a Varian Model 3400 series Gas Chromatograph using a Carbopack. c/o. 3% Carbowax 20m/0.1% H_3PO_4, 30"x1/4" ODx4mm ID glass column operating at a temperature of 130°C and 60°C respectively. The operating temperatures for injector, and detector were 170°C, 175°C respectively. Nitrogen was used as the carrier gas at 55 ml/min. Samples for volatile fatty acids were acidified by adding 0.2 ml of 25% H_3PO_4 to 0.8 ml of sample. A 1μl injection volume was used for the analysis of fatty acids and alcohols. Fatty acid analyses were also performed using a high-pressure liquid chromatograph, equipped with a Bio-Rad, 300x7.8mm Aminex HPX-87H column and an isocratic mobile phase of 0.016 N H_2SO_4 at a flow rate of 0.9 ml/min. Hydrogen was analyzed using a RGA 3 Reduction Gas Analyzer fitted with a 3'x1/8" column packed with 60/80 mesh spherocarb, operating at temperature of 90°C. The detector temperature was set at 264°C. Nitrogen was used as the carrier gas at 20 ml/min. CO_2 and CH_4 were measured with a gas chromatograph equipped with a thermal conductivity detector and a Poropack Q column (Supleco, Inc.) (Jenneman et al., 1986). All gas analyses were performed using gas tight syringes. Calibration curves for gasses were prepared by adding high purity gases with a gastight syringe to 160 ml serum bottles flushed with oxygen free nitrogen and sealed with a black rubber stopper. All products were identified and

quantified by comparision of retention times and peak areas with those of known standards. Identification of fatty acids and alcohols was also confirmed by the addition of internal standards.

3.3 Results

Four anaerobic heterotrophic halophiles designated as VS-732, VS-751, VS-752, VS-511, and one molasses nitrate-using halophile designated TTL-30 were characterized. Strains VS-732, VS-751 and VS-752, and VS-511 were isolated from wells 7-3, 7-5, and 5-1 respectively. All five were gram-negative, non-sporeforming rod shaped bacteria. Cells of strains VS-751 and VS-752 were straight rods, appearing single, in pairs, or occasionally as long chains, and measuring 0.7-0.8 by 2-3.3 μm, and 0.3-0.4 by 2.6-4 μm, respectively. Cells of strains VS-732, VS-511, and TTL-30 were relatively smaller, occuring either singly or in pairs, with dimensions of 0.5-0.8 by 0.7-1.9 μm, 0.5-0.7 by 1.3-2.6 μm, and 0.5 by 1.2-1.5 μm, respectively. Cells of strains VS-732, VS-751, and VS-752 were motile, while that of strains VS-511 and TTL-30 were non-motile.

All five strains were unable to grow in aerated medium and required high concentrations of NaCl for growth. At least 6% NaCl (wt/vol) was required for the growth of all the strains. At NaCl concentrations less than 6% the cells lysed. Strains VS-732 and VS-752 grew at NaCl concentrations ranging between 6 and 25%, with optimum growth occuring at 6% and 9 to 12%, respectively (Fig. 3.1 and Fig. 3.3). The range of NaCl concentrations for the growth of

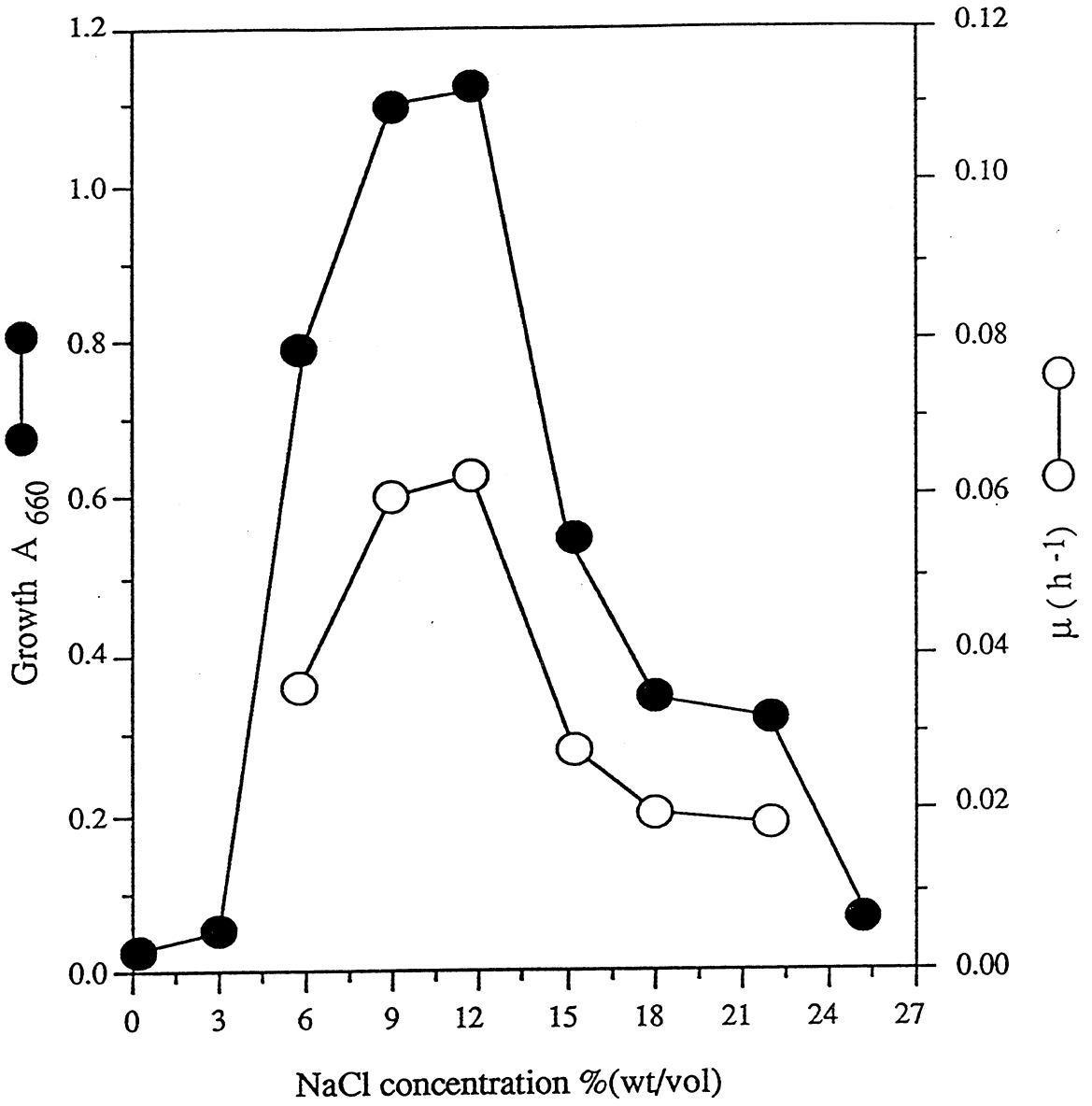

Figure 3.1 Effect of NaCl concentration on the growth of strain VS-732. Cells were grown at 35°C in mineral salts medium containing yeast extract, casamino acids, glucose, and the NaCl concentration indicated. After different incubation periods at 35°C the absorbance of the cultures was measured and the growth rates were calculated from the exponential part of the growth curves.

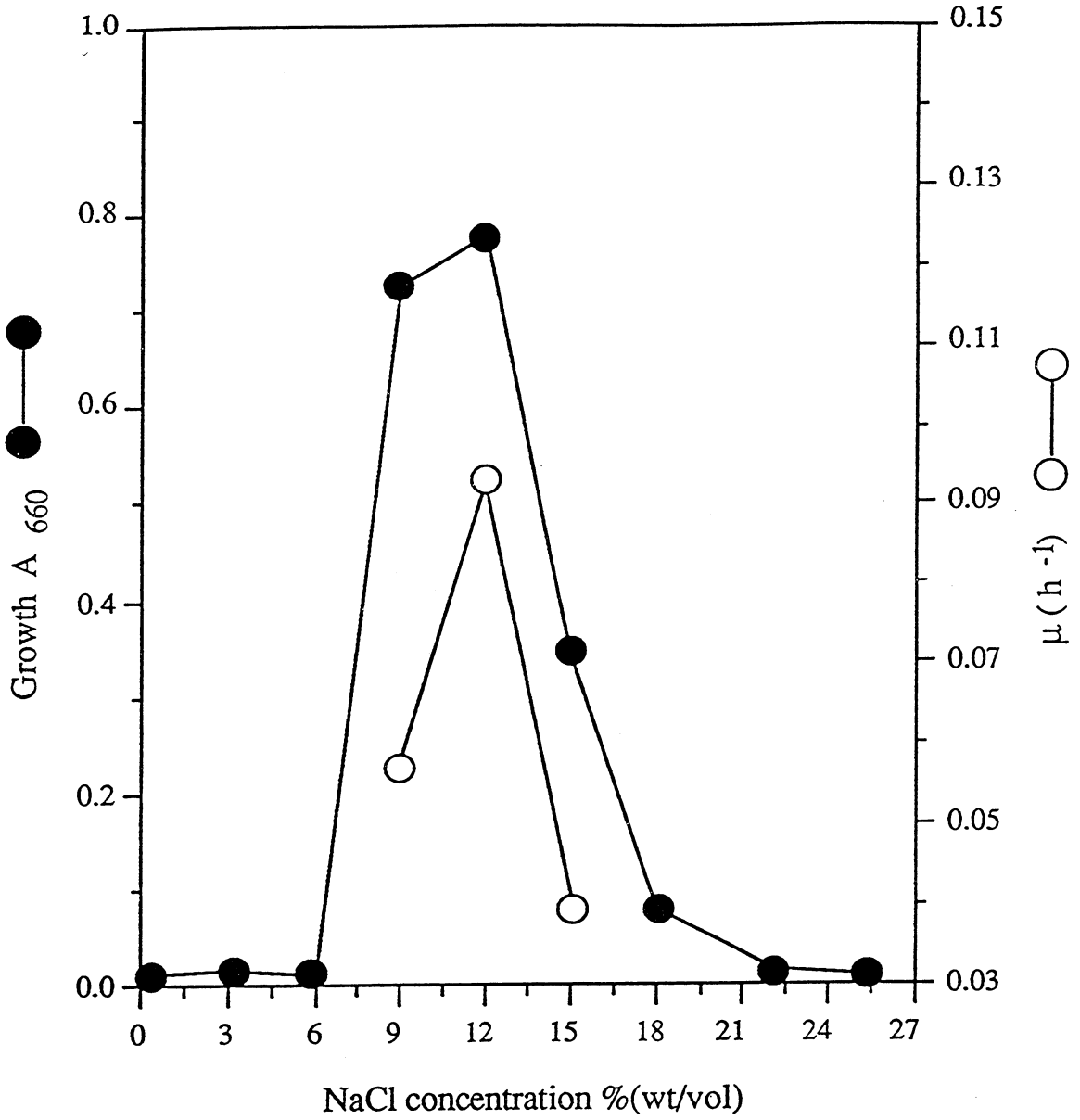

Figure 3.2 Effect of NaCl concentration on the growth of strain VS-751. Cells were grown at 35°C in mineral salts medium containing yeast extract, casamino acids, glucose, and the NaCl concentration indicated. After different incubation periods at 35°C the absorbance of the cultures was measured and the grwoth rates wre calculated from the exponential part of the growth curves.

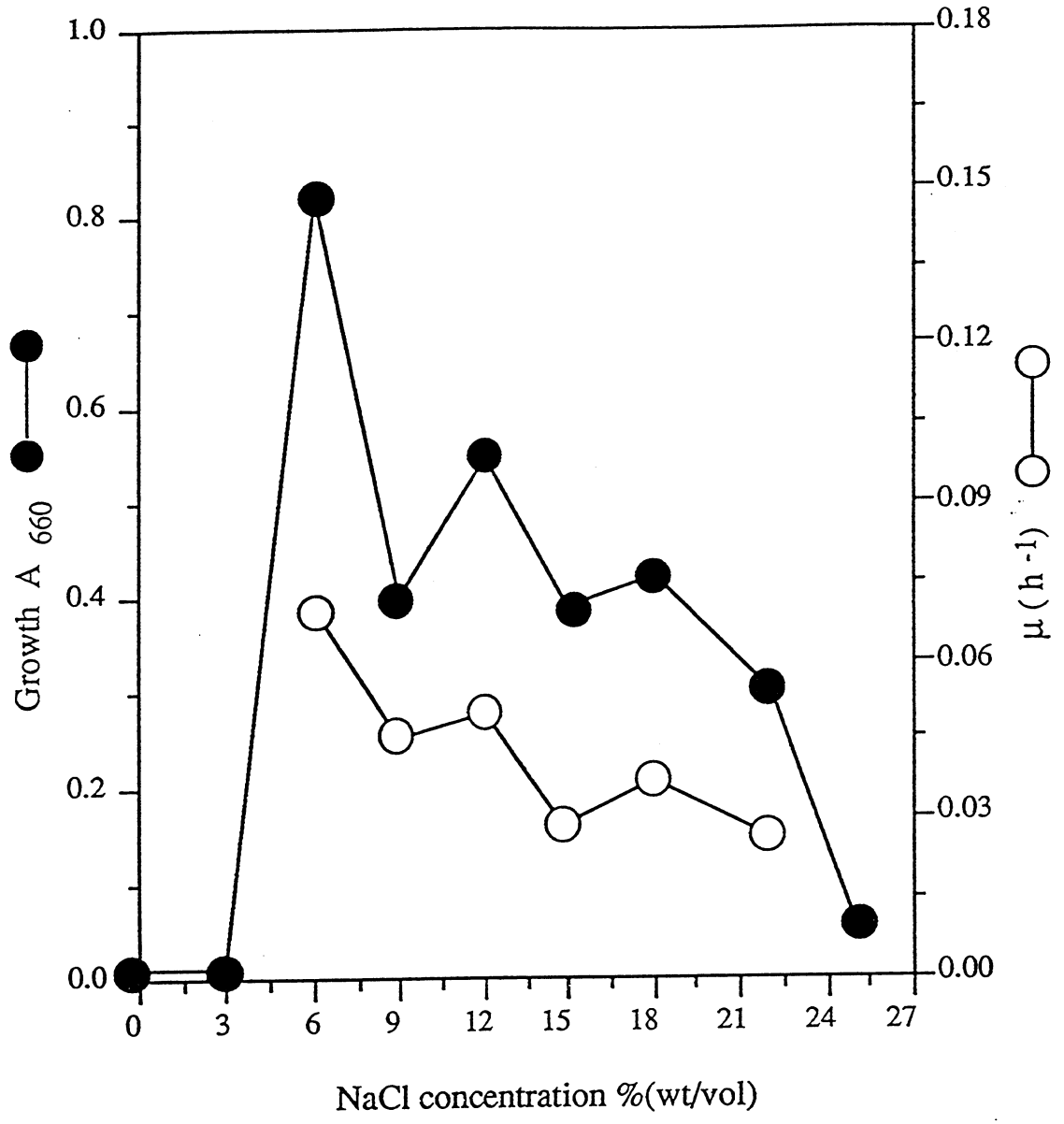

Figure 3.3 Effect of NaCl concentration on the growth of strain VS-752. Cells wre grown at 35°C in mineral salts medium containing yeast extract, casamino acids, glucose, and the NaCl concentration indicated. After different incubation periods at the 35°C the absorbance of the cultures was measured and the growth rates were calculated from the exponential part of the growth curves.

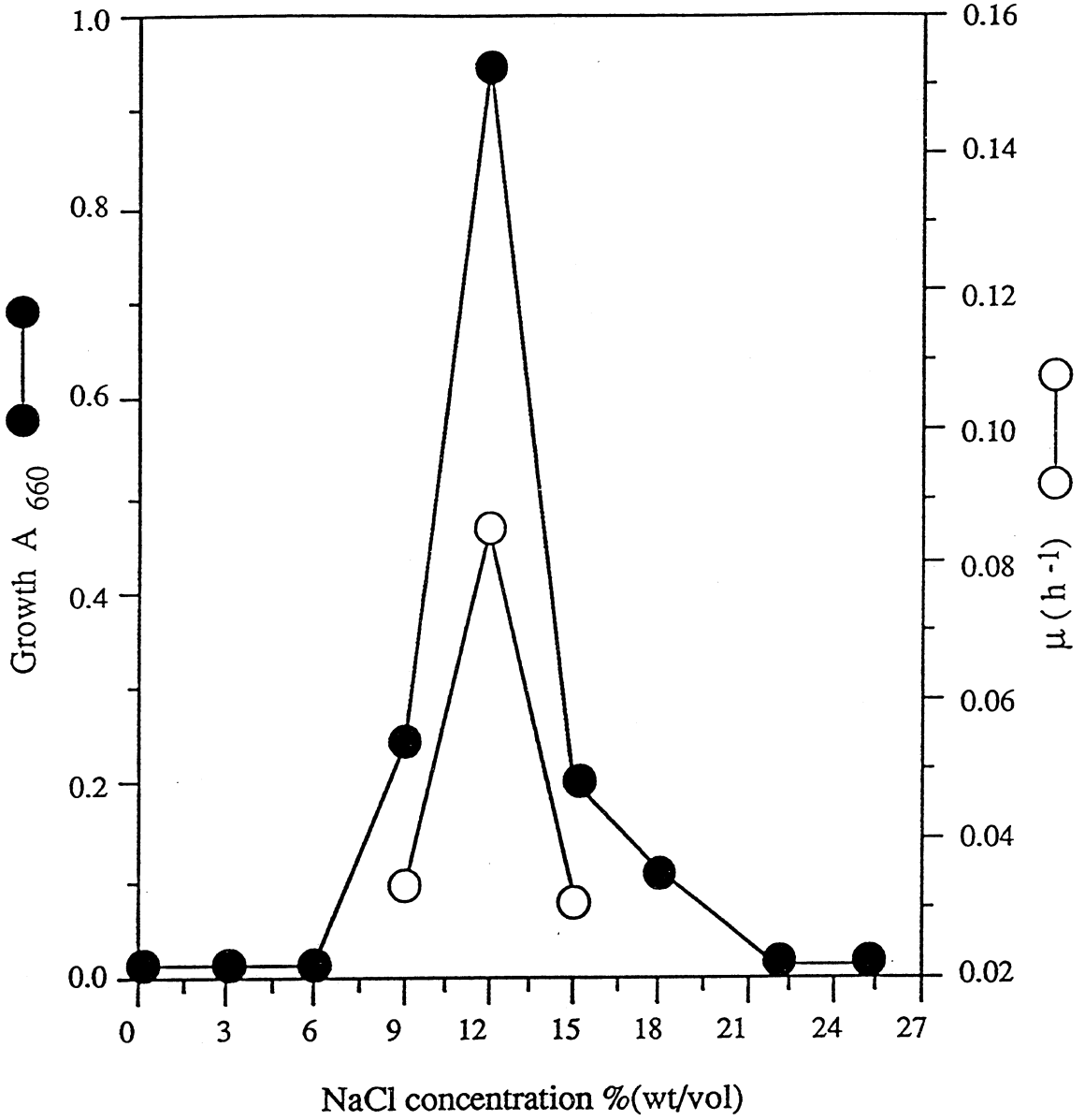

Figure 3.4 Effect of NaCl concentration on the growth of strain VS-511. Cells were grown at 35°C in mineral salts medium containing yeast extract, casamino acids, glucose, and the NaCl concentration indicated. After different incubation periods at 35°C the absorbance of the cultures was measured and the growth rates were calculated from the exponential part of the growth curves.

strains VS-751 and VS-511 was between 9 and 18%, with optimum growth occuring at 12% (Fig 3.2 and Fig. 3.4). The optimal NaCl requirment for strain TTL-30 was 15%, with growth occuring between 6 and 22% (Fig. 3.5). None of the strains grew at NaCl concentrations greater than 25%. The optimum temperature for growth of strains VS-751, VS-752, and TTL-30 was between 23 and 45°C, and for strains VS-732, and VS-511 was between 23 and 37°C. The doubling time of strains VS-751, VS-511, and VS-732 was 7.2, 8, and 11 hours respectively and that of strains VS-752 and TTL-30 was around 10 hours. All strains were catalase and oxidase negative and were inhibited by chloramphenicol, tetracycline, and penicillin, but not cyclohexamide or azide.

The effect of added electron acceptors on the growth of the strains was tested in medium containing glucose as the carbon source (Table 3.1). None of the tested electron acceptors stimulated the growth of the strains, except for sulfite which stimulated the growth of strain TTL-30. Nitrate neither stimulated nor inhibited the growth of the strains. Elemental sulfur, sulfate, thiosulfate, and nitrite inhibited the growth of all the strains. The change of the gas phase from N_2/CO_2 to H_2/CO_2 in tubes containing glucose as the carbon source and no added electron acceptors, stimulated the growth of strains VS-511 and VS-732, but completely inhibited the growth of strain TTL-30 (Table 3.2). The presence of carbon monoxide in the gas phase at any of the tested concentrations in medium with and without glucose, completely inhibited growth of all the strains.

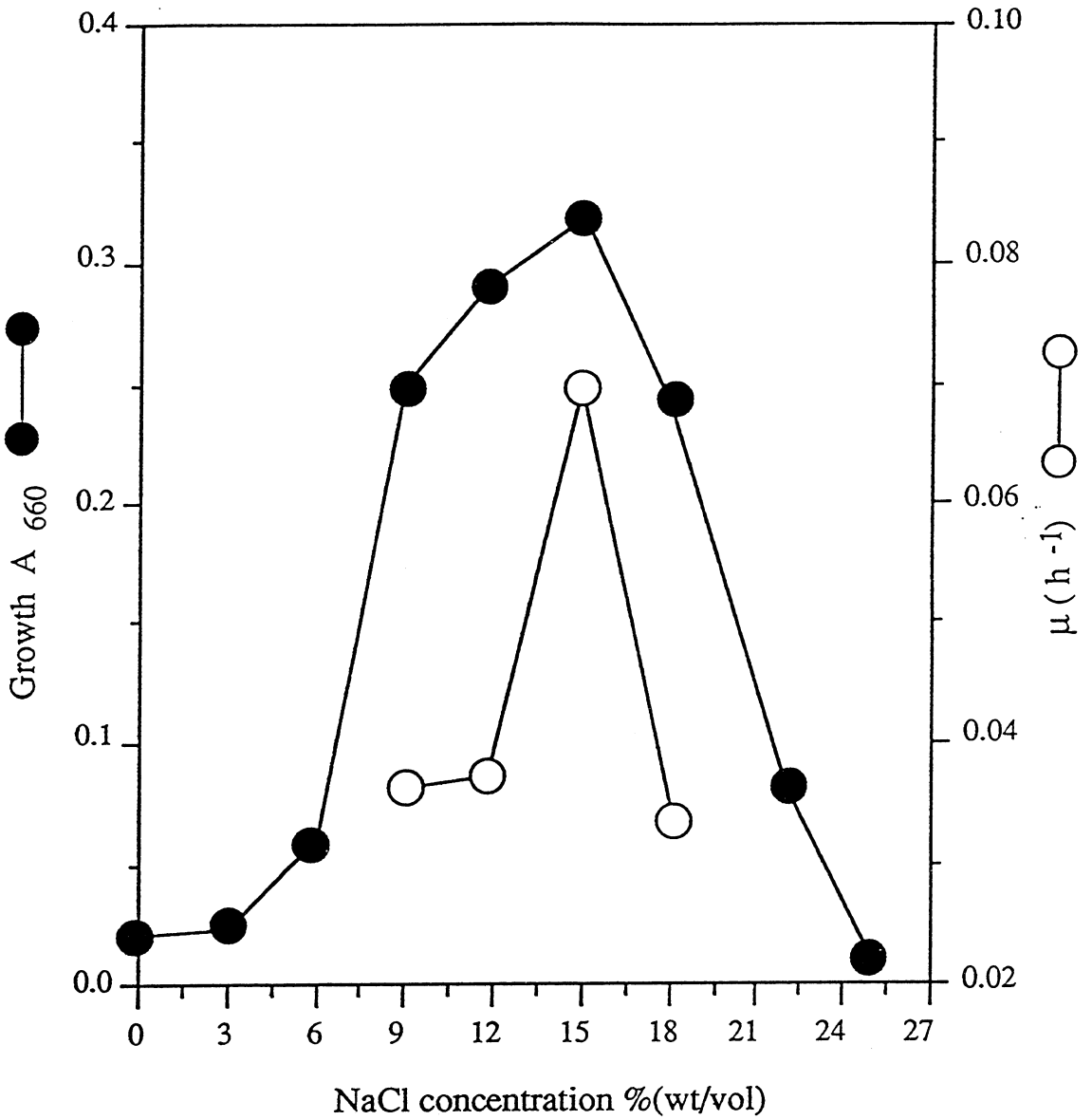

Figure 3.5 Effect of NaCl concentration on the growth of strain TTL-30. Cells were grown at 35°C in mineral salts medium containing yeast extract, casamino acids, glucose, and the NaCl concentration indicated. After different incubation periods at 35°C the absorbance of the cultures was measured and the growth rates were calculated from the exponential part of the growth curves.

Table 3.1. Effect of external electron acceptors on the growth of the halophilic strains.

Electron acceptor[b]	Strain				
	VS-732	VS-751	VS-752	VS-511	TTL-30
None	0.20	0.20	0.15	0.20	0.25
Elemental sulfur	0.04	0.01	0.03	0.02	0.01
Sulfate	0.06	0.02	0.03	0.07	0.00
Thiosulfate	0.01	0.02	0.02	0.05	0.00
Sulfite	0.00	0.00	0.00	0.00	0.40
Nitrate	0.20	0.20	0.15	0.20	0.20
Nitrite	0.05	0.05	0.05	0.04	0.06
-Glucose - e- acceptor	0.00	0.00	0.00	0.00	0.00

[a] Growth was determined by measuring absorbance at 660 nm after incubation at 35°C for 4 days.

[b] Electron acceptors were added at a concentration of 0.3% w/v to mineral salts medium containing glucose (1% w/v) as the sole source of carbon.

Table 3.2. Effect of gas phase on the growth of the halophilic strains[a].

Gas phase[b]	Strains				
	VS-732	VS-751	VS-752	VS-511	TTL-30
N_2/CO_2					
+ Glucose	0.20	0.20	0.15	0.20	0.25
- Glucose	0.00	0.00	0.00	0.00	0.00
H_2/CO_2					
+ Glucose	0.35	0.20	0.15	0.30	0.00
- Glucose	0.00	0.00	0.00	0.00	0.00
CO					
+ Glucose	0.00	0.00	0.00	0.00	0.00
- Glucose	0.00	0.00	0.00	0.00	0.00

[a] Cells were grown in mineral salts medium containing 12% (w/v) NaCl. Where required glucose was added as sol source of carbon at 1% (w/v). Growth was determined by measuring absorbance at 660 nm after incubation at 35°C for 4 days.

[b] Gas phase, N_2/CO_2, 80% N_2: 20% CO_2; H_2/CO_2, 80% H_2: 20% CO_2; CO, 100% CO, 75%CO: 25%N_2, 50%CO: 50%N_2, 25%CO: 75%N_2.

Energy sources for the strains were tested by adding individual carbon source at 10 mM (unless otherwise indicated) to mineral salts medium containing 12% NaCl, and 0.025% yeast extract. A variety of compounds were able to serve as energy sources (Table 3.3). Substrate utilization was indicated by both growth (A_{660}) and product (acetate) formation. Substrates utilized by all the strains included: arabinose, fructose, galactose, glucose, inulin, mannose, maltose, sucrose, and trypticase. Substrates not utilized by any of the strains included the following: ascorbate, butyrate, crotonate, dihydroxybenzoate, gallic acid, inositol, lactate, malate, methanol, methionine, propionate, phenoxyacetate, and resorcinol. The ability of the strains to utilize amino acid mixtures was also tested. Amino acid mixtures such as alanine-glycine, leucine-proline, isoleucine-tryptophan, valine-ornithine, phenyl-alanine-leucine, and histidine-sarcosine were also not utilized by any of the strains.

The glucose fermentation products of the strains were determined in 160 ml serum bottles containing mineral salts medium with 1% (wt/vol) glucose, 0.025% yeast extract and a gas phase of nitrogen. Analysis of culture fluids after 96 hours of incubation at 35°C, by gas and liquid chromatography indicated the following products: ethanol, acetate, formate, CO_2 and H_2 in the case of strains VS-732, and VS-751; acetate, ethanol, CO_2 and H_2 in the case of strains VS-752 and TTL-30; and ethanol, acetate, CO_2 and H_2 in the case of strain VS-511 (Table 3.4). For strain VS-732 an unidentified peak was detected in HPLC chromatograms, as a product

Table 3.3. Substrate utilization by the halophilic strains [a].

Substrate [b]	Acetate produced[c] (mM)				
	VS-732	VS-751	VS-752	VS-511	TTL-30
Arabinose	1.7 ± 0.1 (0.19)[d]	4.6 ± 0.2 (0.28)	6.8 ± 0.4 (0.25)	3.7 ± 0.2 (0.22)	3.0 ± 0.6 (0.22)
Cellobiose	0.9 ± 0.1 (0.14)	3.7 ± 0.2 (0.31)	ND[f] (0.19)	2.6 ± 0.3 (0.23)	-
Ethylene glycol	-[e]	-	-	1.3 ± 0.2 (0.18)	-
Formate	-	-	0.7 ± 0.3 (0.15)	-	-
Fructose	2.7 ± 0.3 (0.25)	3.4 ±0.2 (0.33)	2.4 ± 0.3 (0.22)	4.3 ± 0.3 (0.26)	7.3 ± 0.4 (0.35)
Fucose	3.5 ± 0.3 (0.22)	-	-	2.5 ± 0.4 (0.20)	NA (0.19)
Galactose	2.1 ± 0.1 (0.18)	3.1 ± 0.2 (0.24)	6.0 ± 0.1 (0.28)	2.8 ± 0.2 (0.25)	4.8 ± 0.4 (0.21)
Glucose	6.9 ± 0.5 (0.30)	5.8 ± 0.4 (0.42)	8.2 ± 0.5 (0.32)	6.4 ± 0.2 (0.35)	8.9 ± 0.8 (0.40)
Glucosamine	-	-	2.3 ± 0.2 (0.18)	ND (0.15)	3.1 ± 0.2 (0.15)
Glycerol	-	-	4.6 ± 0.1 (0.25)	1.0 ± 0.2 (0.16)	4.9 ± 0.3 (0.18)
Inulin	4.1 ± 0.2 (0.28)	5.7 ± 0.3 (0.25)	5.7 ± 0.2 (0.28)	6.2 ± 0.3 (0.24)	5.5 ± 0.5 (0.20)
Lactose	-	1.9 ± 0.1 (0.17)	0.9 ± 0.2 (0.15)	ND (0.27)	-
Maltose	4.2 ± 0.1 (0.22)	-	1.5 ± 0.1 (0.19)	5.2 ± 0.4 (0.27)	3.2 ± 0.2 (0.23)
Mannitol	-	-	-	2.6 ± 0.5 (0.23)	-
Mannose	2.5 ± 0.2 (0.19)	3.3 ± 0.2 (0.24)	2.7 ± 0.3 (0.20)	2.1 ± 0.2 (0.22)	5.6 ± 0.2 (0.22)

(continued on next page)

Table 3.3 (continued from previous page)

Substrate [b]	Acetate produced[c] (mM)				
	VS-732	VS-751	VS-752	VS-511	TTL-30
Peptone	2.1 ± 0.2 (0.18)	6.0 ± 0.6 (0.21)	-	ND (0.15)	9.8 ± 0.4 (0.25)
Pyruvate	-	5.1 ± 0.6 (0.21)	3.9 ± 0.3 (0.19)	1.1 ± 0.1 (0.14)	-
Pyrogallic acid	-	-	1.2 ± 0.2 (0.16)	-	1.6 ± 0.3 (0.14)
Rhamnose	-	-	1.0 ± 0.2 (0.15)	-	-
Sorbose	-	-	-	1.1 ± 0.2 (0.15)	-
Succinate	-	-	5.7 ± 0.5 (0.22)	-	-
Sucrose	3.5 ± 0.3 (0.24)	3.4 ± 0.2 (0.25)	2.6 ± 0.3 (0.22)	4.8 ± 0.6 (0.28)	6.7 ± 0.2 (0.27)
Trypticase	1.5 ± 0.2 (0.15)	1.6 ± 0.2 (0.22)	1.6 ± 0.5 (0.19)	2.3 ± 0.2 (0.18)	7.1 ± 0.6 (0.22)
Xylose	3.3 ± 0.4 (0.25)	-	0.8 ± 0.2 (0.15)	2.2 ± 0.2 (0.19)	-

[a] A 2% inoculum grown on the same substrate was employed in all the experiments.

[b] Substrate was added at 10 mM to mineral salts medium described in text, except peptone, trypticase and inulin which were added at 1% (w/v), 1% (w/v), and 1mM respectively. Substrates tested but not utilized include: ascorbate, butyrate, crotonate, dihydroxybenzoate, gallic acid, inositol, lactate, methionine, malate, methanol, propionate, phenoxyacetate, and recorcinol.

[c] Acetate production was determined by gas chromatography after five days of incubation at 35°C. Values are corrected for small amounts of acetate formed in medium without substrate. No acetate formation was found in inoculated, autoclaved control or in uninoculated controls. Values represent mean ± standard deviation of two replicates.

[d] Numbers in parenthesis indicate mean of maximum A_{660} after five days incubation at 35°C.

[e] -, not utilized.

[f] ND, not determined.

Table 3.4. Glucose fermentation products of the anaerobic halophiles isolated from SEVVSU brines [a]

Strain	Glucose Consumed (mmol/l)	Products[b] (mmol/l)					%CR[c]	% HR[d]
		Ethanol	Acetate	Formate	CO_2[e]	H_2[e]		
VS-732[f]	10.2 ± 0.16	10.5 ± 0.10	7.1 ± 0.32	3.3 ± 0.10	17.7 ± 0.38	4.9 ± 0.59	91	88
VS-751	9.6 ± 0.11	13.1 ± 0.35	5.6 ± 0.19	3.1 ± 0.15	18.5 ± 0.19	5.0 ± 0.38	103	101
VS-752	5.7 ± 0.14	6.0 ± 0.02	8.4 ± 0.33	ND[g]	9.7 ± 0.18	2.1 ± 0.07	112	107
VS-511	10.3 ± 0.20	14.4 ± 0.47	6.9 ± 0.16	ND	18.0 ± 0.27	5.5 ± 0.58	98	102
TTL-30	3.8 ± 0.22	1.6 ± 0.10	6.0 ± 0.18	ND	8.3 ± 0.47	1.3 ± 0.05	102	79

[a] Cultures were grown in 160 ml serum bottles containing 30 ml mineral salts medium with 1% (w/v) glucose, 0.025% (w/v) yeast extract, and a gas phase of nitrogen. Volatile acids and alcohols in the liquid phase, and CO_2 and H_2 in the gas phase were analyzed at the begining of the experiment and after 96 hrs of incubation at 35°C.

[b] Values are corrected for small amounts of products formed in medium without substrate. No product formation or substrate loss was found in inoculated, autoclaved controls or in uninoculated controls. Values represent mean ± standard deviation of two replicates.

[c] CR, carbon recovery.

[d] HR, hydrogen recovery.

[e] Values were normalized to 20°C and 1 atmosphere.

[f] An unidentified compound has been detected as a product of glucose fermentation.

[g] Not detected.

of glucose metabolism. Lactate, malate, succinate, butyrate, propionate, valerate, isovelarate, and caproate were not detected in any of the culture fluids.

3.4 Discussion

Most anaerobic fermentative halophilic bacteria reported so far have been isolated from either the bottom sediments of the Dead Sea (Oren, 1983; Oren et al., 1984), the Great Salt Lake (Zeikus et al., 1988), or other hypersaline environments (Rengpipet et al., 1988; Hirotaka et al., 1989). Isolation of these bacteria from oil brines has not been reported, although halophilic methanogens (Belyaev et al., 1990; Gevertz et al., 1991), and halophilic sulfate reducers (Gevertz et al.,1991) have been reported from oil brines and stratal waters associated with oil bearing formations. In the present study several haloanaerobes were isolated from the hypersaline brines of the SEVVSU. Five of the characterized isolates have optimal growth at NaCl concentrations within the range of those required by "moderate halophiles" (Kushner, 1978). All these isolates are strictly anaerobic, obligately halophilic, gram-negative, non-sporing, rod-shaped bacteria capable of growing over a wide range of salt concentrations. All of the SEVVSU isolates differ from each other and from other described haloanaerobes. Tables 3.5 and 3.6 summarize the differences between the SEVVSU isolates and other described haloanaerobic bacteria.

Both strain VS-732 and strain VS-752 grow at NaCl

Table 3.5. Differences between anaerobic halophilic bacteria.

Characteristics	VS-732	VS-751	VS-752	VS-511	TTL-30
Morphology	rod	rod	rod	rod	rod
Gram stain	negative	negative	negative	negative	negative
Size					
Growth (t_d,h)	11	7.25	10	8	10
Opt. temp. range (°C)	20-37	20-45	20-45	20-37	20-45
NaCl conc. range (%w/v)	6-25	9-18	6-25	9-18	6-22
Opt. NaCl conc. (%w/v)	9-12	12	6	12	15
Motility	+	+	+	-	-
Spores	-	-	-	-	-
Habitat	oil-reservoir brines	oil-reservoir brines	oil-reservoir brines	oil-reservoir brines	oil-reservoir brines
End products from glucose	ethanol acetate formate CO_2/H_2	ethanol acetate formate CO_2/H_2	acetate ethanol CO_2/H_2	ethanol acetate CO_2/H_2	acetate ethanol CO_2/H_2

(continued on next page)

Table 3.5. (continued from prevoius page).

Characteristics	*Clostridium lortetti* (Oren, 1983)	*Halobacteroides halobius* (Oren et al., 1984)	*Haloanaerobium prevalens* (Zeikus et al., 1983)	*Halobacteroides acetoethylicus* (Rengpipat et al., 1988)
Morphology	rod	rod	rod	rod
Gram stain	negative	negative	negative	negative
Size	0.5-0.6 x 2.5-10 µm	0.5 x 10-20 µm	0.5 x 1.5 µm	0.4-0.7 x 1-1.6µm
Growth (t_d,h)	8	1	4	7.8-9-5
Temperature range (°C)	37-45	37-45	15-45	15-45
NaCl conc. range (%w/v)	6-12	8-17	5-25	6-20
Opt. NaCl conc. (%w/v)	8-10	10-15	12.5	10
Motility	+	+	-	+
Spores	+	-	-	-
Habitat	Dead sea	Dead sea	Dead sea	Gas-bearing rocks Oil-water injection filter
End products from glucose	acetate butyrate H_2/CO_2	acetate ethanol CO_2/H_2	acetate butyrate CO_2/H_2	ethanol acetate CO_2/H_2

(continued on next page)

Table 3.5. (continued from previous page)

Characteristics	SS-11	SS-15	SS-21	M-20
Morphology	rod	rod	rod	rod
Gram stain	negative	negative	negative	negative
Size	1.0-1.3 x 2.5-3.5μm	0.6-0.8 x 10-20 μm	0.5-0.7 x 2.5-4.0 μm	0.4-0.7 x 1-1.6μm
Growth (t_d,h)	NR[a]	NR	NR	NR
Opt. temp. range (°C)	37-45	37-45	37-45	37-45
NaCl conc. range (%w/v)	2.5-25	2.5-25	5-30	5-20
Opt. NaCl conc. (%w/v)	10	5	15	5
Motility	+	+	+	+
Spores	-	-	-	-
Habitat	Salton sea California	Salton sea California	Salton sea California	Soda lake Nevada
End products from glucose	acetate propionate n-butyrate H_2/CO_2	acetate propionate n-butyrate H_2/CO_2	acetate propionate n-butyrate H_2/CO_2	ethanol acetate lactate pyruvate H_2/CO_2

[a]NR, not reported.

Table 3.6. Comparision of substrate utilization by various fermentative haloanaerobes[a].

Substrate	VS-732	VS-751	VS-752	VS-511	TTL-30	Hb. ace	Hb. halo	Ha. pre	C. lort	SS-11	SS-15	SS-21	M-20
Alanine							-			-	-	-	-
Arabinose	+	+	+	+	+		-			-	-	+	+
Arganine					-					-	-	-	-
Ascorbate	-	-	-	-	-		-						
Cellobiose	+	+	+	+	-	+	-	-	-	-	-	+	+
Chitin								-					
Ethylene glycol	-	-	-	+	-		-						
Formate	-	-	+	-	-								
Fructose	+	+	+	+	+	+	+	-	+	+	+	±	+
Fucose	+	-	-	+	+		-						
Fumarate							-			-	-	-	-
Galactose	+	+	+	+	+	-	+	-	-	-	±	+	+
Gluconate							-			-	±	-	+
Glucose	+	+	+	+	+	+	+	+	+	+	+	+	+
Glucosamine	-	-	+	+	+	+		+		+	-	+	+
Glutamate										+	+	-	-
Glutamine						-							
Glycerol	-	-	+	+	+	-	-			-	-	-	+
Glycine	-				-					+	-	-	-
Inulin	+	+	+	+	+								
Lactate			-	-	-	-							
Lactose	-	+	+	+	-	+	-	-	-	-	-	+	+

(continued on next page)

Table 3.6. (continued from previous page)

Substrate	VS-732	VS-751	VS-752	VS-511	TTL-30	Hb. ace	Hb. halo	Ha. pre	C. lort	SS-11	SS-15	SS-21	M-20
Lysine					-		-			-	+	-	+
Maltose	+	-	+	+	+		+		+	-	+	+	+
Mannitol	-	-	-	+	-		-			-	-	+	-
Mannose	+	+	+	+	+	+	+	+	-	-	+	+	+
Melibiose							-			-	-	+	+
Melizitose							-						
Methionine	-	-	-	-		-		-					
Pectin						-		+					
Peptone	+	+	-	+	+								
Pyruvate	-	+	+	+	-	+	+	-					
Pyrogallic acid	-	-	+	-	+								
Raffinose							+			-	-	±	-
Rhamnose	-	-	+	-	-		-			-	-	-	-
Ribose							-			-	-	-	-
Sorbose	-	-	-	+	-		-			-	-	-	-
Starch						-		-	+	+	+	+	+
Succinate	-	-	+	-	-					-	-	-	-
Sucrose	+	+	+	+	+	+	+		+	-	-	+	+
Trehalose										-	-	+	+
Trypticase	+	+	+	+	+								
Xylose	+	-	+	+	-	+	-			-	-	+	-

[a] Abbreviations: Hb. ace, *Halobacteroides acetoethylicus*; Hb. halo, *Halobacteroides halobius*; Ha. pre, *Haloanaerobium prevalens*; C. lort, *Clostridium lorteti*.

concentrations ranging between 6 and 25% (wt/vol), but differ from each other in their optimal requirement for NaCl (9-12% for VS-732 vs. 6% for VS-752). These strains also differed in their ability to use various tested substrates (Table 3.3), optimal temperature range for growth, generation time, and the pattern of product formation from glucose. Acetate is the major end product of glucose fermentation for strain VS-752, followed by ethanol, CO_2 and H_2. On the other-hand ethanol is the major end product for strain VS-732. Furthermore, in addition to acetate, CO_2 and H_2, formate is one of the major fermentative end products of strain VS-732. Strains VS-751 and VS-511 on the other hand have similar optimal requirement for NaCl (around 12% [wt/vol]) and grow fairly well at NaCl concentrations ranging between 9-18% (wt/vol) [a relatively narrow salt tolerance in comparision with strain VS-732 and strain VS-752 which can grow between 6-25% (wt/vol)]. Strains VS-751 and VS-511 differ from each other in generation time, optimal temperature range for growth, and substrate utilization (Table 3.3). Ethanol is the major end product of glucose fermentation for both these strains. However, for strain VS-751, formate is an additional product of glucose fermentation. The pattern of glucose fermentation of strain VS-751 is similar to that of strain VS-732, however these two strains differ from each other in terms of generation time, optimal temperature range, and substrate utilization (Table 3.3). The glucose fermentation products of strain TTL-30 are similar to that of strain VS-752. However, strain TTL-30 differs from all the strains in terms of salt

tolerance, optimal requirement for NaCl (15% [wt/vol]) and the use of sulfite.

All fermentative haloanaerobes described so far have been of eubacterial origin. All the SEVVSU isolates are inhibited by chloramphenicol, tetracycline, and penicillin, suggesting that they are also eubacteria and not archaebacteria. The SEVVSU isolates differ significantly from the previously described haloanaerobes morphologically, physiologically, and metabolically (Tables 3.5 and 3.6). Strains VS-752 and TTL-30 appear most closely related to *H. halobius* and *H. acetoethylicus* in their mode of sugar fermentation, but differ significantly in size, generation time, optimum salt requirement, optimal temperature requirement for growth and substrate specificity. Strains VS-752 and TTL-30 appear to be more versatile in their ability to utilize a variety of compounds as energy sources. The characteristics of strains VS-732, VS-751 and VS-511 are distinctly different from other haloanaerobes.

On the basis of the fermentation balances presented in Table 3.4, the following reactions are proposed for fermentation of glucose in mineral salts medium by the SEVVSU isolates:

<u>Strain VS-732:</u>

$$1.0 \text{ Glucose} \longrightarrow 1.0 \text{ Ethanol} + 0.7 \text{ Acetate} + 0.3 \text{ Formate} + 1.7\ CO_2 + 0.5\ H_2$$

<u>Strain VS-751:</u>

$$1.0 \text{ Glucose} \longrightarrow 1.4 \text{ Ethanol} + 0.6 \text{ Acetate} + 0.3 \text{ Formate} + 1.9\ CO_2 + 0.5\ H_2$$

<u>Strain VS-752:</u>

$$1.0 \text{ Glucose} \longrightarrow 1.1 \text{ Ethanol} + 1.5 \text{ Acetate} + 1.7\ CO_2 + 0.4\ H_2$$

Strain VS-511:

1.0 Glucose ---> 1.4 Ethanol + 0.7 Acetate + 1.8 CO_2 + 0.5 H_2

Strain TTL-30:

1.0 Glucose ---> 0.4 Ethanol + 1.6 Acetate + 2.7 CO_2 + 0.3 H_2

Ethanol, acetate, CO_2/H_2 are the only products of glucose fermentation detected for strains VS-752, VS-511 and TTL-30. This pattern of product formation closely resembles that seen for *H. halobius* and *H. acetoethylicus* which ferment glucose according to the following overall reactions:

(*H. halobius*)

1.0 Glucose ---> 1.6 Ethanol + 0.6 Acetate + 1.4 CO_2 + 0.9 H_2

(*H. acetoethylicus*)

1.0 Glucose ---> 0.7 Ethanol + 0.9 Acetate + 2.7 CO_2 + 1.1 H_2

Strains VS-752, VS-511, and TTL-30 are all gram-negative, non-sporeforming eubacteria, and have same end products from glucose fermentation, similar to *Halobacteroides* sp. Based on these characteristics it is possible that strains VS-752, VS-511, TTL-30, *H. halobius*, and *H. acetoethylicus* are members of the same genus. However, strains VS-752, VS-511, and TTL-30 differ significantly from the *Halobacteroides* sp. in terms of substrate utilization as they are more versatile in their ability to utilize a variety of substrates as energy sources. Strains VS-752, VS-511, and TTL-30 also differ from these described species in their utilization of glycerol and arabinose. Strain VS-511 differs from strain VS-752, strain TTL-30, and the *Halobacteroides* sp. in its use of ethylene glycol, mannitol, and sorbose as the sole carbon

and energy source. Strain TTL-30 differs from strain VS-752, strain VS-511, and the *Halobacteroides* sp. in its inability to utilize pyruvate. Furthermore it is interesting that strains VS-752 and strain TTL-30 have the ability to utilize the aromatic compound pyrogallic acid. The differences between the *Halobacteroides* sp. and strains VS-752, VS-511, and TTL-30 may support their inclusion in a new genus.

For strains VS-732 and VS-751, formate is one of the major end products of glucose fermentation in addition to acetate, ethanol, CO_2 and H_2. In the case of strain VS-732, an additional unidentified compound was also detected as a product, which may account for 10% of the unrecovered carbon (Table 3.4). Formate has never been detected as a product of glucose fermentation for any of the previously described haloanaerobes (Table 3.5). Thus, it appears that these new isolates represent the first example of formate-producing haloanaerobe. Based on these observations and other characteristics (Tables 3.5 and 3.6) that differentiate strains VS-732 and VS-751 from the other haloanaerobes, strains VS-732 and VS-751 are also members of a new genus. Additional work is necessary to more accurately determine the taxonomic and phylogenetic status of these strains.

All the isolates from the SEVVSU are strictly anaerobic and obligately halophilic. Thus, any accidental release of these microorganisms into non-saline oxygenated environments such as surface ponds and streams, during the pilot test, would not pose a health or environmental hazard, since these organisms can not

survive under such conditions. All the isolates are capable of producing substantial amounts of gas, solvents, acids, and at times polymers and emulsifiers (V. K. Bhupathiraju, P. K. Sharma, and M. J. McInerney, unpublished observations). All of these compounds have previously been shown to enhance oil recovery. Also, when these isolates are starved for a carbon source, an approximate one order magnitude reduction in size of cells is observed. This indicates that the strains are capable of forming ultramicrobacteria (UMB). The formation of UMB has been shown to be useful in effectively plugging porous formations in laboratory models (McLeod et al., 1988; Lappin-Scott et al., 1988), mainly because of their ability to deeply penetrate smaller pores, and such organisms have been succesfully used in field trials (Sheehy, 1990). The ability of the SEVVSU isolates to utilize a fermentable carbohydrate and produce useful products that could enhance oil recovery make them suitable candidates for microbial selective plugging processes in hypersaline environments.

REFERENCES

Balch, W. E., and R. S. Wolfe. 1976. New approach to the cultivation of methanogenic bacteria: 2-mercaptoethanesulfonic acid (HS-CoM)-dependent growth of *Methanobacterium ruminatium* in a pressurized atmosphere. Appl. Environ. Microbiol. 32:781-791.

Belyaev, S. S. I. A. Charackhchian, I. A. Borzenkov, E. I. Milyokhina, and V. G. Kuzetsuva. 1990. The activities of microbiological processes in stratal waters of oil fields, p. 425-443. In C. B. Fliermans and T. C. Hazen (ed.), Proceedings of the First International Symposium on Microbiology of the Deep Subsurface, WSRC Information Services, Aiken, SC.

Bhupathiraju, V. K., P. S. Sharma, M. J. McInerney, R. M. Knapp, K. Fowler, and W. Jenkins. 1991. Isolation and characterization of novel halophilic anaerobic bacteria from oil field brines, pp. 131-144. In E. C. Donaldson (ed.), Microbial enhancement of oil recovery-recent advances. Elsevier Press, Amsterdam.

Elazarie-Volcani, B. 1943. Bacteria in the bottom sediments of the dead sea. Nature (London) 152:274-275.

Gevertz. D., J. R. Paterek, M. E. Davey and W. A. Wood. 1991. Isolation and characterization of anaerobic halophilic bacteria from oil reservoir brines, p. 115-129. In E. C. Donaldson (ed.), Microbial enhancement of oil recovery-recent advances. Elsevier Science Publishing Co., New York.

Grula, E. A., H. H. Russel, and M. M. Grula. 1985. Field trails in central Oklahoma using *Clostridium* strains for microbially enhanced oil recovery, p. 144-150. In J. E. Zajic and E. C. Donaldson (ed.), Microbes and Oil Recovery, Vol. 1. Bioresources Publications, El Paso, TX.

Hirotaka. S., Y. Hiroshi, and H. Koki. 1989. Isolation of strictly anaerobic halophiles from the aerobic surface sediments of hypersaline environments in California and Nevada. FEMS Microbiology Lett. 57:191-196.

Javaheri, M., G. E. Jenneman, M. J. McInerney, and R. M. Knapp. 1985. Anaerobic production of biosurfactant by *Bacillus licheniformis* Strain JF-2. Appl. Environ. Microbiol. 50:698-700.

Jenneman, G. E., M. J. McInerney, and R. M. Knapp. 1986. Effect of nitrate on biogenic sulfide production. Appl. Environ. Microbiol. 51:1205-1211.

Knapp, R. M., M. J. McInerney, D. E. Menzie, and R. A. Raiders. 1989. Microbial field pilot study. Final report for the period ending March 31, 1988. Bartlesville Project Office, U. S. Department of

Energy, Bartlesville, OK.

Kushner, D. L. J. 1978. Life in high salt and solute concentrations: Halophilic Bacteria, p. 317-368. In D. J. Kushner (ed.), Microbial Life in Extreme Environments, Academic Press, London.

Lappin-Scott, H. M., F. Cusak, and J. W. Costerton. 1988. Nutrient resuscitation and growth of starved cells in sandstone cores: a novel approach to enhanced oil recovery. Appl. Environ. Microbiol. 54:1373-1382.

McLeod, F. A., H. M. Lappin-Scoot, and J. W. Costerton. 1988. Plugging of a model rock system by using starved bacteria. Appl. Environ. Microbiol. 54:1365-1372.

McInerney, M. J., and D. W. S. Westlake. 1990. Microbially enhanced oil recovery, p. 409-445. In H. L. Ehrilch and C. L. Brierley (ed.), Microbial mineral recovery. McGraw-Hill Publishing Co., New York.

Oren, A. 1983. *Clostridium lortetti* sp. nov. a halophilic obligately anaerobic bacterium producing endospores with attached gas vacoules. Arch. Microbiol. 136:42-48.

Oren, A., W. G. Weisberg, M. Kessel, and C. R. Woese. 1984. *Halobacteroides halobius* gen. nov., sp. nov., a moderately halophilic obligately anaerobic bacterium from the bottom sediments of the dead sea. System. Appl. Microbiol. 5:58-70.

Oren, A., B. J. Paster, and C. R. Woese. 1984. *Haloanaerobiaceae*: a new family of moderately halophilic, obligately anaerobic bacteria. System. Appl. Microbiol. 5:71-80

Oren, A., H. Pohla, and E. Stackebrandt. 1987. Transfer of *Clostridiun lortetii* to a new genus *Sporohalobacter lortetii* comb. nov., and description of *Sporohalobacter marismortui*. System. Appl. Microbiol. 9:239-246.

Oren, A. 1988. Anaerobic degradation of organic compounds at high salt concentrations. Antonie van Leeuwenhoek 54:267-277.

Pfiffner, S. M., M. J. McInerney, G. E. Jenneman, and R. M. Knapp. 1986. Isolation of halotolerant, thermotolerent, facultative polymer-producing bacteria and the characterization of the exopolymer. Appl. Environ. Microbiol. 51:1224-1229.

Raiders, R. A., R. M. Knapp, and M. J. McInerney. 1989. Microbial selective plugging and enhanced oil recovery. J. Ind. Microbiol. 4:215-230.

Rengpipat, S., T. A. Langworthy, and G. J. Zeikus. 1988. *Halobacteroides acetoethylicus* sp. nov., a new obligately anaerobic

halophile isolated from deep subsurface hypersaline environments. System. Appl. Microbiol. 11:28-35.

Rodrigues-Valera, F. 1988. Halophilic bacteria, Vol.1, CRC press, BocaRaton, Florida.

Sheehy, A. J. 1990. Field studies on microbial EOR. Paper SPE/DOE 20254. Presented at the SPE/DOE Seventh Symposium on Enhanced Oil Recovery, Tulsa, Okla. Society of Petroleum Engineers, Dallas, TX.

Smith, R. J., and A. G. Collins. 1985. Microbial enhanced oil recovery: A review, p.1-18. In J. E. Zajic and E. C. Donaldson (ed.), Microbes and Oil Recovery, Vol.1. Bioresources Publications, El Paso, TX.

Udegbunam, E. O., R. M. Knapp, M. J. McInerney, and R. S. Tanner. 1991. Potential of microbially enhanced oil recovery (MEOR) in petroleum reservoirs of the Mid-Continent region. Bull. Okla. Geol. Sur. in press.

Zeikus, J. G., T. E. Thompson, T. J. Phelps, and T. A. Langworthy. 1983. Isolation and description of *Haloanaerobium prevalens* gen. nov., sp. nov., an obligately anaerobic halophile common to Great Salt Lake sediments. Curr. Microbiol. 9:225-234.

4. BACTERIAL TRANSPORT AND ACTIVITY IN UNCONSOLIDATED POROUS MATERIALS

4.1 Introduction

Self-propulsion by bacteria has been proposed as an important mechanism for bacterial penetration in subterranean formations, especially in aquifers with slow flow rates (McInerney, 1991). Without applied advective force, the penetration rate of a bacterium to be used in enhanced oil recovery, *Bacillus* strain BCI-INC, through sandstone cores with permeabilities greater than 0.1 μm^2 was close to the velocities of most waterfloods (0.6 to 1.3 cm/h) (Jenneman et al., 1985). In unconsolidated porous materials, rates of penetration by some motile strains of *Escherichia coli* up to 0.1 m/d were observed under static conditions (Reynolds et al., 1989). Thus, it is clear that some bacteria can penetrate either consolidated or unconsolidated porous medium without fluid flow and suggests that self-propulsion may be an important mechanism for the propagation of bacteria in aquifers or portions of aquifers where groundwater velocities are low. Little information is available on the mechanisms of self-propulsion of bacteria through porous media in the absence of fluid flow. To understand how to manipulate the growth of bacteria in subsurface, it is important to understand the mechanisms that control bacterial transport. While there are many physiochemical and biological factors important for microbial penetration (Harvey, 1991; Jenneman et al., 1985; Reynolds et al., 1989; McInerney, 1991), our work focuses on biological factors that

affect transport.

Mechanisms by which bacteria penetrate porous material under static conditions are growth, motility, chemotaxis, or a combination of these modes of locomotion. The importance of growth is implicated since the movement of coliform bacteria follows the movement of nutrients from leaking septic tanks and sewer lines (Hagedorn, 1981), suggesting that conditions favorable for bacterial growth are also the conditions that favor greater bacterial penetration. Without any hydrostatic head or a differential pressure, bacteria have been shown to penetrate through consolidated and unconsolidated porous media under conditions which favor growth (Chang and Yen, 1984; 1985; Jenneman et al., 1985; Montgomery et al., 1990). Reynolds et al. (1989) showed that strains with faster growth rates had the fastest penetration rates in nutrient-saturated, sand-packed cores. The penetration rates of *E. coli* strains RP1616 and RP5232 were shown to decrease when the substrate concentration in sand-packed cores was increased (Reynolds et al., 1989). This suggests that the rates of substrate utilization, and consequently, the growth rates of individual bacterial species, may determine penetration rates under nutrient-saturated conditions.

In addition to growth, motility also seems to be important, since a motile bacterium, *Enterobacter aerogenes*, penetrated through nutrient-saturated Berea sandstone 3 to 8 times faster than a nonmotile bacterium, *Klebseilla pneumonia* (Jenneman et al., 1985). In sand-packed cores, several motile strains of *E. coli* had

on average 4 times faster penetration rates than nonmotile mutants (Reynolds et al., 1989). The mechanisms by which nonmotile organisms penetrate porous media are not well understood. An equation which included factors such as pore volume and cell volume successfully predicted the penetration rates of non-motile cells (Reynolds et al., 1989). This indicates that the nonmotile cells may penetrate the core by growing throughout the available pore volume or pore space.

The fact that the penetration of a mutant which is capable of chemotaxis toward but not the metabolism of galactose was the same whether or not a galactose gradient was present in the core suggested that chemotaxis may not be required for bacterial penetration through unconsolidated porous media (Reynolds et al., 1989). Interestingly, nonchemotactic strains (RP5232 and RP1616) had faster penetration rates in sand-packed cores than did the parental chemotactic strain RP437 (Reynolds et al., 1989). The reason for this may be related to the mode of growth in porous materials, as the loss of chemotaxis may increase apparent dispersion of the nonchemotactic cells being transported.

In the present study, mechanisms and modes of transport of *E. coli* strains were studied in anaerobic, nutrient-saturated, Ottawa sand-packed cores under static conditions. Growth and metabolism of strain RW262 was monitored inside cores, and the role of these two factors in bacterial transport was investigated. A paired comparison between the movement of a nonchemotactic strain RP5232 and its parental chemotactic strain RP437 showed that

nonchemotactic cells move through the core in a diffuse manner. Also, mode of transport of nonmotile cells in sand-packed cores was determined.

4.2 Materials and Methods

4.2.1 Bacterial strains and growth conditions. The characteristics of the four *Escherichia coli* strains used are listed in Table 4.1. Strain RW262 was grown anaerobically in galactose-nitrate medium (GNM) containing (per 100 ml): 0.45 g of D-galactose, 0.3 g of $NaNO_3$, 1.12 g of K_2HPO_4, 0.48 g of KH_2PO_4, 2 ml of Tanner's mineral solution, and 1 ml of Tanner's trace metal solution (Tanner, 1989). *E.coli* strains RP437, RP5232, and RP2912 were grown anaerobically in motility growth medium (MGM) which contained (per 100 ml): 0.45 g of galactose, 0.5 g of peptone, 0.5 g of NaCl, 1.12 g of K_2HPO_4, 0.48 g of KH_2PO_4, 0.2 g of $(NH_4)_2SO_4$, 0.025 g of $MgSO_4.7H_2O$, 0.025 g of L-methionine, and 0.00005 g of $Fe_2(SO_4)_3.H_2O$. The pH of both MGM and GNM was 7.0. Cultures were incubated at 35°C under static conditions. All the strains, except strain RW262, were maintained on slants of MGM with 2% (wt/vol) agar. Strain RW262 was maintained on agar slants of GNM. Cultures were transferred to fresh slants every 15 days. The purity of the cultures was routinely checked microscopically and by gram-reaction. The motility of each strain was checked by using MIO broth (Difco Laboratories) and by microscopic examination.

4.2.2 Anaerobic preparation of growth media. Anaerobic procedures used for cultivation, and media preparation have been

TABLE 4.1 Characteristics of the *E. coli* strains used

Strain[a]	Phenotype	Specific growth rate[b] (h^{-1})
RW262	Wild-type, motile	0.69 ± 0.00
RP437	Wild-type, motile	0.27 ± 0.02
RP5232	Chemotactic mutant, motile	0.50 ± 0.03
RP2912	Nonmotile	0.37 ± 0.03

[a]Strains RP437, RP5232, and RP2912 were kindly provided by J.S. Parkinson. Strain RW262 was a gift from F. Zimain. The genotype of all strains used in the study has been described previously (Reynolds et al., 1989).
[b]Values represent means ± standard deviations of triplicate cultures.

described previously (Balch and Wolfe, 1976; Bryant, 1972). A medium or solution was adjusted to pH 7.0 and boiled under N_2 (100%), cooled to room temperature and brought into the anaerobic chamber. The medium was then transferred to anaerobic serum tubes, which were sealed with black rubber bungs and aluminum seals before autoclaving. The gas phase of all anaerobically prepared media and solutions was that of the anaerobic chamber, about 1 to 5% H_2 with the balance being N_2.

4.2.3 Core preparation. Commercially available sand (100 to 200 mesh size) was used as the porous material. The sand was suspended in concentrated HCl overnight to remove organic contaminants, rinsed with distilled water until the sand slurry had a pH of 7.0, and then dried at 125°C overnight.

Two types of core chambers were used. Glass core chambers were used to determine the rate of growth of strain RW262 inside the cores where the entire contents of the core were removed at a given time interval. Plastic core chambers were used when the core was cut into five sections in order to monitor the bacterial transport along the length of the core.

The glass core chamber (1.25 by 9.0 cm) was constructed by fusing together the top ends of two borosilicate serum tubes (Reynolds et al., 1989). The plastic core chamber (1.25 by 12 cm) was prepared by cutting off the closed end of a plastic culture tube. The internal dimensions of stoppered cores were 1.25 x 8 cm for glass cores and 1.25 by 10 cm for plastic cores.

Both types of core chambers were packed as described

previously (Reynolds et al., 1989). Glass core chambers, with the bottom end fitted with a rubber serum stopper (size 20), were placed in a vertical position in a test tube rack. The test tube rack was brought into the anaerobic chamber, placed in a sonicating water bath, and each core was filled with the respective growth medium. Each core was then filled with sand which displaced excess growth medium. The open end of each core chamber was closed with a gray butyl rubber stopper (13 by 20 mm), which had a filter plug inserted into it. The filter plug insert aided in uniform distribution of bacteria after inoculation and reduced the volume of liquid near the stopper. To prevent liquid escaping from the core during autoclaving, both ends of the glass core chamber were crimp sealed and submersed in a 2-liter glass bottle containing same medium which saturated the inside of the core. Plastic core chambers were prepared in an identical manner except that the ends of the plastic core were stoppered by 13 mm (1/2") vacutainer stoppers. Since plastic cores could not be crimp sealed, they were autoclaved in a test tube press.

The porosity, pore volume, and permeability of both glass and plastic cores were determined as described previously (Jenneman et al., 1985) and the data are given in Table 4.2.

4.2.4 Core experiments. The growth and metabolism of strain RW262 in sand-packed cores was compared to that observed in liquid culture. Glass cores saturated with GNM were prepared and each core was inoculated with 0.1 ml of an exponential phase culture of strain RW262. The cores were incubated at room temperature in a

TABLE 4.2 Characteristics of the porous media used

Core Type	Parameters[a]		
	Pore volume (ml)	Porosity (%)	Permeability (μm^2)
Glass core	5.00 ± 0.01	35.7 ± 0.07	7.25 ± 0.25
Plastic core	6.20 ± 0.01	38.7 ± 0.06	7.15 ± 0.35
Section number			
1	1.47 ± 0.05		
2	1.12 ± 0.00		
3	0.97 ± 0.07		
4	1.03 ± 0.01		
5	1.54 ± 0.08		

[a]Values represent means ± standard deviations of duplicate cores or core sections.

horizontal position inside the anaerobic chamber. At about 5 h intervals, duplicate cores were removed and the contents of each glass core were extracted by adding 5 ml of sterile 20 mM potassium phosphate buffer (pH 7.0) and vortexing the slurry for 30 seconds. Since the pore volume of an 8 cm long core was 5.0 ± 0.01 ml (Table 4.2), a 1:2 dilution was obtained when 5 ml of buffer was used for extraction. The liquid fraction was analyzed for concentration of viable cells, substrate, and fermentation end products. These data were compared to data obtained from anaerobic liquid cultures of strain RW262, inoculated with the same culture used to inoculate the cores and incubated at room temperature in serum bottles containing 50 ml of GNM.

The growth and metabolism of the strains at different locations in the core with time was followed using plastic cores. Since the pore volume of plastic cores was greater than the volume of glass cores (Table 4.2), each plastic core was inoculated with 0.2 ml of an exponential phase cultures. At each time interval, duplicate plastic cores were removed and analyzed. Each plastic core was marked at 2 cm intervals, which divided the core into 5 sections. Each section was separated from the others by cutting the core with a hot nichrome wire. The nichrome wire was used to minimize the chance of contamination and disturbance of the porous matrix during sectioning of the core. The pore volume of each section was determined; the two end sections had pore volumes of about 1.5 ml each while the middle three sections had pore volumes of about 1.0 ml each (Table 4.2). To the contents of each section,

2 ml portion of the buffer was added and the slurry was mixed and the liquid fraction was analyzed as discussed above. This resulted in a 1:3 dilution of the contents of the middle three sections and 1:2.33 dilution of the contents of the two end sections.

4.2.5 Extraction efficiency. The percent recovery of bacterial cells and cellular protein in the liquid fraction was measured to determine the efficiency of washing procedure in removing bacterial cells from the sand matrix.

The percent recovery of viable cells in the liquid fraction was determined by inoculating about 2 x 10^7 cells/ml for strain RW262 and 2 x 10^6 cells/ml for strain RP5232 into duplicate cores without galactose added. After 48 h of incubation, average number of viable cells recovered in the liquid fraction was about 1 x 10^7 cells/ml and 3 x 10^6 cells/ml for strain RW262 and RP5232 respectively, showing that little or no adsorption of cells occurred in the absence of growth.

The efficiency of the phosphate buffer wash in removing cellular protein from the porous matrix was determined by comparing the amount of protein present in untreated cores to that removed from washed cores. Four glass cores saturated with MGM were each inoculated with 8 x 10^7 cells/ml of strain RP2912. After 7 d of incubation, the entire contents of each core were extracted with 5 ml of phosphate buffer as described above. The sand slurry from two cores was vortexed and these cores were designated as washed cores. The liquid fraction of each washed core was centrifuged (10,000 x g, 4°C, 10 min.) and the cell pellet was suspended in 1

ml of 1N NaOH. The cells were digested by boiling the cells in alkali for 10 min. and the amount of protein was determined. For the untreated cores, the liquid obtained after extraction with buffer was centrifuged as above to concentrate the cells. The cell pellet was suspended in 1 ml of 1N NaOH and the cell suspension was added to the tube containing the sand from which the liquid had been removed. The alkali-sand slurry was vortexed for 1 min. for uniform distribution of NaOH and then boiled for 10 min. to digest the cells. The amount of protein in the slurry was determined. The average protein concentration of the washed cores was 527.0 ± 4.0 μg/ml, while that of the untreated cores was 575.0 ± 7.0 μg/ml. Thus, about 92.5 ± 0.5 % of total cell protein was recovered in the liquid fraction after washing. These data showed that cell concentration measured in the liquid fraction after extraction accurately represented the cell concentration in the porous matrix. Thus, in this study, viable cell concentrations in the liquid fraction are reported as the cell concentrations in the entire porous contents.

4.2.6 Growth measurement. Samples from sand-packed cores and liquid cultures were serially diluted in 20 mM potassium phosphate buffer (pH 7.0) aerobically and duplicate plates of plate count agar were inoculated. Colonies were counted after aerobic incubation of the plates for 24 h at 35°C.

The specific growth rate of the strains in liquid cultures was determined from the change in absorbance at 600 nm (McInerney et al., 1979).

4.2.7 Analytical Methods. The D-galactose concentration was measured enzymatically (Boehringer Mannheim GmbH, Mannheim W. Germany). The type and amount of short chain monocarboxylic fatty acids were determined by high pressure liquid chromatography (HPLC) using an ion exclusion column (Amos and McInerney, 1989). Nitrate was analyzed by anion-exchange HPLC (Smolenski and Suflita, 1987). Protein was determined by the bicinchroninic acid method (Smith et al., 1985).

4.3 Results

4.3.1 In-situ growth and metabolic activity. Interfaces of solid-matrix influence the rate of growth and metabolism of microbes (Hattori and Hattori, 1976; van Loosdrecht et al., 1990). Both growth and metabolism have been suggested as important factors that determine the penetration rates of bacterial species in porous media under nutrient-saturated conditions (McInerney, 1991; Reynolds et al., 1989). Thus, in order to understand the bacterial transport through porous media, it was important to measure directly the in-situ bacterial growth and metabolism inside cores used in this study.

The effect of the porous solid matrix on the growth rate of strain RW262 was determined by a parallel comparison of the rate of growth in liquid cultures to that observed in porous media. In order to determine the effect of porous media on the metabolism of strain RW262, a comparison of the fermentation end products in liquid cultures and porous media was performed. A change in the

nature of fermentation end-product inside porous media would indicate a shift in the metabolism of galactose by strain RW262.

Figure 4.1A shows that the doubling time of strain RW262 in GNM broth was approximately 1 h [specific growth rate (μ) of 0.69 per h]. However, under similar experimental conditions, the cell population of strain RW262 inside of the cores increased exponentially, but with a doubling time of 2 h (μ of 0.35 per h). This showed that the rate of growth of strain RW262 was slower in porous media than in liquid cultures. Acetate was the only fermentation end product detected either in liquid cultures or in porous media with about 1.7 mmol of acetate produced per mmol of galactose used, and about 0.6 mmol of acetate produced per mmol of nitrate used. Thus the metabolism of galactose by strain RW262 was not affected by solid-matrix interfaces. In liquid cultures, after 5 h of incubation at the room temperature, 1.6 mM acetate was detected and acetate concentration increased progressively up to 3.2 mM at 12.5 h of incubation (data not shown). In contrast, detectable acetate was observed only after 35 h of incubation of strain RW262 inside the cores (Fig. 4.1B). An appreciable decrease in galactose and nitrate concentrations, concomitant with acetate accumulation was detected only after 35 h of incubation of cores. This shows that the lag-period before active metabolism by strain RW262 was detected was much longer inside cores than in liquid cultures.

4.3.2 Transport of motile cells. The fact that strain RW262 penetrated through 8-cm-long glass cores within 20 h at a rate of

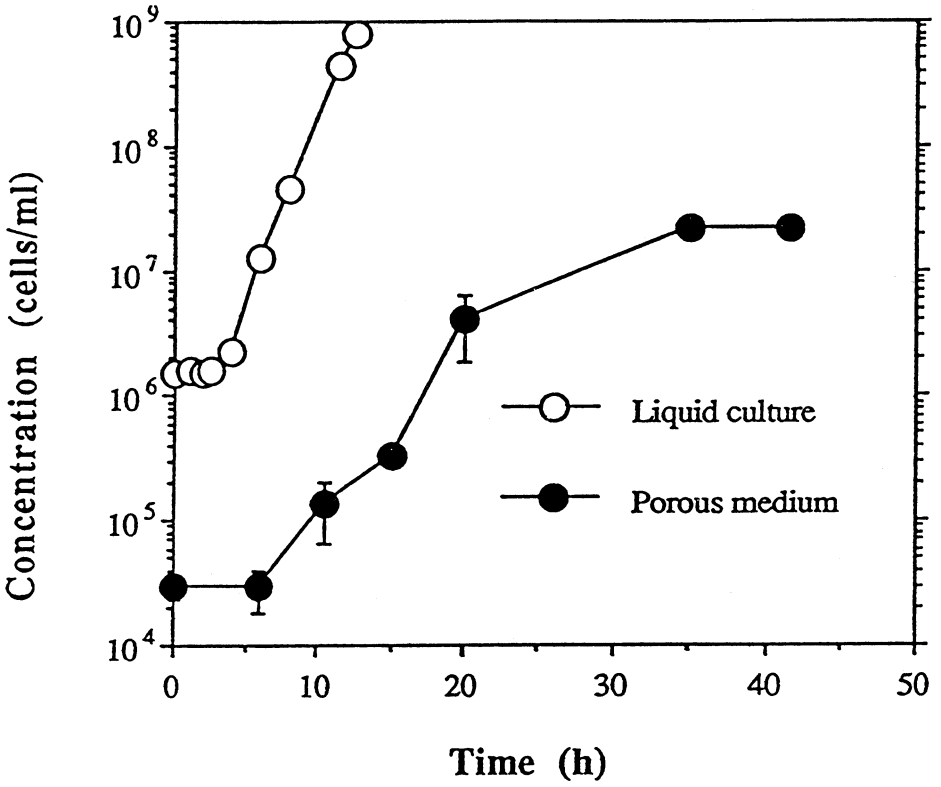

FIGURE 4.1A Growth of *E. coli* RW262 in GNM-saturated, sand-packed cores and liquid cultures. The cell detection limit in cores was 300 cells/ml. Source of inoculum and experimental conditions were identical for both cores and liquid cultures.

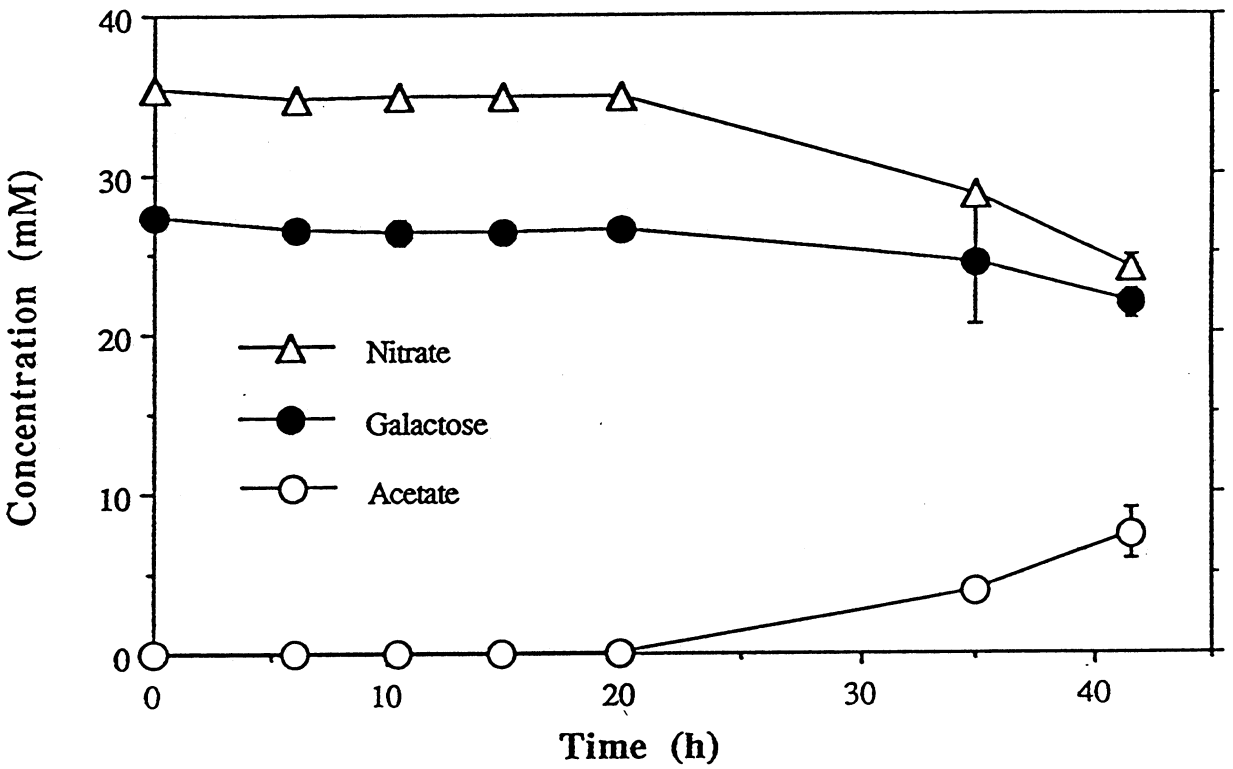

FIGURE 4.1B Metabolism of strain RW262 with time in nutrient-saturated, sand-packed cores. Concentration of galactose, nitrate, and acetate was determined from the contents of cores used in Figure 4.1A.

0.4 cm/h before detectable acetate production or galactose consumption occurred inside of the cores (Fig. 4.1B) indicated that the transport of bacterial cells in cores may not have been dependent on the generation of a substrate or product gradient. This does not support the hypothesis of Reynolds et al. (1989) that, under conditions in which growth is restricted, cell penetration is a result of the consumption of practically all the locally available substrate. In order to determine whether all of the locally available substrate was consumed during penetration, the concentration of viable cells, substrate, and fermentation end-products in different sections of 10-cm-long plastic core with time was determined.

About 2 x 10^7 cells/ml were inoculated in GNM-saturated cores, and immediately after inoculation, all the cells were localized only in the front section of the core (Fig. 4.2A). After six hours of incubation, viable cells were observed in the front two sections of the cores and with continued incubation, the presence of viable cells was sequentially detected in the remaining sections. The appearance of viable cells in a section was followed by an increase in cell concentration, indicating that bacterial growth occurred in that section. As the cells penetrated through the core, high cell concentrations ($\geq 10^5$cells/ml) were detected in each new section, suggesting that the front of the moving cells was not dispersed, and that strain RW262 grew and moved through the core in a band-like fashion.

Strain RW262 penetrated through 10-cm-long core within 25 h at

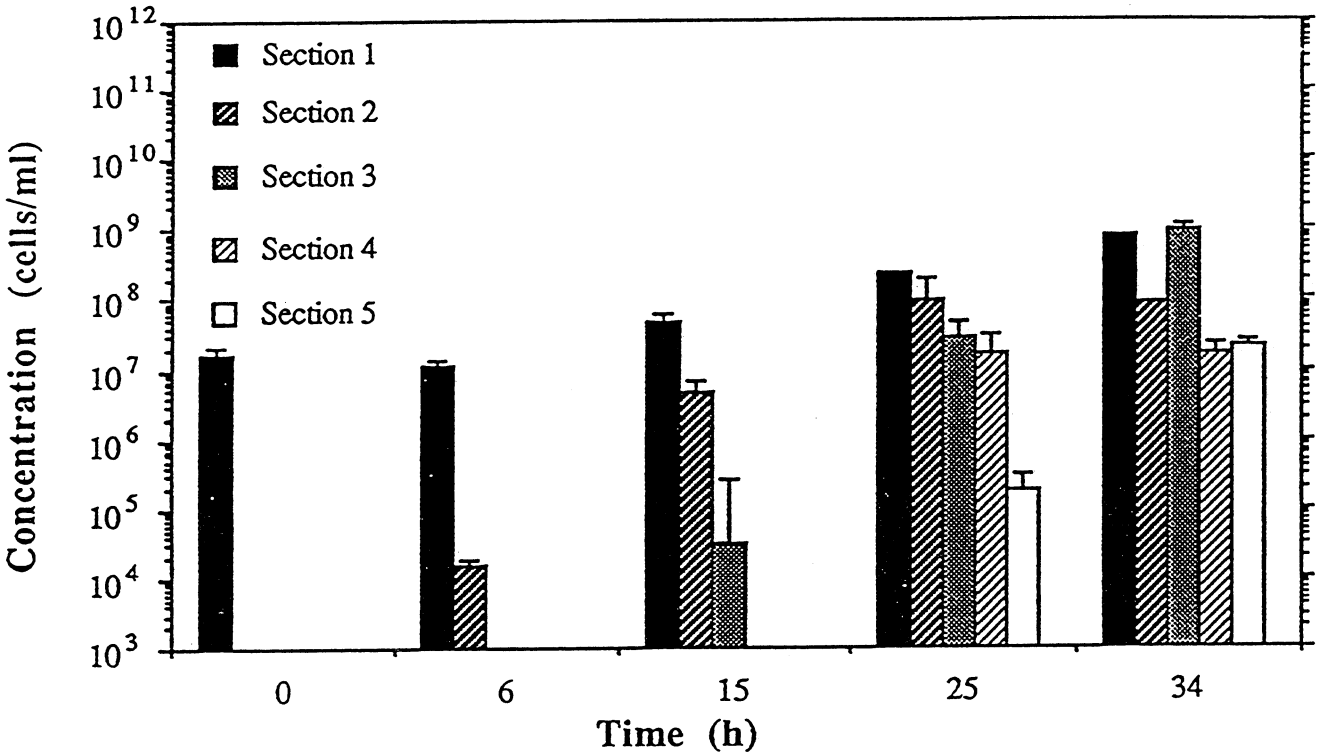

FIGURE 4.2A Growth of strain RW262 in different sections of GNM-saturated, 10-cm-long plastic cores with time. At the indicated times, duplicate cores were cut into five 2.0-cm-long sections and contents of each section were analyzed. The cell detection limit in cores was 300 cells/ml.

a rate of 0.4 cm/h. At 25 h of incubation, in the front section of the core only about 22% of the available galactose was metabolized, with the production of 14 mM of acetate (about 2 acetate/galactose) (Fig. 4.2B). Active metabolism, as evidenced by acetate production, was sequentially observed in 3rd, 4th and 5th section of the core only after 34 h of incubation, 9 h after the breakthrough time of cells (Fig. 4.2C). These data showed that cell propagation preceded an appreciable depletion of the galactose or the accumulation of large amounts of acetate.

In order to preclude any ambiguity about whether a galactose gradient was produced during cell penetration, the experiment was repeated using a lower galactose concentration (3.5 mM) which should be rapidly metabolized in the front few sections during cell penetration. After 11.5 h of incubation, strain RW262 had penetrated into the fourth section of the core (Fig. 4.3). However, only about 39% of available galactose was consumed in the first section of the core and little or no detectable change in galactose concentration was observed in the other sections of the core. This showed that the propagation of cells preceded any appreciable utilization of the substrate and was consistent with the data presented in Figures 4.1 and 4.2.

In our previous study (Reynolds et al., 1989), the presence or absence of galactose did not affect the penetration rate of strain RW262 through MGM-saturated sand-packed cores. However, it was of interest to determine whether the absence of galactose affected the mode of transport. About 2.2 x 10^7 cells/ml of strain RW262 were

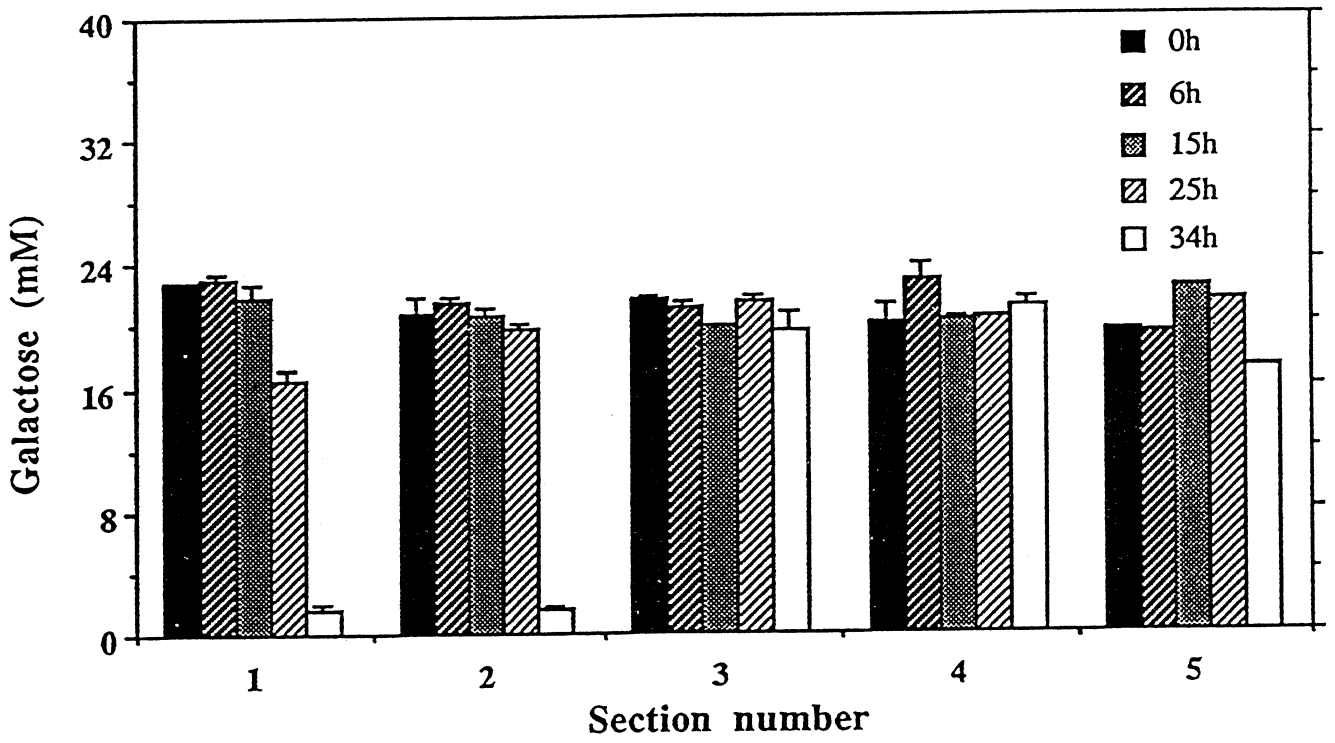

FIGURE 4.2B Galactose consumption by strain RW262 in different sections of GNM-saturated, 10-cm-long plastic cores with time. Galactose was determined in the contents of cores used in Furgure 4.2A.

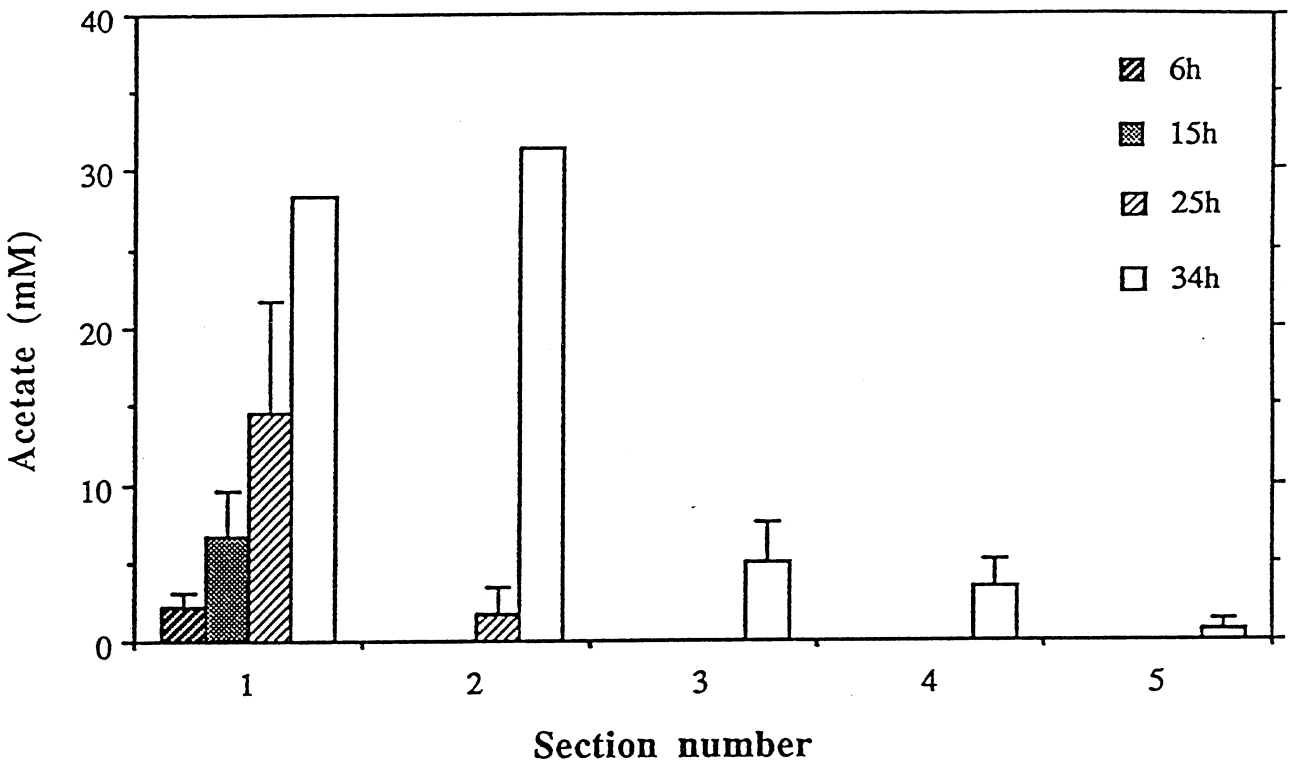

FIGURE 4.2C Acetate production by strain RW262 in different sections of GNM-saturated, 10-cm-long plastic cores with time. Acetate was determined in the contents of cores used in Figure 4.2A. Acetate was below detection limits in any section immediately after inoculation.

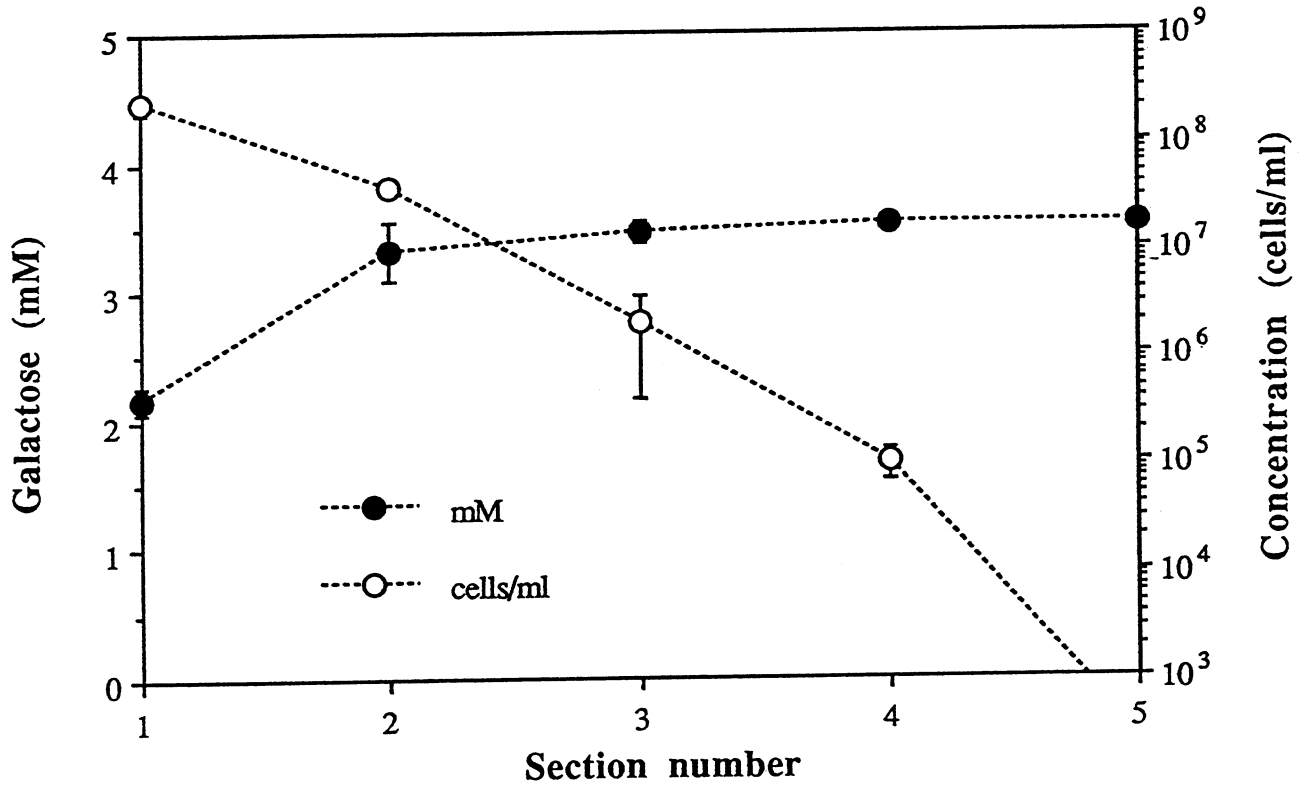

FIGURE 4.3 Cell concentration and galactose consumption by strain RW262 in different sections of plastic cores with lower galactose concentration at 11.5 h of incubation. Experimental conditions were identical to that in Figure 4.2, except that initial galactose concentration was 3.5 mM. Bacterial cells penetrated through the core within 24 ± 0 h.

inoculated into 10-cm-long plastic cores saturated with medium without galactose added. Figure 4.4 shows that the cells had penetrated up to the 4th section of the core after 24.5 h of incubation. This penetration time was comparable to that observed in cores with galactose (Fig. 4.2), showing that the penetration rate of strain RW262 was not affected by the absence of galactose. The total number of viable cells in all the five sections was about 3×10^7 cells/ml, showing that no or little growth occurred in the absence of galactose. Interestingly, after 24.5 h of incubation, about 1×10^7 cells/ml were still present in the first section and the front of the moving cells in the 4th section contained only about 11% of the original population. Adler and Dahl (1967) showed that under conditions conducive to chemotaxis but not growth, bacterial cells migrate away from the origin and move along a capillary tube as a band containing a high fraction of the original population. The fact that only about 11% of the initial population was present in the fourth section after 24.5 h suggested that strain RW262 did not penetrate the core as a band and under non-growth conditions, bacterial transport occurred by a process resembling diffusion.

4.3.3 Importance of chemotaxis. In our previous work (Reynolds et al., 1989), motile chemotactic mutants (*E. coli* strains RP5232 and RP1616) had faster penetration rates than that of the chemotactic parental strain (RP437). The reason for this may be related to the mode of growth through unconsolidated materials. The chemotactic strain which can sense a nutrient-rich

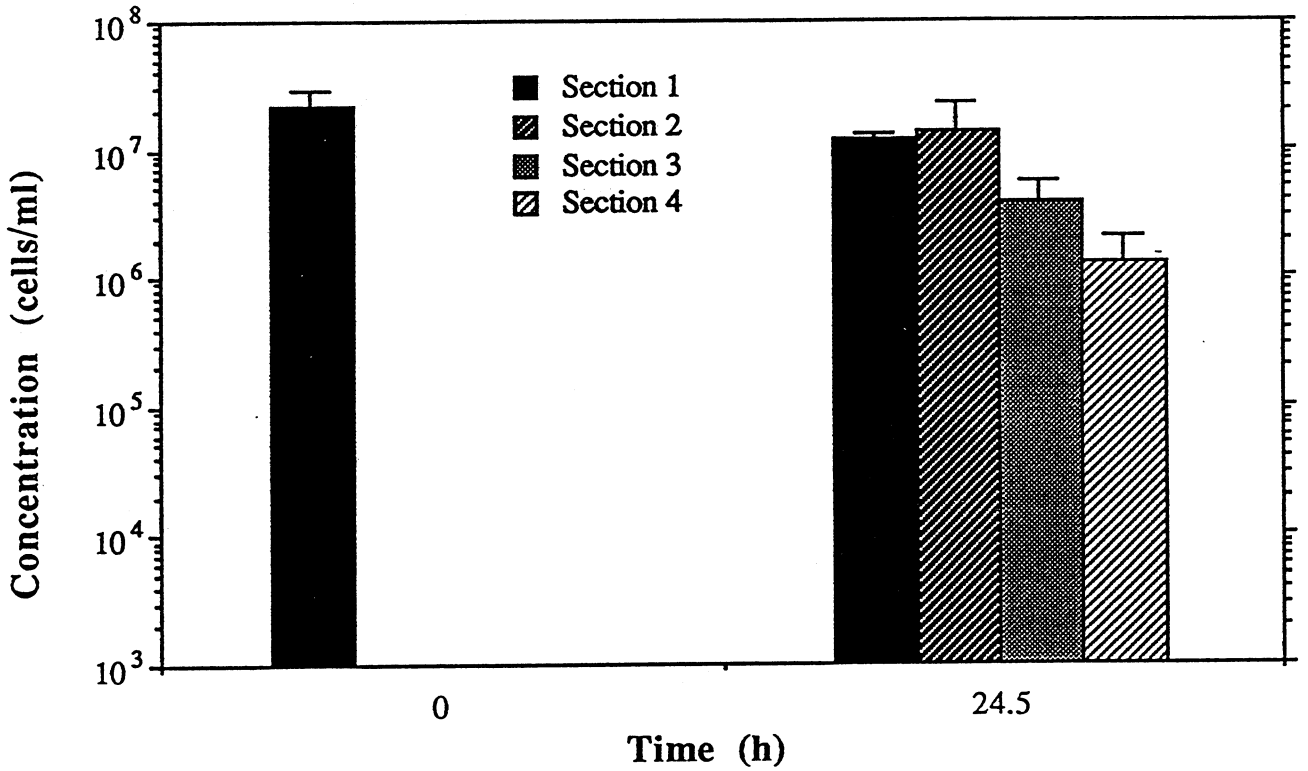

FIGURE 4.4 Transport of strain RW262 through 10-cm-long plastic cores without galactose added.

environment in all three directions may be able to grow throughout the available pore space and thus take a longer time to penetrate through the core. Non-chemotactic strains, which cannot sense a nutrient gradient, move through the core in a diffuse manner and the route taken by the fastest cells may have been less tortuous than that of the chemotactic strains. In order to determine the mode of growth and transport, a paired comparison between the motile, non-chemotactic strain RP5232 and its parental chemotactic strain RP437 was conducted. The change in cell concentration was determined for each strain, along the length of MGM-saturated plastic cores with time. As shown in Figure 4.5A, the chemotactic strain RP437 progressively grew and moved through the core with a large number of cells ($\geq 10^6$ cells/ml) accumulating in each section of the core before cells were detected in the next section. This suggested that chemotactic cells moved through the core in an ordered fashion resembling a band of cells. In contrast, the mode of transport of the motile, non-chemotactic strain RP5232 was different (Fig. 4.5B). A small cell concentration ($\geq 10^3$cells/ml) appeared in new sections at various incubation time intervals (5 h, 11.5 h, 19.5 h, and 24.5 h), indicating that front of the moving cells was more dispersed than that observed with RP437. After 11.5 h of incubation, strain RP5232 migrated into the 3rd section of the core. With continued incubation, at 19.5 h, no increase in cell number was observed in 3rd section, although about 10^3 cells/ml was detected in the 4th section. This is in contrast to the pattern of penetration observed for the chemotactic strains RP437 (Fig. 4.5A)

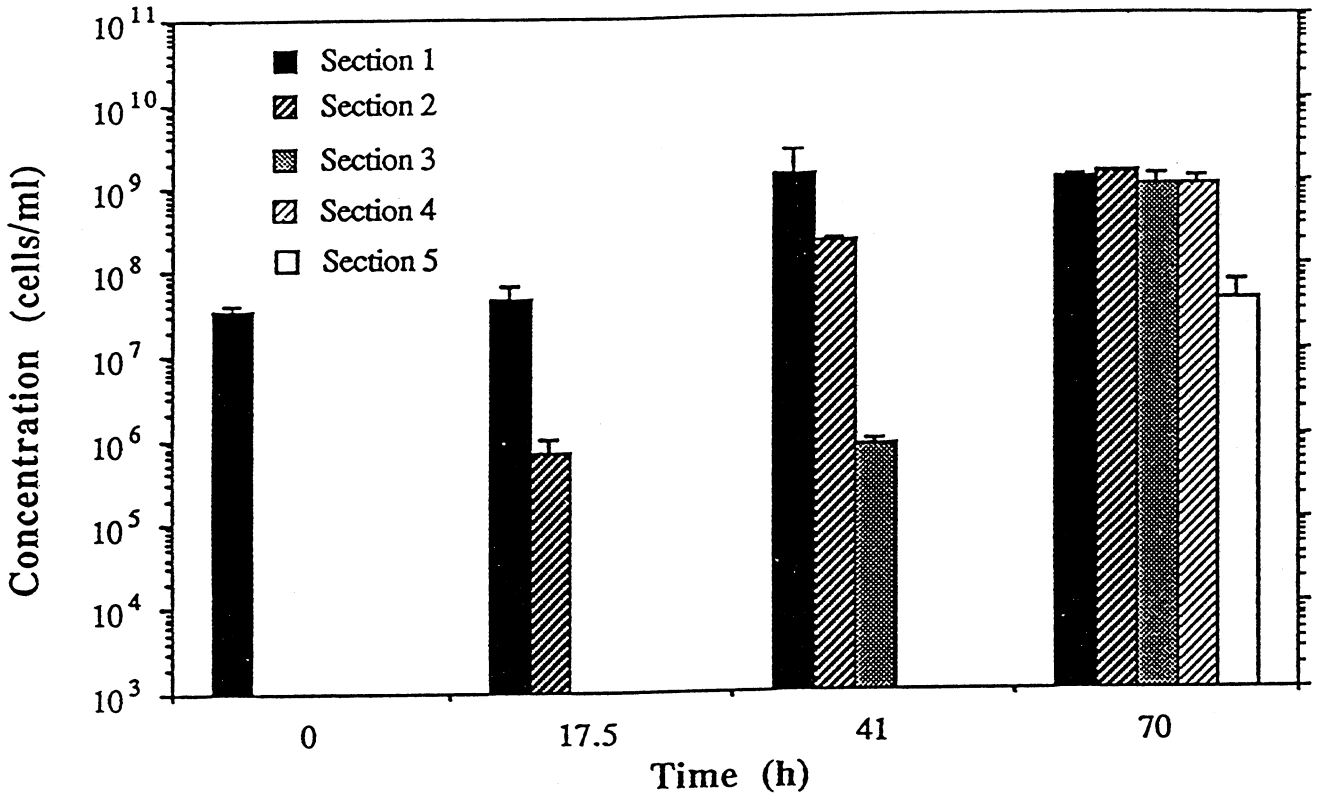

FIGURE 4.5A Growth and transport of the chemotactic strain RP437 through MGM-saturated, 10-cm-long plastic cores.

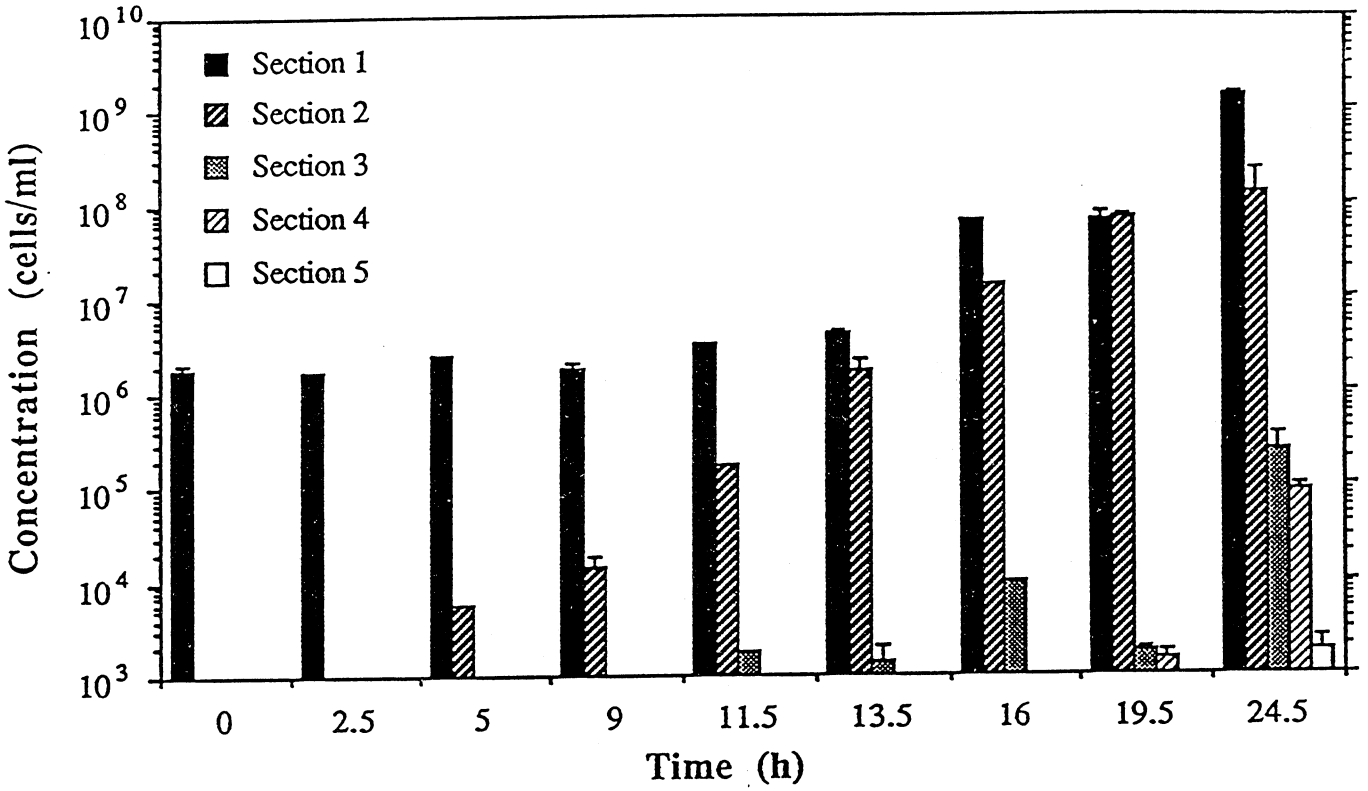

FIGURE 4.5B Growth and transport of the non-chemotactic strain RP5232 through MGM-saturated, 10-cm-long plastic cores.

and RW262 (Fig. 4.2), where presence of viable cells in a section was followed by an increase in cell number in that section. These data showed that strain RP5232 did not move through the core in an ordered fashion and bacterial transport occurred in a more diffuse manner than that observed with the chemotactic strains.

4.3.4 Transport of non-motile cells. One possible mode of penetration of non-motile bacteria in porous media would be to perceive growth occurring in a filamentous fashion (Jenneman et al., 1985). Thus, penetration rate would be a function of the length of the cell and the core. However, the actual penetration rates for non-motile cells were shown to be much slower than that predicted by this relationship and it was proposed that the actual path taken by the non-motile cells is more tortuous than a straight line (Jenneman et al., 1985; Reynolds et al., 1989). In order to determine whether non-motile cells penetrate the core by growing throughout the available pore space, the cell concentration of strain RP2912 was determined along the length of MGM-saturated plastic cores with time (Fig. 4.6). After 24 h of incubation, high cell concentrations ($\geq 10^8$ cells/ml) were observed in the front two sections and cells had migrated into the 3rd section of the core. With continued incubation (37 h), the cell concentration increased from 4×10^4 cells/ml to 8×10^6 cells/ml in the third section and no viable cells were detected in the rest of the sections. Interestingly, about 10^5 cells/ml moved into the 4th section at 48.5 h, but only after a further increase in the cell concentration in the 3rd section. Similarly, the appearance of viable cells in the

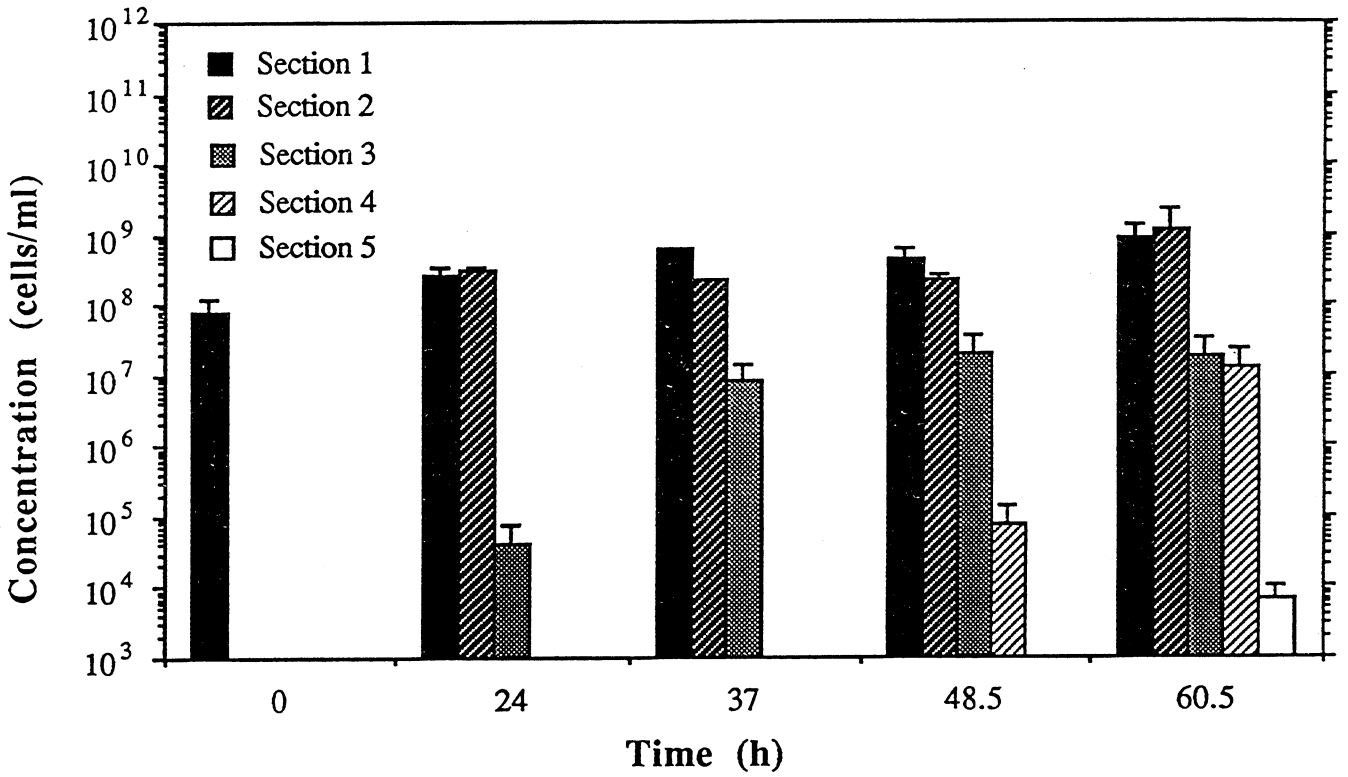

FIGURE 4.6 Growth and transport of the non-motile strain RP2912 through MGM-saturated, 10-cm-long cores.

5th section occurred only after an increase in cell concentration from 7 x 10^4 cells/ml to 1 x 10^7 cells/ml in the 4th section. These data show that non-motile cells grew and moved through the core in an ordered rather than a diffuse fashion.

4.3.5 Mechanisms of transport. Adler and Dahl (1967) showed that movement of non-chemotactic bacteria through capillary tubes could be described by an equation for diffusion of a thin layer of cells in a column of liquid, for which the plot of time versus the square of the distance that fastest cells have moved from origin (L^2) gives a straight line with a y intercept of 0. Our assay is similar to the frontier assay used by Adler and Dahl (1967), in which penetration time is a function of the time for the fastest cell to penetrate a known length the core.

The penetration time for each strain was plotted against the square of the distance (length) of the core traveled by the fastest moving cells. Figure 4.7A shows a comparison between the nonchemotactic strain RP5232 and its parental chemotactic strain RP437. The linear relationship obtained for strain RP5232 indicated that nonchemotactic cells moved through the core by a random process resembling diffusion. In contrast, a curvilinear relationship between penetration time and the square of the core length (cm) was obtained for strain RP437 (Fig. 4.7A) indicative of a nonrandom process resembling chemotaxis. A curvilinear relationship was also obtained for wild type chemotactic strain RW262 (Fig. 4.7B). Although the curvilinear relationship appeared to be the best fit for the penetration of nonmotile cells (RP2912)

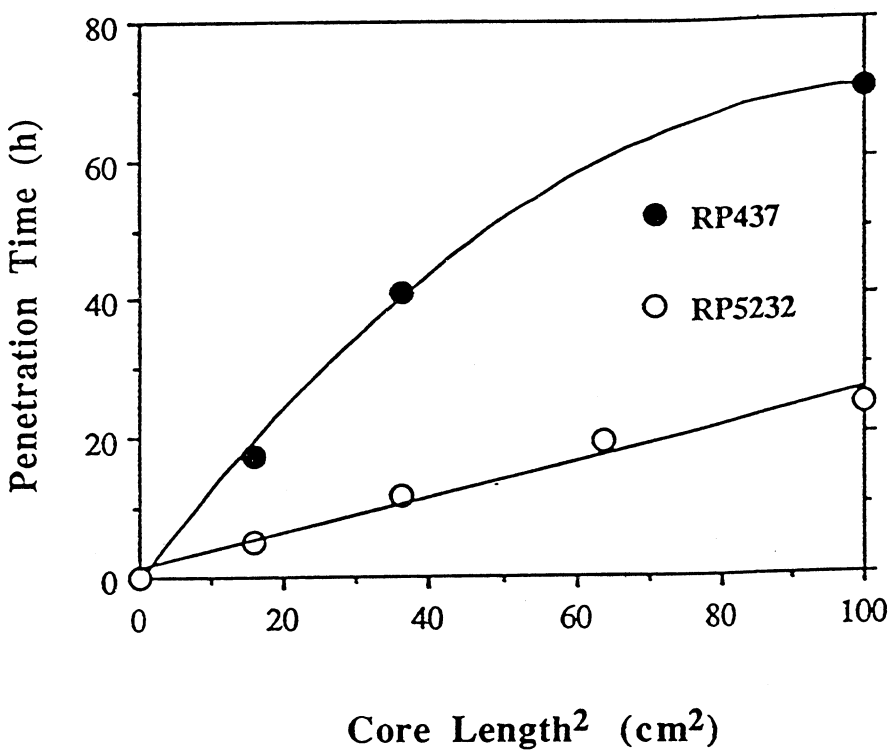

FIGURE 4.7A Mechanisms of penetration through sand-packed cores by chemotactc and nonchemotactic strains of *E. coli*. The data of Figures 4.2, 4.5, and 4.6 were used to obtain a relationship between the penetration time (h) and square of distance travelled from origin (cm^2). Data for chemotactic strain RP437 were fit to a linear equation (r^2 = 0.972) and for nonchemotactic strain RP5232 to a second order polynomial curve (r^2 = 0.998). The first appearance of viable cells in a section was used as a criteria to determine the length of the core travelled by each strain (Fig. 4.2, 4.5, and 4.6). At 0 h incubation, a value of 0 was presumed for core length (cm^2) and penetration time.

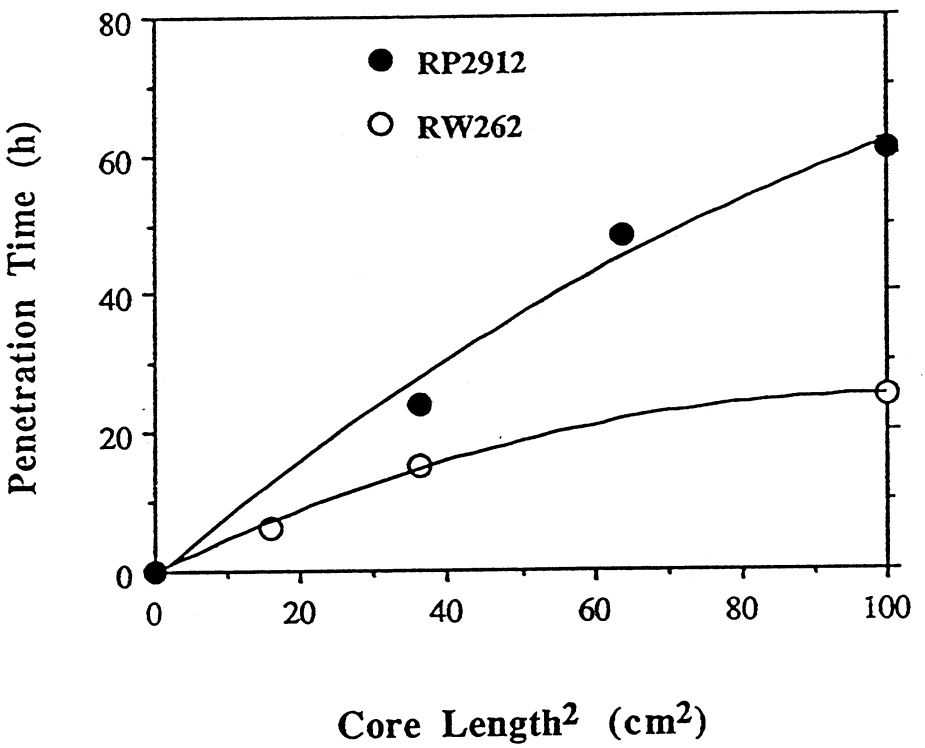

FIGURE 4.7B Mechanisms of penetration through sand-packed cores by motile and nonmotile strains of *E. coli*. Data for chemotactic strain RW262 and nonmotile strain RP2912 were fit to a second order polynomial curve (r^2 of 0.996 and 0.988, respectively). See legend of Figure 4.7A for further details.

(Fig. 4.7B), a linear relationship can not be ruled out since an r^2 of 0.971 was obtained using a linear fit to the penetration data for strain RP2912. However, the mode of movement of strain RP2912 (Fig. 4.6) clearly showed that non-motile cells moved through sand-packed cores in band-like fashion.

4.4 Discussion

In order to develop accurate conceptual and mathematical models to predict bacterial movement in the subsurface, a clear understanding of how bacteria progagate through porous media, and how biological and physiochemical factors affect bacterial propagation, is required. Mathematical approaches (Chang et al., 1991; Corapcioglu and Hardas, 1984; 1985; Knapp et al., 1988; Sarkar et al., 1991; Molz et al., 1986) for modeling growth and transport through porous materials assume that exponential growth occurs. However, since the pore structure of subsurface material could limit the availability of nutrients which would influence bacterial growth rates, it was important to verify whether exponential growth does occur in porous materials. Exponential growth of *E. coli* (RW262) did occur within porous material. However, the rate of growth was half as fast as that observed in liquid cultures, and the apparent lag time before the growth of RW262 was detected also increased inside of the cores. Under identical experimental conditions, the lag time for growth to be detected within cores for another *E. coli* strain (RP405) was six times longer than that observed in liquid culture (Sharma and

McInerney, 1992). Our results show that the metabolism of galactose by *E. coli* strain RW262 was not altered inside of the cores, since acetate was the only non-gaseous end product detected in either the cores or liquid cultures. Under similar experimental conditions, acetate and ethanol were the only end products of glucose fermentation by an anaerobic, halophilic strain TTL-30, detected either in the sand-, limestone-, or sandstone-packed cores or liquid cultures (Sharma and McInerney, 1992). However, the presence of a porous material did affect the apparent lag-time before the metabolism of galactose was observed. Although a 100-fold increase in cell concentration (from about 10^4 to about 10^6 cells/ml) of strain RW262 within 20 h of incubation inside of the cores was observed, indicating that some metabolism must have occurred, the production of acetate was not observed until 35 h after inoculation. This is 7 times longer than the time observed in liquid cultures.

The effect of porous material on bacterial growth may be related to the pore-size. Zvyagintsev and Pitryuk (1973) showed that the microbial growth rate decreased and the lag time increased when small capillary tubes with decreasing rectangular cross-section were used, suggesting that small pore spaces restrict microbial growth. The cell yield of strain RW262 grown in nutrient-saturated cores packed with glass beads of different size ranges decreased with decreasing bead size and pore-size (Sharma and McInerney, 1992), suggesting that smaller pores sizes restrict bacterial growth. Another possibility is that the presence of a

solid surface affects bacterial growth and metabolism. Conflicting evidence exists as to what effects surfaces have on bacterial metabolism and whether bacterial metabolism is even affected by surfaces (van Loosdrecht et al., 1990). Cultures of *E. coli* grown in the presence of styrene-diphenylbenzene copolymer, polytetrafluoroethylene, and pyrophyllite (consisting of silicic acid and alumina) particles had higher respiration and glucose consumption rates compared to suspended cultures without the solids (Morisaki, 1983). In another study the rate of substrate oxidation decreased when *E. coli* cultures were grown in the presence of an anion exchange resin, Dowex 1 (Hattori and Hattori, 1976). Hattori and Hattori (1976) attributed the slower bacterial activity to a reduction of the surface area of adhered cells that is exposed to the substrate and oxygen. However, van Loosedrecht et al. (1990) suggest that in these experiments, the presence of the resin resulted in slower diffusion of the substrate and oxygen to the cells, and consequently, bacterial activity was decreased. Further work is required to determine if the sizes of pores physically constrain cell division and growth, and whether the presence of a surface directly influences bacterial activity or whether the observed effects can be explained based on the mass transfer limitations of nutrients through the pores.

Several phenomenological mathematical models to predict microbial growth in porous media for the microbial enhancement of oil recovery (Chang et al., 1991; Knapp et al., 1988; Sarkar et al., 1991) or for the movement of microorganisms in groundwater

(Corapcioglu and Haridas, 1984; 1985; Molz et al., 1986) have been developed. These models consist of species conservation equations that describe the change in concentration of bacterial cells, substrates, or products within the porous medium. These models have not been verified because of the difficulty in obtaining statistically reliable data on the actual concentrations of cells, substrates, and products in porous materials which are required to test the accuracy of simulated values from the individual species conservation equations. Also, kinetic parameter estimates and actual stoichiometric equations relating substrate use, product formation, and growth in porous material are not available. The utility of our experimental system lies in the fact that a large number of cores can be prepared with little variation in the important hydrogeological factors such as porosity, permeability, and pore volume. Thus, the observed variations are the result of the treatment and not from differences in the physical system and reproducible data can be obtained on the in-situ microbial growth and metabolic activity required for model verification. Data such as that shown in Figures 4.2 and 4.3 on the change in the concentrations of cells, substrates and products in different sections of the cores can be compared with primary dependent variables for the individual species conservation equations to determine whether these models accurately simulate microbial growth in porous media.

The amount of galactose used for growth and product formation in the core can be calculated. The consumption of galactose by

RW262 inside of the cores was coupled with nitrate utilization, since galactose disappearence and acetate production occurred concominantly with the utilization of nitrate (Fig. 4.1B). An average ratio of about 1.7 mmol of acetate per mmol of galactose and about 3 mmol of nitrate per mmol of galactose was obtained. The yield of cells in the core, calculated from the final change in cell concentration of 2×10^7 cells per ml of pore fluid and amount of galactose used (2.2 mM), was 1×10^7 cells per mmol of galactose. Assuming that the average dry weight of a single cell is 2.8×10^{-13} g (Ingraham et al., 1983), the cell yield expressed in units of mass is 0.003 mg (dry wt) per mmol of galactose. From this information, an equation can be derived that describes the use of galactose for product formation and cell synthesis within the core (equation 4.1). In this equation, the average empirical formula for a bacterial cell is used (Bu'lock and Kristiansen, 1987) and it is assumed that HCO_3^- and NH_4^+ are made in amounts stoichiometrically equal to that of acetate and nitrate as would be predicted from the stoichiometry of nitrate respiration by *E. coli* (Gottshalk, 1986; Thauer et al., 1977). The carbon recovery calculated from this equation was 87%. However, the hydrogen recovery is too high (155%) indicating that not all of the nitrate was stoichiometrically reduced to ammonium.

$$1.00 \text{ galactose} + 2.95\ NO_3^- \text{ ----> } 1.70 \text{ acetate}^- + 1.70\ HCO_3^- + 2.95\ NH_4^+ + 2.48\ OH^- + 0.11 \text{ cells } (CH_{1.8}O_{0.5}N_{0.2}) \quad (4.1)$$

Our data reported herein and elsewhere (Jenneman et al., 1985; McInerney, 1991; Reynolds et al., 1989) allow us to develop conceptual models of how chemotactic and nonchemotactic motile bacteria and non-motile bacteria propogate through porous materials. For the chemotactic wild-type strains of *E. coli*, the mode of propogation resembled an ordered or band-like movement since an increase in cell concentration occurred in one section before cells were detected in the next section, and the concentration of the front of cells was always high ($>10^5$ per ml). This mode of growth through the core was also observed for both of the chemotactic, motile strains, RW262 and RP437. This suggests that the cells grew throughout the available pore-space of a unit section of the core before cells entered the next section by motility or perhaps physical displacement. However, the propagation of the isogenic, nonchemotactic strain RP5232 was different. A small concentration of cells ($<10^3$ per ml) appeared in new sections indicating that the front of moving cells was dispersed. Also, the appearance of cells in a section was not always accompanied with growth in that section before the cells moved into another section. These results suggest that strain RP5232 moved in a diffuse rather than an ordered fashion through the porous material. The analysis of penetrations times versus the square of the core length (Fig. 4.7) is consistent with the kind of movement Alder and Dahl (1967) described as diffusion for strain RP5232 and ordered or band-like for the two chemotactic strains. This difference in the mode of propagation may be the reason why

chemotactic strains had slower penetration rates than did nonchemotactic strains through porous media (Reynolds et al., 1989). Chemotactic strains grew throughout the available pore space, suggesting that they sensed chemicals in all three dimensions and had a route of transport that was for more tortuous than nonchemotactic cells. Nonchemotactic cells which are unable to sense chemicals would have a mode of movement that would be more unidirectional and thus would take less time to penetrate the core. The directional locomotive response of bacteria to certain stimuli has been suggested as an important mode of bacterial transport in aquifers with low flow rates (Harvey, 1991). Chemotactic migration toward or away from a given chemical should be proportional to the population density and to the concentration gradient of the attractant or repellant. This mode of transport could provide a mechanism whereby microorganisms can propagate throughout the entire porous matrix rather than being localized in the dominant flow channels.

One interesting finding from the analysis of the concentrations of substrates, products, and cells throughout the core was that cells completely penetrated the core before an appreciable depletion of galactose or accumulation of acetate occurred. After 25 h of incubation, cells of RW262 had completely penetrated the core, but there was little or no change in galactose or acetate concentrations within the core, except for the first section, until 34 h of incubation, about 9 hours after cell penetration (Fig. 4.2 and 4.3). These data suggest that cell

migration preceded the generation of noticeable substrate or end-product gradients. The penetration rate of RW262 in cores without galactose added (Fig. 4.4) was comparable to that observed in cores with galactose, suggesting that the migration of cells through the core was not dependent on galactose. If the movement of RW262 was not in response to galactose, then the presence or absence of galactose should not affect the mode of movement of RW262 through the core. However, RW262 appeared to move through cores without galactose added in a diffuse manner rather than in an ordered band-like fashion observed in cores with galactose added. Although these data do not rule out the possibility that the cells migrated through the core in response to a very small galactose gradient, it may be that the cells migrated in response to a chemical other than galactose present in the core. Apart from galactose, the other major chemical difference observed between cores with and without galactose added was the presence of fermentation end-products in the cores with galactose added. It could be that under growing conditions, small amounts of end-products could have acted as a repellent. The fact that the penetration rate of RW262 was not affected by the presence or absence of galactose indicates that chemotaxis may not increase the rate of penetration through porous material, suggesting that the rate of penetration may depend on motility and growth rate.

If motility is important for penetration, the question of how nonmotile organisms penetrate porous materials is an interesting one. Our data indicated that the growth and penetration of the

nonmotile strain RP2912 through cores, like that of chemotactic, motile strains, occurred in an ordered, band-like manner from the point of inoculation. These data support a theoretical model (Reynolds et al., 1989) which was developed based on the concept that, as nonmotile cells grow, they fill the locally available pore space and new cells are physically displaced into the next portion of the porous material. An equation (4.2) based on the pore volume and the average volume of a bacterial cell was developed to predict the penetration time of nonmotile cells (Reynolds et al, 1989):

$$t_p = t_d \, l_x \, [\ln(V_x/V_c)/\ln 2] \qquad (4.2)$$

where t_p is the penetration time (in hours), t_d is the doubling time (in hours), l_x is the length of the core (in centimeters), V_x and V_c are the specific liquid volume of the core (milliliters per centimeter) and the average volume of a bacterial cell (1.2 μm^3), respectively.

The accuracy of this model in predicting the penetration times of the nonmotile strain RP2912 (doubling time of 1.9 h in liquid culture) was tested using pentration times obtained under two different experimental conditions. First, penetration times of RP2912 were determined by inserting a syringe needle containing 0.2 ml of culture into a 8-cm long core (V_x of 0.62 ml) and the penetration time was calculated from the time that viable cells were detected in a syringe filled with medium inserted into the distal end of the core (Reynolds et al., 1989). For the second

condition, 0.2 ml of a culture of RP2912 (about 10^8 cells/ml) was injected inside of each 10-cm long core (V_x of 0.6 ml) and the movement of the cells was monitored along the length of the core with time (Fig. 4.6). Immediately after inoculation, all the cells were localized in the first section of the core (within the first 2 cm). For the first condition, equation 4.2 predicts a penetration time of 135 h which is about 45% longer than the observed penetration time of 93 h (Reynolds et al., 1989). Equation 4.2 was a poorer predictor of penetration times for the second experimental condition. Strain RP2912 penetrated through 10-cm long cores within about 62 h, while the predicted time from equation 4.2 (135 h) is about two times longer. In this model, the movement of cells occurs by a process resembling physical displacement where nonmotile cells grow and fill the available pore space before cells enter the next section of porous material. Assuming that the average volume of an *E. coli* cell is 1.2 μm^3 (see Reynolds et al., 1989 for calculation), a cell population of about 8×10^{11} cells would be required to completely fill a unit section of core with a pore volume of about 1 ml. The data in Fig. 4.6 suggest that a cell population between 10^7 and 10^8 is reached before cells are detected in the next section. This is much lower than that required to fill completely all of the available pore space. It may suggest that a critical cell density must be reached before non-motile cells enter the next section, or perhaps all that is needed for nonmotile cells to penetrate is to grow end to end without completely filling the pore space.

Interestingly, although the pore volumes of the cores used for the two experimental conditions were very similar, the penetration rates observed for strain RP2912 for each condition were different, 0.08 versus 0.16 cm/h for first and second condition, respectively. The reason for this discrepency may be explained based on the need to reach a critical cell density within each unit section of the porous material before cells are displaced into the next section. In the second experimental condition, a large concentration of cells was directly injected into the core rather than allowing cells to migrate from a syringe needle as occurred in the first condition. By having a large initial cell population within the core, the time required to achieve the critical cell density needed for displacement into the next section would be shorter. This would result in shorter penetration times and faster penetration rates. Thus, more realistic models may require an expression to estimate the time required to acheive the critical cell population needed for displacement.

Other important factors for the movement of nonmotile cells through porous materials include pore-size and gas-production. The rate of penetration of nonmotile cells increased linearly with an increase in the pore-size from 10 μm to 80 μm (Sharma and McInerney, 1991), suggesting that transport of nonmotile cells is influenced by the size of pore throats. The reason why transport of nonmotile cells is influenced by the confining pore-space may be related to the requirement of critical cell density for the movement of nonmotile cells. The lag-time for bacterial growth

increases with a decrease in the pore-size (Zvyagintsev and Pitryuk, 1973). Thus, the time required to obtain critical cell density and consequently, the rate of penetration of nonmotile cells would also increase with a decrease in the pore-size. Reynolds et al. (1989) showed that the rate of penetration of gas-producing nonmotile strains of *E. coli* was six times faster in sand-packed cores compared to that observed for isogenic mutants that lacked the ability to produce gas, suggesting that gas production increases the rate of penetration of nonmotile cells. In heterogenous consolidated systems, where conditions would be conducive for the generation of localized pressure gradients, gas production may act to push nonmotile cells through the porous material. Since the mode of growth of chemotactic, motile strains is similar to that of nonmotile strains, the above model (equation 4.2) may be useful in predicting penetration times if factors such as coefficients of motility and chemotaxis are included.

It is clear that active microbial communities exist at depths of several hundreds to thousands of meters below the surface (Balkwill, 1989; Bhupathiraju et al., 1991; Chapelle and Lovely, 1990; Francis et al., 1989; Fredrickson et al., 1989; Hicks and Fredickson, 1989; Jones et al., 1989; Madsen and Bollag, 1989; Phelps et al., 1989; Sinclair and Ghiorse, 1989). The recent studies of the deep aquifers underlying the Savannah River plant, South Carolina, raise the question of how microorganisms became associated with these sediments which are several hundreds of meters below the surface (Sargent and Fliermans, 1989). The most

likely explanations are that the organisms were transported to their present locations by percolation of surface water downward or groundwater from aquifer recharge areas, or that the microorganisms were present in the sediments at the time of deposition. The first two explanations were thought to be unlikely since the colonization of aquifers below the Congaree (about 50 m below the surface) by the percolation of surface waters would require the movement of bacteria against an upward hydraulic gradient, and the distance from the recharge areas to the deeper aquifers is so large, and the tendency of bacteria to attach to particles is so great, that it is difficult to envision how bacteria could travel over such distances. However, our current and previous studies (Jenneman et al., 1985; McInerney, 1991; Reynolds et al., 1989; Sharma and McInerney, 1991) clearly show that bacteria by growth and self-populsion move through consolidated and unconsolidated porous materials at rates greater than 0.1 m/d which is almost twice the average groundwater velocities reported for the deeper aquifers under the Savannah River plant (Sargent and Fliermans, 1989). The fact that microorganisms can grow through porous materials suggests that the constant removal of microorganisms from the groundwater by the filtering action of the porous material may not always occur. Thus, the organisms in these aquifers may not have been completely isolated from those on the surface since the time of sediment deposition, and self-propulsion may have played an important role in the colonization of deep aquifers.

REFERENCES

Adler, J. and M. M. Dahl. 1967. A method for measuring the motility of bacteria and for comparing random and non-random motility. J. Gen. Microbiol. 46:161-173.

Amos, D. A., and M. J. McInerney. 1989. Poly-B-hydroxyalkanoate in *Syntrophomonas wolfei*. Arch. Microbiol. 152:172-177.

Balch, W. E., and R. S. Wolfe. 1976. New approach to the cultivation of methanogenic bacteria: 2-mercaptoethanesulfonic acid (HS-CoM)-dependent growth of methanobacterium ruminantium in a pressurized atmosphere. Appl. Environ. Microbiol. 32:781-791.

Balkwill, D. L. 1989. Numbers, diversity, and morphological characteristics of aerobic, chemoheterotrophic bacteria in deep subsurface sediments from a site in South Carolina. Geomicrobiol. J. 7:33-52.

Bhupathiraju, V. K., P. K. Sharma, M. J. McInerney, R. M. Knapp, K. Fowler, and W. Jenkins. 1991. Isolation and characterization of novel halophilic anaerobic bacteria from oil field brines, pp. 131-144. In: E. C. Donaldson (ed.), Microbial Enhancement of Oil Recovery-Recent Advances, Elsevier Science Publishers, The Netherlands.

Bryant, M. P. 1972. Commentary on the Hungate technique for culture of anaerobic bacteria. Am. J. Cln. Nutr. 25:1324-1328.

Bu'lock, J. and B. Kristiansen. 1987. Basic Biotechnology. Academic Press Inc., London.

Chapelle, F. H., and D. R. Lovely. 1990. Rates of microbial metabolism in deep coastal plain aquifers. Appl. Environ. Microbiol. 56:1865-1874.

Chang, M. M., R. S. Bryant, T. H. Chung, and H. W. Gao. 1991. Modeling and laboratory investigations of microbial transport phenomena in porous media. Topical report NIPER-548, U. S. Department of Energy, Bartlesville, Oklahoma.

Chang, P. L., and T. F. Yen. 1984. Interaction of *Escerichia coli* B and B/4 and Bacteriophage T_4D with Berea sandstone rock in relation to enhanced oil recovery. Appl. Environ. Microbiol. 47:544-550.

Chang, P. L., and T. F. Yen. 1985. Interaction of *Pseudomonas putida* ATCC 12633 and Bacteriophage T_4D in Berea sandstone rock. Appl. Environ. Microbiol. 50:1545-1547.

Corapcioglu, M. Y., and A. Haridas. 1984. Transport and fate of microorganisms in porous media: a theoretical investigation. J. Hydrol. 72:149-169.

Corapcioglu, M. Y., and A. Haridas. 1985. Microbial transport in soils and groundwater: a numerical model. Adv. Water Res. 8:188-200.

Francis, A. J., J. M. Slater, and C. J. Dodge. 1989. Denitrification in deep subsurface sediments. Geomicrobiol. J. 7:103-116.

Fredrickson, T. R. Garland, R. J. Hicks, J. M. Thomas, S. W. Li, and K. M. McFadden. 1989. Lithotrophic and heterotrophic bacteria in deep subsurface sediments and their relation to sediment properties. Geomicrobiol. J. 7:53-66.

Gottshalk, G. 1986. Bacterial metabolism. Springer-Verlag, New York, Inc., USA.

Hagedorn, C. 1981. Transport and fate: bacterial pathogens in groundwater, pp. 153-172. In Microbial Health Considerations of Soil Disposal of Domestic Wastewaters. U. S. Environmental Protection Agency, No. EPA-6001 9-83-017.

Harvey, R. W. 1991. Parameters involved in modeling movement of bacteria in groundwater, pp. 89-114 In: C. J. Hurst (ed.), Modeling the Environmental Fate of Microorganisms, American Society for Microbiology, Washington, DC.

Hattori, R., and T. Hattori. 1976. The physical environment in soil microbiology: an attempt to extend principles of microbiology to soil microorganisms. Crit. Rev. Microbiol. 4:423-461.

Hicks, R. J., and J. K. Fredrickson. 1989. Aerobic metabolic potential of microbial populations indigenous to deep subsurface environments. Geomicrobiol. J. 7:67-76.

Ingraham, J. L., O. Maaloe, and F. C. Neidhardt, F. C. 1983. Growth of bacterial cell. Sinauer Associates Inc., Massachusetts.

Jenneman, G. E., M. J. McInerney, and R. M. Knapp. 1985. Microbial penetration through nutrient-saturated Berea sandstone. Appl. Environ. Microbiol. 50:383-391.

Jones, R. E., R. E. Beeman, and J. M. Suflita. 1989. Anaerobic metabolic processes in deep terrestrial subsurface. Geomicrobiol. J. 7:117-130.

Knapp, R. M., F. Civan and M. J. McInerney. 1988. Modeling growth and transport of microorganisms in porous formations, pp. 676-679. In: R. Vichnevetsky, P. Borne, and J. Vignes (eds.), IMACS 1988 Proceedings of the 12th World Congress on Scientific Computation, Vol. 3, pp. 676-679.

Madsen, E. L., and J. M. Bollag. 1989. Aerobic and anaerobic microbial activity in deep subsurface sediments from the Savannah River plant. Geomicrobiol. J. 7:93-102.

McInerney, M. J. 1991. Use of models to predict bacterial penetration and movement within a subsurface matrix, pp. 115-135. In: C. J. Hurst (ed.), Modeling the Environmental Fate of Microorganisms. American Society for Microbiology, Washington, DC.

McInerney, M. J., M. P. Bryant, and N. Pfenning. 1979. Anaerobic bacterium that degrades fatty acids in syntrophic association with methanogens. Arch. Microbiol. 122:129-135.

Molz, F. J., M. A. Widdowson, and L. D. Benefield. 1986. Simulations of microbial growth dynamics coupled to nutrient and oxygen transport in porous media. Water Resour. Res. 22:1207-1216.

Montgomery, A. D., M. J. McInerney, and K. L. Sublette. 1990. Microbial control of the production of hydrogen sulfide by sulfate reducing bacteria. Biotechnol. Bioeng. 35:533-539.

Morisaki, H. 1983. Effect of solid-liquid interface on metabolic activity of *E. coli*. J. Gen. Appl. Microbiol. 29:195-204.

Phelps, T. J., E. G. Raione, D. C. White, and C. B. Fliermans. 1989. Microbial activities in deep subsurface environments. Geomicrobil. J. 7:79-92.

Reynolds, P. J., P. Sharma, G. E. Jenneman, and M. J. McInerney. 1989. Mechanisms of microbial movement in subsurface materials. Appl. Environ. Microbiol. 55:2280-2286.

Sargent, K. A., and C. B. Fliermans. 1989. Geology and hydrology of the deep subsurface microbiology sampling sites at the Savannah River plant, South Carolina. Geomicrobiol. J. 7:3-13.

Sarkar, A. K., M. M. Sharma, and G. Georgiou. 1991. Compositional numerical simulation of MEOR process, pp. 331-344. In: E. C. Donaldson (ed.), Microbial Enhancement of Oil Recovery-Recent Advances, Elsevier Science Publishers, The Netherlands.

Sinclair, J. L., and W. C. Ghiorse. 1989. Distribution of aerobic bacteria, protozoa, algae, and fungi in deep subsurface

sediments. Geomicroiol. J. 7:15-32.

Sharma, P. K., and M. J. McInerney. 1991. Kinetics of microbial growth in unconsolidated porous media. 1991 ASM Annual Meeting. Dallas, Tex., 5-9 May 1991.

Sharma, P. K., and M. J. McInerney. 1992. Effects of solid interfaces on bacterial growth and activity in subsurface environments. In preparation for Appl. Environ. Microbiol.

Smith, P. K., R. I. Krohn, G. T. Hermanson, A. K. Mallia, F. H. Gartner, M. D. Provenzano, E. K. Fujimoto, N. M. Goeke, B. J. Olson, and D. C. Klenk. 1985. Measurement of protein using bicinchroninic acid. Anal. Biochem. 150:76-85.

Smolenski, W. J., and J. M. Suflita. 1987. Biodegradation of cresols isomers in anoxic aquifers. Appl. Environ. Microbiol. 53:710-717.

Tanner, R. S. 1989. Monitoring sulfate-reducing bacteria: comparison of enumeration bacteria. J. Micro. Methods. 10:83-90.

Thauer, R. K., H. K. Jungermann, and K. Decker. 1977. Energy conservation in chemotrophic anaerobic bacteria. Bact. Rev. 41:100-180.

van Loosdrecht, M. C. M., Lyklema J., Norde W., and Zehnder, J. B. 1990. Influence of interfaces on microbial activity. Microbiol. Rev. 54:75-87.

Zvyagintsev, D. G., and A. P. Pitryuk. 1973. Growth of microorganisms of various sizes under continuous flow and static conditions. Mikrobiologiya. 42:60-64.

5. MATHEMATICAL MODELING OF MEOR PROCESSES

5.1 Introduction

Our previous studies have focused on testing the feasibility of a microbial process to selectively plug high permeability zones and thereby improve sweep efficiency and increase oil recovery (Jenneman et al., 1984; Raiders et al., 1986 and 1989). We have shown (1) that viable bacteria and the nutrients required for growth can be transported through Berea sandstone cores, (2) that the in situ growth of bacteria results in significant reductions in permeability, (3) that the permeability reduction is selective for high permeability cores and improves sweep efficiency even under conditions where cross flow of fluids between regions occurs, and (4) that additional oil is recovered as a result of improved microscopic displacement and sweep efficiences. Associated with the laboratory work, a mathematical model was developed (Knapp et al., 1988) to quantify the growth of bacteria, product formation, and substrate consumption during MEOR processes and to predict permeabilty reduction as a result of those microbial activities in porous media.

The one-dimension mathematical model has been modified to include three-phases and seven-species. The model is specified into three stages that correspond to the initial injection, the incubation, and the continued injection processes that occur during core flood experiments. A third-order upwind difference scheme is used to represent convective transport because it reduces numerical dispersion and oscillation. The simulator efficiency is enhanced

by varying time step sizes during computation of the incubation process.

The model is simplified to a one-phase, zero-dimension system to simulate microbial growth and metabolism in nutrient-saturated, sand-packed cores incubated under static conditions. Comparisons between the numerical solutions and experimental results show that the proposed model does capture the essential characteristics of microbial activities during MEOR processes.

5.2 Microbial Activities

There are two reactions that describe the microbiological processes that occur during a MEOR process. The first is the growth of bacteria coupled to glucose and ammonium ion consumption. Equation 5.1 describes the conversion of these substrates to make a microbial cell (Bu'lock and Kristiansen, 1984):

$$C_6H_{12}O_6 + 1.2NH_4^+ \rightarrow 6CH_{1.8}O_{0.5}N_{0.2} + 3H_2O \qquad (5.1)$$

The second reaction is the growth-associated production of acetate (CH_3COO^-), carbon dioxide (CO_2), and nitrogen (N_2) [or ammonium (NH_4^+)] by the degradation of glucose coupled to the reduction of nitrate (NO_3^-) (Equation 5.2):

$$5C_6H_{12}O_6 + 8NO_3^- \rightarrow 10CH_3COO^- + 10CO_2 + 4N_2 + 14H_2O + 2H^+ \qquad (5.2)$$

As a result, the behavior of seven species must be described during in situ microbial growth: glucose ($C_6H_{12}O_6$), ammonium (NH_4^+), nitrate (NO_3^-), cellular biomass ($CH_{1.8}O_{0.5}N_{0.2}$), acetate (CH_3COO^-), carbon dioxide (CO_2), and nitrogen (N_2) (for consolidated core flood

experiments only).

5.3 Assumptions

The following assumptions were used in development of the model equations.

1. One-dimensional, horizontal, linear flow with the effects of gravity ignored.
2. Homogeneous, isotropic, and incompressible porous medium.
3. Three phases, Newtonian fluids, and oil, water, and gas.
4. Isothermal process for microbial transport, growth, and metabolism.
5. Both glucose and ammonium nitrate are limiting for growth.
6. Biomass in the core is divided into that suspended in the flowing water phase, and that retained on the pore surfaces.
7. Nutrients suspended in the flowing phase are assumed to fully penetrate and saturate the sessile phase so that anaerobic microbial growth and metabolism occur in the same fashion in both the flowing phase and the sessile phase.

5.4 Model Equations

5.4.1 Conservation Equations for Species

The transport of each species suspended in the flowing water phase is described by a specific convection-dispersion equation:

$$\frac{\partial(\phi C_i)}{\partial t} = -\frac{\partial(u_f C_i)}{\partial x} + \frac{\partial}{\partial x}(\phi K_D \frac{\partial C_i}{\partial x}) \tag{5.3}$$

where, u_f is the Darcy flux; K_D is dispersion coefficient; ϕ is the

updated porosity; R_i is the rate of generation or consumption of individual species. Equation 5.3 can be applied to each of the following species: acetate (A), biomass (B), nitrogen (N), glucose (S1), ammonium ($S2^+$), and nitrate ($S2^-$). However, the production of carbon dioxide (C) can be estimated from that of acetate according to the chemical balance described by Equation 5.2:

$$\frac{\partial C_C}{\partial t} = \omega \frac{\partial C_A}{\partial t}, \quad \omega = \frac{(MW)_C}{(MW)_A} \tag{5.4}$$

where, C_C and C_A are respectively the concentrations for CO_2 and acetate, and $(MW)_C$ and $(MW)_A$ are the molecular weights for CO_2 and acetate, respectively.

The accumulation of the biomass attached to pore surfaces is assumed to be the net result of biomass retention, detachment, and growth:

$$\frac{\partial}{\partial t}(\rho_B \sigma) = R_r - R_d + R_{Bs} \tag{5.5}$$

where, R_r, R_d, and R_{Bs} are the rates for retention, detachment, and growth respectively, ρ_B is density of biomass, and σ is the fraction of pore space occupied by the retained cells.

5.4.2 Rate Equations for Species

The biomass retention rate is considered to be proportional to the biomass $u_f C_B$ entering a given area, and to the applicable plugging capacity $(1-\sigma)\rho_B$ of the porous medium (Cernansky and Siroky, 1985):

$$R_r = K_r(u_f C_B)(1 - \sigma)\rho_B \tag{5.6}$$

where, K_r is the kinetic coefficient of retention, C_B is the mass concentration of biomass in the flowing phase, σ is the updated volume fraction of the sessile phase, and ρ_B is density of biomass.

Biomass detachment is a function of the biomass $\sigma\rho_B$ attached to pore surfaces, and the shear force $u_f[(\mu_w)/K_f]$ between the stream of suspended and retained cells (Cernansky and Siroky, 1985):

$$R_d = K_d(\sigma\rho_B)\, u_f \frac{\mu_w}{K_f} \tag{5.7}$$

where, K_d is the kinetic coefficient of detachment, μ_w is the viscosity of the flowing phase, and K_f is the updated permeability of the porous medium to the flowing phase, defined as (Civan et al., 1989):

$$K_f = K_o\left(\frac{\phi}{\phi_o}\right)^3, \quad \phi = \phi_o(1 - \sigma) \tag{5.8}$$

where, K_o and ϕ_o are initial permeability and porosity, respectively.

The growth rate R_{Bs} for retained biomass, limited by availability of the two substrates (glucose and ammonium), can be expressed using a modified version of the Monod equation (Bu'lock and Kristainsen, 1984):

$$R_{Bs} = \mu_{Bm}\left(\frac{C_{S1}}{K_{B/S1} + C_{S1}}\right)\left(\frac{C_{S2^+}}{K_{B/S2^+} + C_{S2^+}}\right)(\sigma\rho_B) \tag{5.9}$$

where, μ_{Bm} is maximum specific growth rate for bacteria, C_{S1} and C_{S2+}

are mass concentrations for glucose and ammonium, respectively, $K_{B/S1}$ and $K_{B/S2+}$ are the Monod saturation constants for the consumption of glucose and ammonium, respectively.

Biomass generation in the flowing water phase is considered to be a dynamic balance of various mass exchange processes including bacterial growth, retention, and detachment:

$$R_B = R_{Bf} - R_r + R_d \tag{5.10}$$

where, R_r and R_d are biomass retention and detachment rates described in Equations (5.6) and (5.7), and R_{Bf} is the growth rate for bacterial cells in the flowing phase (Bu'lock and Kristiansen, 1984):

$$R_{Bf} = \mu_{Bm}\left(\frac{C_{S1}}{K_{B/S1} + C_{S1}}\right)\left(\frac{C_{S2^+}}{K_{B/S2^+} + C_{S2^+}}\right)C_B \tag{5.11}$$

where, C_B is the concentration of bacterial cells in the flowing phase.

The production rates for acetate and nitrogen are given respectively as (Bajpai and Reuss, 1982):

$$R_A = \begin{cases} 0, & if C_{S1} \le C_{S1}^* \\ \mu_{Am}\dfrac{C_{S1} - C_{S1}^*}{K_{A/S1} + C_{S1} - C_{S1}^*}(C_B + \sigma\rho_B), & if C_{S1} > C_{S1}^* \end{cases} \tag{5.12}$$

$$R_N = \begin{cases} 0, & if C_{S2^-} \le C_{S1}^* \\ \mu_{Nm}\dfrac{C_{S2^-} - C_{S2^-}^*}{K_{N/S2^-} + C_{S2^-} - C_{S2^-}^*}(C_B + \sigma\rho_B), & if C_{S2^-} > C_{S2^-}^* \end{cases} \tag{5.13}$$

where, R_A and R_N are production rates for acetate and N_2,

respectively, μ_{Am} and μ_{Nm} are the maximum specific production rates for acetate and nitrogen, respectively, $K_{A/S1}$ is the saturation constant for production of acetate by the consumption of glucose, $K_{N/S2-}$ is the saturation constant for the net production of nitrogen by consumption of nitrate, and C^*_{S1} and C^*_{S2-} are critical concentrations of glucose and nitrate, respectively.

The production rate of CO_2 is proportional to that of acetate:

$$R_C = \omega R_A \tag{5.14}$$

A typical substrate consumption equation can be used to describe the utilization of glucose and ammonium nitrate (Bu'lock and Kristiansen, 1984):

$$R_{S1} = -\frac{R_{Bf} + R_{Bs}}{Y_{B/S1}} - \frac{R_A + R_C}{Y_{(A+C)/S1}} - m_{S1}(C_B + \sigma\rho_B) \tag{5.15}$$

$$R_{S2^+} = -\frac{R_{Bf} + R_{Bs}}{Y_{B/S2^+}} \tag{5.16}$$

$$R_{S2^-} = -\frac{R_N}{Y_{N/S2^-}} - m_{S2-}(C_B + \sigma\rho_B) \tag{5.17}$$

where, R_{S1}, R_{S2+}, and R_{S2-} are the consumption rates of glucose, ammonium, and nitrate, respectively, $Y_{B/S1}$ is the yield coefficient for biomass per unit amount of glucose, $Y_{(A+C)/S1}$ is the yield coefficient for both acetate and CO_2 per unit glucose; $Y_{B/S2+}$ and $Y_{N/S2-}$ are the yield coefficients for biomass per unit amount of ammonium, and nitrogen per unit amount of nitrate, respectively, and m_{S1} and m_{S2-} are maintenance coefficients for the consumption of glucose and

nitrate, respectively.

5.4.3 Multiphase-Flow Equations

After significant microbial plugging and biogenic gas production, the simultaneous flow of oil, water, and gas phases can occur in the porous medium when fluid flow is initiated after the incubation period. A three-phase, transport model was developed to describe this process.

Consider linear horizontal flow. If capillary pressure is neglected, and the gas is assumed to dissolve in both the oil and water phases, a complete set of equations for pressure and saturations along the one-dimensional core system can be derived after an appropriate rearrangement (Fanchi et al., 1982):

$$\phi C_t \frac{\partial p}{\partial t} = \beta_o \frac{\partial}{\partial x}(\psi_o \frac{\partial p}{\partial x}) + \beta_w \frac{\partial}{\partial x}(\psi_w \frac{\partial p}{\partial x}) + \beta_g [\frac{\partial}{\partial x}(\psi_g \frac{\partial p}{\partial x}) + q_g] \quad (5.18)$$

$$\frac{\partial}{\partial t}(\phi \frac{S_o}{B_o}) = \frac{\partial}{\partial x}(\psi_o \frac{\partial p}{\partial x}) \quad (5.19)$$

$$\frac{\partial}{\partial t}(\psi \frac{S_w}{B_w}) = \frac{\partial}{\partial x}(\psi_w \frac{\partial p}{\partial x}) \quad (5.20)$$

$$\frac{\partial}{\partial t}[\phi(\frac{S_g}{B_g} + \frac{R_{so}S_o}{B_o} + \frac{R_{sw}S_w}{B_w})] = \frac{\partial}{\partial x}(\psi_g \frac{\partial p}{\partial x}) + q_g \quad (5.21)$$

$$\beta_o = B_o - R_{so}B_g, \quad \beta_w = B_w - R_{sw}B_g, \quad \beta_g = B_g \quad (5.22)$$

$$C_t = C_o S_o + C_w S_w + C_g S_g \quad (5.26)$$

$$\psi_o = \frac{K\lambda_o}{B_o}, \quad \psi_w = \frac{K\lambda_w}{B_w}, \quad \psi_g = K(\frac{\lambda_g}{B_g} + \frac{R_{so}\lambda_o}{B_o} + \frac{R_{sw}\lambda w}{B_w}) \tag{5.23}$$

$$\lambda_o = \frac{K_{ro}}{\mu_o}, \quad \lambda_w = \frac{K_{rw}}{\mu_w}, \quad \lambda_g = \frac{K_{rg}}{\mu_g} \tag{5.24}$$

$$q_g = \frac{1}{\rho_{CS}}\frac{\partial C_C}{\partial t} + \frac{1}{\rho_{NS}}\frac{\partial C_N}{\partial t} \tag{5.25}$$

$$C_o = -\frac{1}{B_o}\frac{\partial B_o}{\partial p} + \frac{B_g}{B_o}\frac{\partial R_{so}}{\partial p} \tag{5.27}$$

$$C_w = -\frac{1}{B_w}\frac{\partial B_w}{\partial p} + \frac{B_g}{B_w}\frac{\partial R_{sw}}{\partial p}, \quad C_g = -\frac{1}{B_g}\frac{\partial B_g}{\partial p} \tag{5.28}$$

$$S_o + S_w + S_g + \sigma = 1, \quad \phi = \phi_o(1 - \sigma) \tag{5.29}$$

where, p is pressure, S_o, S_w, and S_g are saturations for oil, water, and gas, respectively, B_o, B_w, and B_g are formation volume factors for oil, water, and gas, respectively, R_{so} and R_{sw} are gas solubilities in oil and water, respectively, K_{ro}, K_{rw}, and K_{rg} are relative permeabilities to oil, water, and gas, respectively, μ_o, μ_w, and μ_g are viscosities for oil, water, and gas, respectively, C_t is total compressibility, C_o, C_w, and C_g are compressibilities for oil, water, and gas, respectively, q_g is the total gas production (including CO_2 and N_2), and ρ_{CS} and ρ_{NS} are respectively the densities of CO_2 and N_2 at the standard conditions.

5.5 Simplification and Specification

Let μ_{ss} be the specific growth rate for biomass in the two-substrate system:

$$\mu_{ss} = \mu_{Bm}\left(\frac{C_{S1}}{K_{B/S1} + C_{S1}}\right)\left(\frac{C_{S2^+}}{K_{B/S2^+} + C_{S2^+}}\right) \tag{5.30}$$

thus, the biomass retention equation 5.6 can be rewritten:

$$\frac{\partial\sigma}{\partial t} = K_I u_f C_B(1 - \sigma) - K_d u_f \sigma \frac{\mu_w}{K_f} + \mu_{ss}\sigma \tag{5.31}$$

If injection rate u_f is specified, the species equation 5.3 can be simplified to:

$$\frac{\partial C_i}{\partial t} = -\frac{u_f}{\phi}\frac{\partial C_i}{\partial x} + \frac{1}{\phi}\frac{\partial}{\partial x}(\phi K_D \frac{\partial C_i}{\partial x}) + \phi_o C_i \frac{\partial\sigma}{\partial t} + R_i \tag{5.32}$$

However, based on the different mechanisms and flow patterns corresponding to the initial injection, incubation, and post incubatory injection periods, further specifications can be made for each period.

5.5.1 Static Core System

Nutrient-saturated, sand-packed cores were inoculated with bacteria and incubated without fluid flow. These cores did not contain crude oil. To simulate microbial activity in such cores, the general model was reduced to a zero-dimension system by cancelling the convection and dispersion terms and eliminating the equations describing the sessile phase reactions. The result was a set of ordinary differential equations (Table 5.1).

5.5.2 Initial Inoculation

Since the period when sterile medium is injected into the core is short relative to the time required for significant bacterial growth and metabolism to occur, little bacterial plugging or

Table 5.1 Static, unconsolidated core process.

Type	Equation
Biomass	$\frac{dC_B}{dt} = \mu_{Bm}\left(\frac{C_{S1}}{K_{B/S1} + C_{S1}}\right)\left(\frac{C_{S2^+}}{K_{B/S2^+} + C_{S2^+}}\right)C_B$
Acetate	$\frac{dC_A}{dt} = \mu_{Am}\left(\frac{C_{S1} - C^*_{S1}}{K_{A/S1} + C_{S1} - C^*_{S1}}\right)C_B$
CO_2	$\frac{dC_C}{dt} = \omega\frac{dC_A}{dt}, \quad where, \ \omega = \frac{(MW)_C}{(MW)_A}$
N_2	$\frac{dC_N}{dt} = \mu_{Nm}\left(\frac{C_{S2^-} - C^*_{S2^-}}{K_{N/S2^-} + C_{S2^-} - C^*_{S2^-}}\right)C_B$
Glucose	$\frac{dC_{S1}}{dt} = -\frac{1}{Y_{B/S1}}\left(\frac{dC_B}{dt}\right) - \frac{1}{Y_{(A+C)/S1}}\left(\frac{dC_A}{dt} + \frac{dC_C}{dt}\right) - m_{S1}\,C_B$
Ammonium	$\frac{dC_{S2^+}}{dt} = -\frac{1}{Y_{B/S2^+}}\left(\frac{dC_B}{dt}\right)$
Nitrate	$\frac{dC_{S2^-}}{dt} = -\frac{1}{Y_{N/S2^-}}\left(\frac{dC_N}{dt}\right) - m_{S2^-}\,C_B$
Initial Conditions	$(C_B)_{t=0} = C_B^\circ, \ (C_{S1})_{t=0} = C_{S1}^\circ, \ (C_{S2+})_{t=0} = C_{S2+}^\circ$ $(C_{S2-})_{t=0} = C_{S2-}^\circ, \ (C_A)_{t=0} = 0, \ (C_C)_{t=0} = 0, \ (C_N)_{t=0} = 0$

biogenic gas production is observed during nutrient injection. Residual oil and biogenic gas are immobile. Thus, the flow of a single fluid phase, water, is assumed to occur during this nutrient injection. The pressure equation can then be expressed using Darcy's equation.

It is also assumed that growth and metabolism occur only in the flowing phase during the initial injection period. Growth, metabolite production, and substrate consumption in the sessile phase during initial inoculation are assumed to not occur. The specified model for the inoculation period with the appropriate initial and boundary conditions is shown in Table 5.2.

5.5.3 Incubation Period

During the incubation period, injection of fluid into the core is discontinued to allow microbial growth and metabolism to occur. Hence, the rate controlled retention and detachment terms disappear from Equation 5.31, and the convection terms are dropped from the convection-dispersion Equation 5.32. Although molecular diffusion for each species exists during incubation, the molecular diffusion is much smaller than the rates of species generation and consumption, and is ignored in Equation 5.32. Under this condition, the model is reduced to a set of ordinary differential equations applied to each grid block. Each block behaves like a single batch fermenter with no mass exchange with adjacent blocks. This simplification provides an opportunity to enhance model efficiency by appropriately increasing time step sizes during the incubation computation. Also, the pressure is assumed to be

Table 5.2 Specified model equations for the initial inoculation period.

Type	Equation
Species	$\frac{\partial C_i}{\partial t} = -\frac{u_f}{\phi}\frac{\partial C_i}{\partial x} + \frac{1}{\phi}\frac{\partial}{\partial x}(\phi K_D \frac{\partial C_i}{\partial x}) + \phi_0 C_i \frac{\partial \sigma}{\partial t} + R_i$ $\frac{\partial C_c}{\partial t} = \omega \frac{\partial C_N}{\partial t}, \quad \omega = \frac{(Mol.\ Wt.)_C}{(Mol.\ Wt.)_A}$ where, i = A, B, N, S1, $S2^+$, $S2^-$
Sessile	$\frac{\partial \sigma}{\partial t} = K_r u_f C_B (1 - \sigma) - K_d \sigma u_f \frac{\mu_w}{K_f}$
Pressure	$\frac{\partial p}{\partial x} = -u_f \frac{\mu_w}{K_f}$
Initial Conditions	$(C_i)_{t=0} = C_i^0, \quad (\sigma)_{t=0} = \sigma^0, \quad (p)_{t=0} = p^0$
Boundary Conditions	$\left[u_f C_i - \phi K_D \frac{\partial C_i}{\partial x}\right]_{x=0} = u_f (C_i)_{inlet}, \quad \left[\frac{\partial C_i}{\partial x}\right]_{x=L} = 0$ $(p)_{x=0} = P_{inj}$

uniform along the core because no flow occurs and the pressure gradient terms in Equation 5.18 are dropped. A simplified model for the incubation process is summarized in Table 5.3.

5.5.4 Post Incubation Injection Period

During this period, as a result of microbial plugging and biogenic gas production, the simultaneous flow of oil, water, and gas phases occurs. Although much of the gas may be dissolved in the oil phase, some gas may flow as a free phase through its own channels through the core, particularly near the outlet of the core. The rate-controlled retention and detachment of bacteria may again become active during the prolonged fluid injection. It is assumed that growth and metabolism in the sessile phase can be "lumped" into the planktonic phase during this period. A general, three-phase and seven-species model for this period is summarized in Table 5.4.

5.6 Numerical Solutions

The partial differential equations are solved using the method of lines (Ames, 1977). Spatial derivatives are approximated by finite difference formulas while temporal derivatives remain continuous. The numerical solutions are carried out using the 1(2)-order Runge-Kutta-Fehlberg method (Fehlberg, 1969).

The first-order spatial derivative corresponding to convective transport for species i in Equation 5.32 is replaced with a third-order upwinding formula resistant to numerical dispersion and oscillation (Leonard, 1984):

Table 5.3 Model equations for incubation period.

Type	Equation
Species	$\frac{\partial C_i}{\partial t} = \phi_o C_i \frac{\partial \sigma}{\partial t} + R_i$
	$\frac{\partial C_C}{\partial t} = \omega \frac{\partial C_A}{\partial t}, \quad \omega = \frac{(Mol.\ Wrt.)_C}{(Mol.\ Wrt.)_A}$
	where, i = A, B, N, S1, $S2^+$, $S2^-$
Sessile	$\frac{\partial \sigma}{\partial t} = \mu_{ss}\sigma$
Pressure	$\phi C_t \frac{\partial p}{\partial t} = B_g\left(\frac{1}{\rho_{CS}}\frac{\partial C_C}{\partial t} + \frac{1}{\rho_{NS}}\frac{\partial C_N}{\partial t}\right) + \phi\frac{\partial \sigma}{\partial t}$
Initial Conditions	$(C_i)_{t=T_s} = (C_i)^s, \quad (\sigma)_{t=T_s} = (\sigma)^s, \quad (p)_{t=T_s} = (p)^s$

Table 5.4 Model equations for post injection period.

Type	Equation
Species	$\frac{\partial C_i}{\partial t} = -\frac{u_f}{\phi}\frac{\partial C_i}{\partial x} + \frac{1}{\phi}\frac{\partial}{\partial x}(\phi K_D \frac{\partial C_i}{\partial x}) + \phi_o C_i \frac{\partial \sigma}{\partial t} + R_i$ $\frac{\partial C_C}{\partial t} = \omega \frac{\partial C_A}{\partial t}, \quad \omega = \frac{(Mol.\ Wt.)_C}{(Mol.\ Wt.)_A}$ where, i = A, B, N, S1, $S2^+$, $S2^-$
Sessile	$\frac{\partial \sigma}{\partial t} = K_r u_f C_B (1 - \sigma) - K_d \sigma u_f \frac{\mu_w}{K_f}$
Pressure	$\phi C_t \frac{\partial p}{\partial t} = \beta_o \frac{\partial}{\partial x}(\psi_o \frac{\partial p}{\partial x}) + \beta_w \frac{\partial}{\partial x}(\psi_w \frac{\partial p}{\partial x} + \beta_g [\frac{\partial}{\partial x}(\psi_g \frac{\partial p}{\partial x})$
Saturations	$\frac{\partial}{\partial t}(\phi \frac{S_o}{B_o}) = \frac{\partial}{\partial x}(\psi_o \frac{\partial p}{\partial x}), \quad \frac{\partial}{\partial t}(\phi \frac{S_w}{B_w}) - \frac{\partial}{\partial x}(\psi_w \frac{\partial p}{\partial x})$ $\frac{\partial}{\partial t}[\phi(\frac{S_g}{B_g} + \frac{R_{so}S_o}{B_o} + \frac{R_{sw}S_w}{B_w})] = \frac{\partial}{\partial x}(\psi_g \frac{\partial p}{\partial x}) + q_g$
Initial Conditions	$(C_i)_{t=Tw} = C_i^w, \ (\rho)_{t=Tw} = \rho^w, \ (p)_{t=Tw} = p^w$ $(S_j)_{t=Tw} = S_j^w, \ j = o, w, g$
Boundary Conditions	$\left[u_f C_i - \phi K_D \frac{\partial C_i}{\partial x}\right]_{x=0} = u_f (C_i)_{inlet}, \quad \left[\frac{\partial C_i}{\partial x}\right]_{x=L} = 0$ $(p)_{x=0} = p_{inlet}$

$$\left[\frac{\partial C_i}{\partial x}\right]_j = \frac{(C_i)_{j-2} - 6(C_i)_{j-1} + 3(C_i)_j + 2(C_i)_{j+1}}{6\Delta x} + O(\Delta x^3) \qquad (5.33)$$

Since the concentration $(C_i)_0$ required in Equation 5.33 does not exist, the first-order spatial derivative at j = 2 is expressed by the two-point central weighting scheme:

$$\left[\frac{\partial C_i}{\partial x}\right]_2 = \frac{(C_i)_3 - (C_i)_1}{2\Delta x} + \theta(\Delta x^2) \qquad (5.34)$$

The dispersion term for species i in Equation 5.32 is a second-order spatial derivative and is approximated with a second-order central finite difference scheme:

$$\left[\frac{\partial}{\partial x}(\phi K_D \frac{\partial C_i}{\partial x})\right]_j = \frac{(\phi K_D)_{j+½}[(C_i)_{j+1} - (C_i)_j] - (\phi K_D)_{j-½}[(C_i)_j - (C_i)_{j-1}]}{\Delta x^2} + O(\Delta x^2) \qquad (5.35)$$

To approximate the second-order spatial derivatives in the pressure Equation 5.18, a second-order central difference scheme is used:

$$\left[\frac{\partial}{\partial x}(\psi_1 \frac{\partial p}{\partial x})\right]_j = \frac{(\psi_1)_{j+½}(p_{j+1} - p_j) - (\psi_1)_{j-½}(p_j - p_{j-1})}{\Delta x^2} + O(\Delta x^2) \qquad (5.36)$$

Consider a first-order approximation to the oil and water saturation equations, 5.19 and 5.20, respectively:

$$\frac{\left[\frac{\phi S_o}{B_o}\right]_j^{n+1} - \left[\frac{\phi S_o}{B_o}\right]_j^{n}}{\Delta t} = \left[\frac{\partial}{\partial x}(\psi_o \frac{\partial p}{\partial x})\right]_j^{n+1} + O(\Delta t) \qquad (5.37)$$

$$\frac{\left[\frac{\phi S_w}{B_w}\right]_j^{n+1} - \left[\frac{\phi S_w}{B_w}\right]_j^{n}}{\Delta t} = \left[\frac{\partial}{\partial x}(\psi_w \frac{\partial p}{\partial x})\right]_j^{n+1} + O(\Delta t) \tag{5.38}$$

Through discretization in space and time, the model equations are transferred to a set of finite difference equations.

Since the incubation time is much longer than either the initial injection period or post injection period, the simulator's execution time inversely depends on the time step sizes used during the incubation period computation.

Although biomass growth, product formation, and substrate consumption occur at exponential rates, when large amounts of substrate are present, the rates of growth, production and consumption decrease with time as the limiting substrate is consumed during incubation. Hence, it is reasonable that the time step size can be increased at an appropriate geometric rate during incubation.

Let Δt_0 be an initial time step size, and θ a time-step-varying factor. Thus the time step size may increase in the following manner :

$$\Delta t_n = \theta \Delta t_{n-1} = \theta^{n-1} \Delta t_o \tag{5.39}$$

5.7 Model Validation

5.7.1 Static Core Systems

The anaerobic microbial growth and activity in nutrient-saturated sand-packed cores under static conditions were described

in Section 4 of this report. The results of experiments using *Escherichia coli* strain RW262 were used to test the predictions of the microbial growth equations in our model. The medium contained galactose as the sole added carbon source and nitrate served as the external electron acceptor. Galactose consumption and fermentation-end-product formation were determined at various time intervals (see section 4). The yield coefficients required as model parameters were estimated stoichiometrically from chemical balance equations. Other kinetic parameters used as input data are given in Table 5.5. Comparisons between simulator and experimental results are given in Figures 5.1 to 5.5. A good match was achieved for galactose consumption (5.1), nitrate consumption (5.2), and acetate production (5.4). Biomass growth rate (5.3) calculated by the simulator did not follow the experimental data because the model did not account for the six hour lag phase. However, the final cell concentration was predicted accurately by the model.

From chemical balance equations (see section 4), the degradation of one mole of galactose should result in production of about two moles of acetate and about two moles of CO_2. The results from the simulator satisfy these mass-balance criteria (5.4 & 5.5) and follow the experimental results.

5.7.2 MEOR Core Floods

Experimental studies have been conducted to investigate microbial mechanisms involved in recovery of the oil remaining after waterflooding (Knapp et al., 1991). In these experiments, halophilic bacteria and nutrients required for their growth

Table 5.5 Kinetic parameters for static unconsolidated core systems

Symbols	Definitions	Values	Units	Source Comments
μ_{Bm}	max specific growth rate for biomass	0.60169	1/hr	experiment (Knapp et al., 1990)
μ_{Am}	max specific growth rate for acetate	3.35000	1/hr	estimated*
μ_{Nm}	max specific production rate for N_2	1.21000	1/hr	estimated*
$K_{B/S1}$	saturation const for biomass on galactose	1.34500	mg/cm^3	estimated*
$K_{B/S2+}$	saturation const for biomass on NH_4^+	1.23400	mg/cm^3	estimated*
$K_{A/S1}$	saturation const for acetate on galactose	0.01000	mg/cm^3	estimated*
$K_{N/S2-}$	saturation const for N_2 on NO_3^-	0.01000	mg/cm^3	estimated*
C_{S1}^*	critical concentration for galactose	0.03000	mg/cm^3	Bajpai and Reuss, 1982
C_{S2-}^*	critical concentration for NO_3^-	0.03000	mg/cm^3	Bajpai and Reuss, 1982
m_{S1}	coeff of energy maintenance by galactose	0.00010	mg/mg.hr	estimated*
m_{S2-}	coeff of energy maintenance by NO_3^-	0.00010	mg/mg.hr	estimated*

* by trial and error

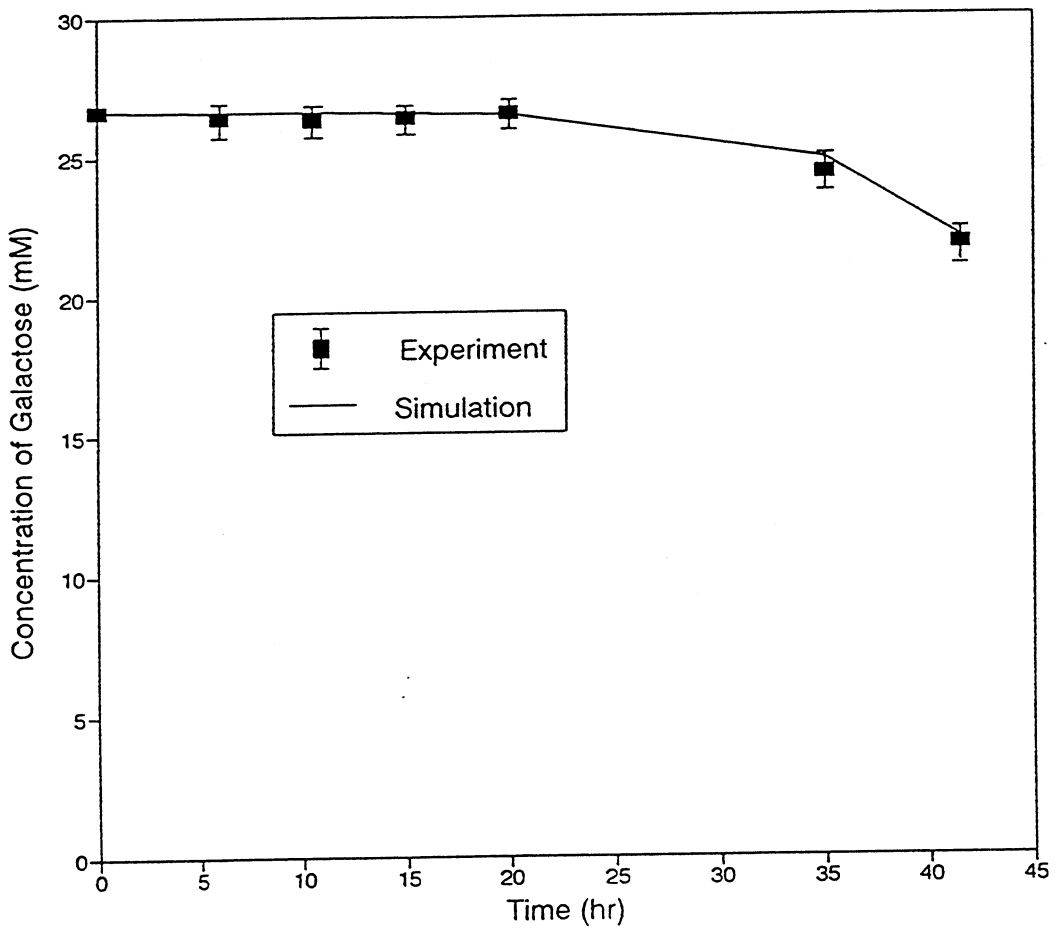

Figure 5.1 Consumption of galactose during batch fermentation

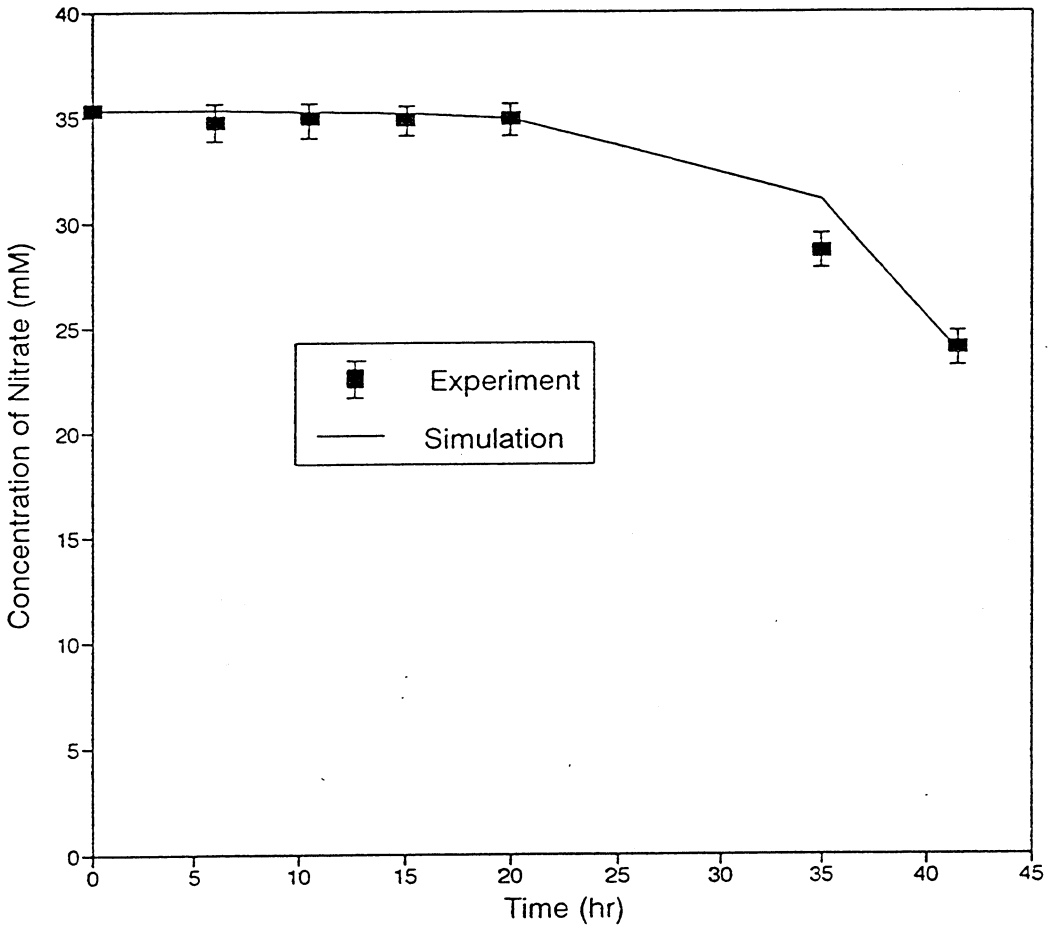

Figure 5.2 Consumption of nitrate during batch fermentation

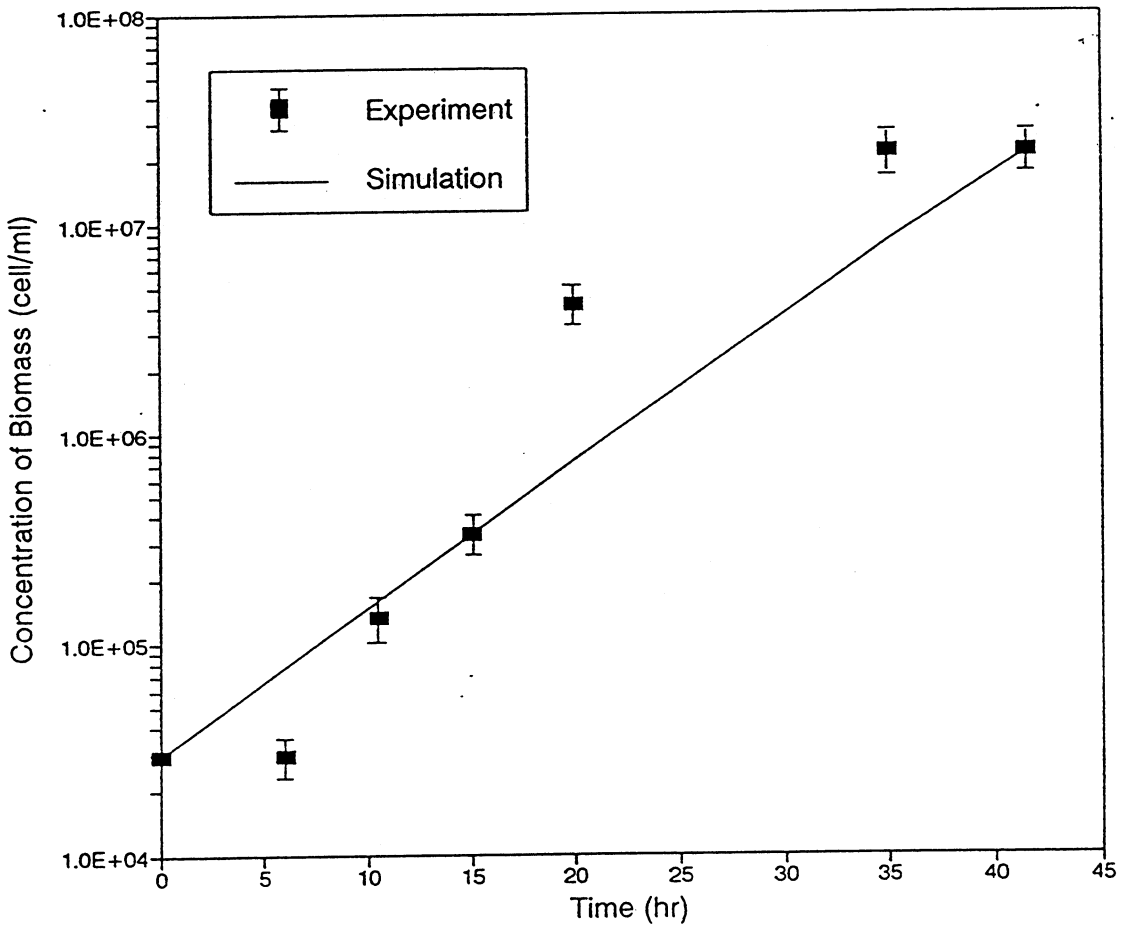

Figure 5.3 Growth of biomass during batch fermentation

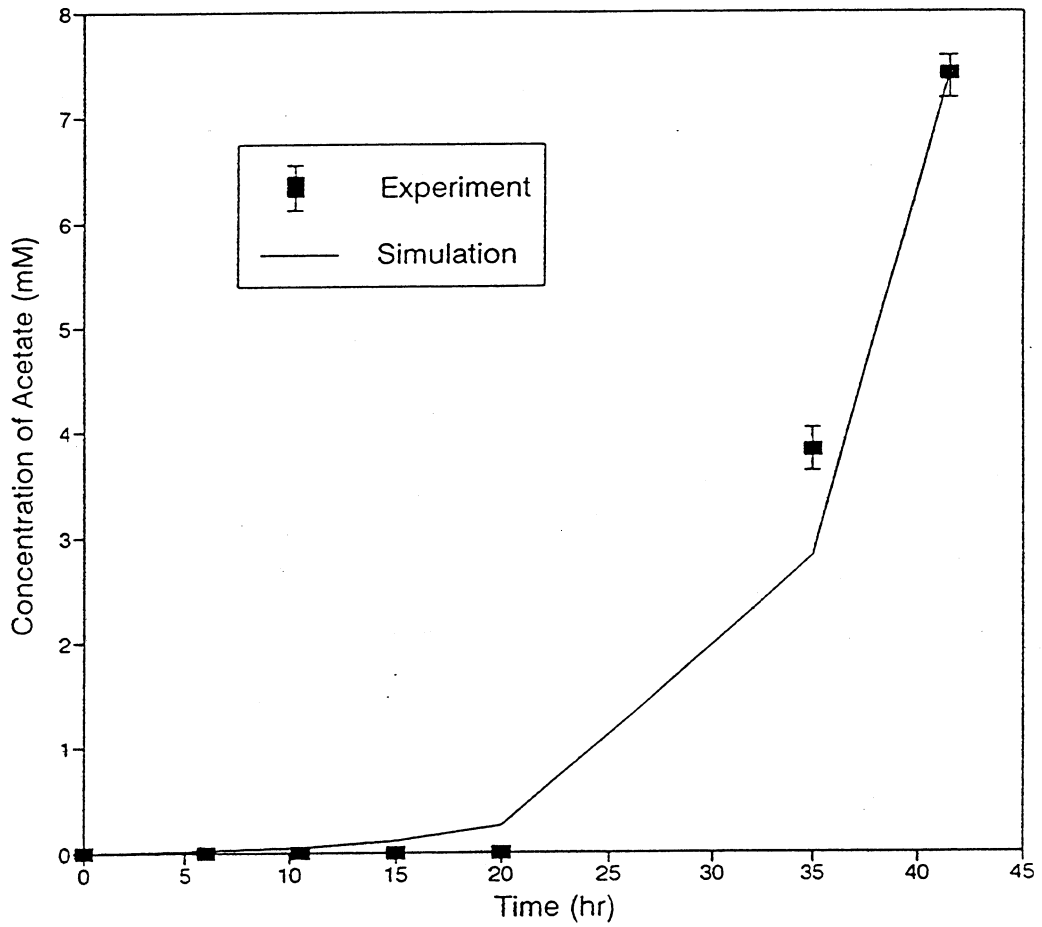

Figure 5.4 Production of acetate during batch fermentation

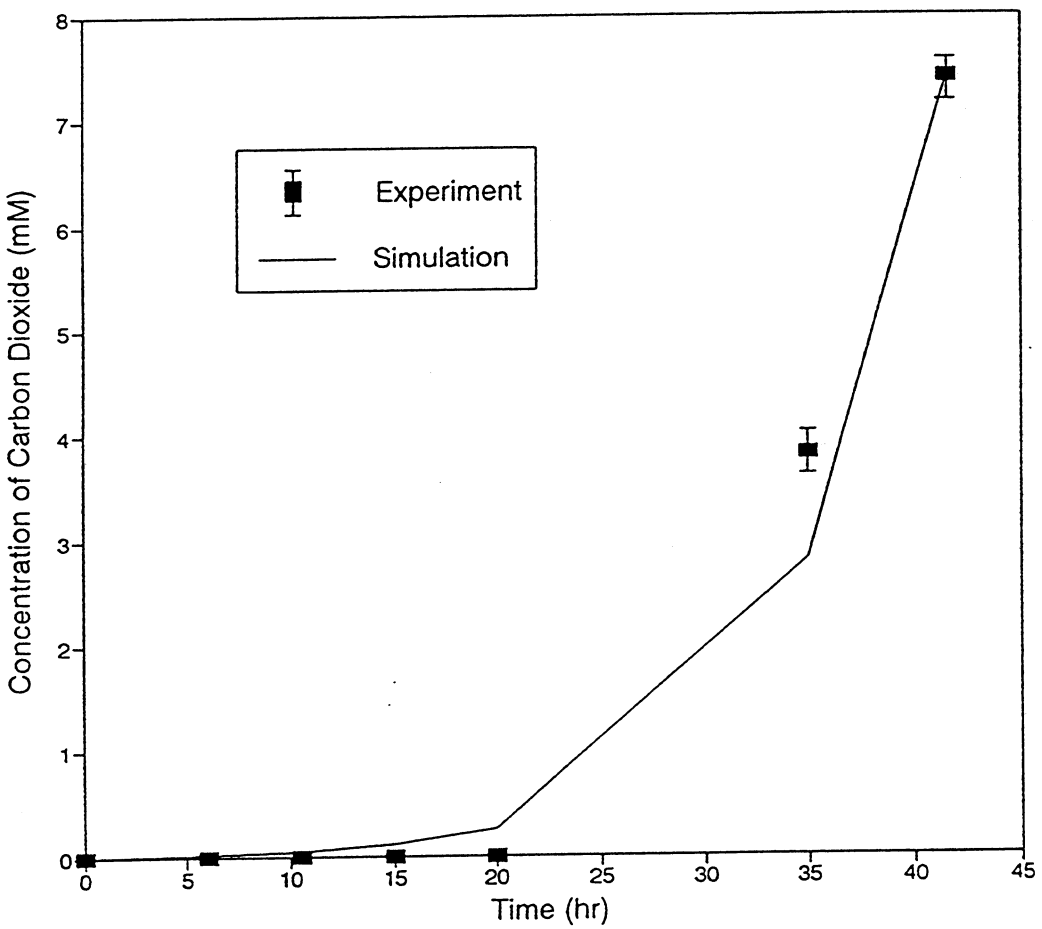

Figure 5.5 Production of CO_2 during batch fermentation

(glucose and ammonium nitrate) were injected into oil-saturated Berea sandstone cores. The experiment conducted on core #6 (Knapp et al., 1991) was selected as a practical case to test the predictions of the mathematical model. The input data for core #6 required for the simulation are given in Tables 5.6 to 5.8. The simulation of 14 nutrient treatments (a total of 121 days) that were conducted in core #6 required about 40 minutes run-time on an Encore MultiMax computer. Comparisons between simulated and experimental results are given in Figures 5.6 to 5.12.

In this experiment, no oil or gas was recovered during the first two treatments. This may be due to the lag time required for microbial growth. Therefore, it seems reasonable that maximum specific growth and production rates (μ_{Bm}, μ_{Am}, and μ_{Nm}) be designated as zero for simulation during the first two treatments. During treatments three and four, oil and gas production increased slightly, suggesting that growth and production rates are very small. Significant bacterial growth and metabolism occurred after treatment five since large amounts of by-products were detected in the effluent samples. Reasonable matches between experimental and simulation results were obtained for most product productions (N_2, Figure 5.7; Total gas, Figure 5.8; and acetate, Figure 5.9). Simulation gives equal amounts of production for acetate and CO_2 based on the chemical balance equations (section 4); however, the estimate of CO_2 production by the simulator was greater than that measured during the experiment, Figure 5.6. It may be that some CO_2 may have dissolved in the water or have been trapped in the core.

Table 5.6 Initial data for MEOR process in Core #6

Symbol	Definition	Value	Units	Source Comments
D	diameter of core #6	5.1	cm	measured (Knapp et al., 1991)
L	length of core #6	15.2	cm	measured (Knapp et al., 1991)
ϕ_0	initial porosity of core #6	0.22	cm^3/cm^3	measured (Knapp et al., 1991)
K_w^0	initial permeability to water	55.0	md	measured (Knapp et al., 1991)
μ_w	water viscosity	1.4	cp	measured (Knapp et al., 1991)
S_{or}	residual oil saturation after water flood	0.296	cm^3/cm^3	measured (Knapp et al., 1991)
S_{wc}	connate water saturation after oil flood	0.274	cm^3/cm^3	measured (Knapp et al., 1991)
D_i	molecular diffusivity	0.044	cm^2/hr	reference (Faust et al., 1960)
α_l	longitudunal dispersivity	0.01	cm	reference (Menzie et al., 1989)
τ	tortuosity factor for core #6	1.4	cm/cm	reference (de Marsily, 1972)
ρ_{CO2}	density for CO_2 at standard conditions	1.977	mg/cm^3	reference (Weast, 1982)
ρ_{N2}	density for N_2 at standard conditions	1.2506	mg/cm^3	reference (Weast, 1982)
ρ_B	density of biomass	791.7	mg/cm^3	reference (Reynolds et al., 1989)
W_{cell}	total weight of single cell	9.5×10^{-10}	mg/cell	reference (Reynolds et al., 1989)
K_r	coefficient of biomass retention	1.0×10^{-3}	cm^2/mg	reference (Cernansky and Siroky, 1985)
K_d	coefficient of biomass detachment	1.6722×10^{-23}	$cm^2.hr/mg$	reference (Cernansky and Siroky, 1985)
C_{S1}^*	critical concentration for glucose	0.03	mg/cm^3	reference (Rajpai and Reus, 1962)
$C_{S2^-}^*$	critical concentration for NO_3^-	0.03	mg/cm^3	reference (Rajpai and Reus, 1962)
m_{S1}	coeff of energy maintenance by glucose	0.000018	mg/mg.hr	estimated*
m_{S2^-}	coeff of energy maintenance of NO_3^-	0.000047	mg/mg.hr	estimated*
$K_{B/S1}$	saturation const for biomass on glucose	0.045	mg/cm^3	estimated*
$K_{B/S2+}$	saturation const for biomass on NH_4^+	0.045	mg/cm^3	estimated*
$K_{A/S1}$	saturation const for acetate on glucose	4.5×10^{-3}	mg/cm^3	estimated*
$K_{N/S2^-}$	saturation const for N_2 on NO_3^-	1.6×10^{-3}	mg/cm^3	estimated*
$Y_{B/S1}$	yield coeff of biomass on glucose	0.8202	mg/mg	calculated**
$Y_{B/S2+}$	yield coeff of biomass on NH_4^+	6.8247	mg/mg	calculated**
$Y_{(A+C)/S1}$	yield coeff of acetate and CO_2 on glucose	1.1441	mg/mg	calculated**
$Y_{N/S2^-}$	yield coeff of N_2 on NO_3^-	0.2259	mg/mg	calculated**
nx	number of grid blocks along core #6	100	cm/cm	given
Δt_0	initial time step size	0.002	hr	given
θ	time-step-varying factor	1.005	hr/hr	given

* by trial and error

** from Equations 5.1 and 5.2

Table 5.7 Injection data for MEOR process in Core #6

Treatment Number	Injection Time* (hr)	Injection Rate* (cm^3/hr)	Injected Biomass** ($cells/cm^3$)	Injected Glucose* (mM)	Injected Nitrate* (mM)	Injected Ammonium* (mM)
1	1	46.8	9.9×10^8	59.0	37.5	47.5
2	1	46.8	9.9×10^8	59.0	37.5	47.5
3	1	46.8	9.9×10^8	59.0	37.5	47.5
4	1	46.8	9.9×10^8	59.0	37.5	47.5
5	1	46.8	0.0	59.0	37.5	47.5
6	1	46.8	0.0	59.0	37.5	47.5
7	1	46.8	0.0	59.0	37.5	47.5
8	1	46.8	0.0	59.0	37.5	47.5
9	1	46.8	0.0	59.0	37.5	47.5
10	1	46.8	0.0	59.0	37.5	47.5
11	1	46.8	0.0	59.0	37.5	47.5
12	1	46.8	0.0	59.0	37.5	47.5
13	1	46.8	0.0	59.0	37.5	47.5
14	1	46.8	0.0	59.0	37.5	47.5

* measured (Knapp et al., 1991)

** estimated

Table 5.8 Incubation data for MEOR process in Core #6

Treatment Number	Incubation Time (day)	Maximum Specific Growth Rate of Biomass (1/hr)	Maximum Specific Production Rate of Acetate (1/hr)	Maximum Specific Production Rate N_2 (1/hr)
1	14	0.00000*	0.00*	0.00*
2	10	0.00000*	0.00*	0.00*
3	6	0.00120*	0.02*	0.09*
4	6	0.00120*	0.02*	0.09*
5	14	0.60169**	0.02*	0.10*
6	14	0.60169**	0.04*	0.10*
7	11	0.60169**	0.10*	0.10*
8	10	0.60169**	0.12*	0.10*
9	8	0.60169**	0.20*	0.10*
10	6	0.60169**	0.20*	0.10*
11	7	0.60169**	0.20*	0.10*
12	6	0.60169**	0.20*	0.10*
13	6	0.60169**	0.20*	0.10*
14	3	0.60169**	0.20*	0.10*

* estimated by trial and error

** measured (Knapp et al., 1990)

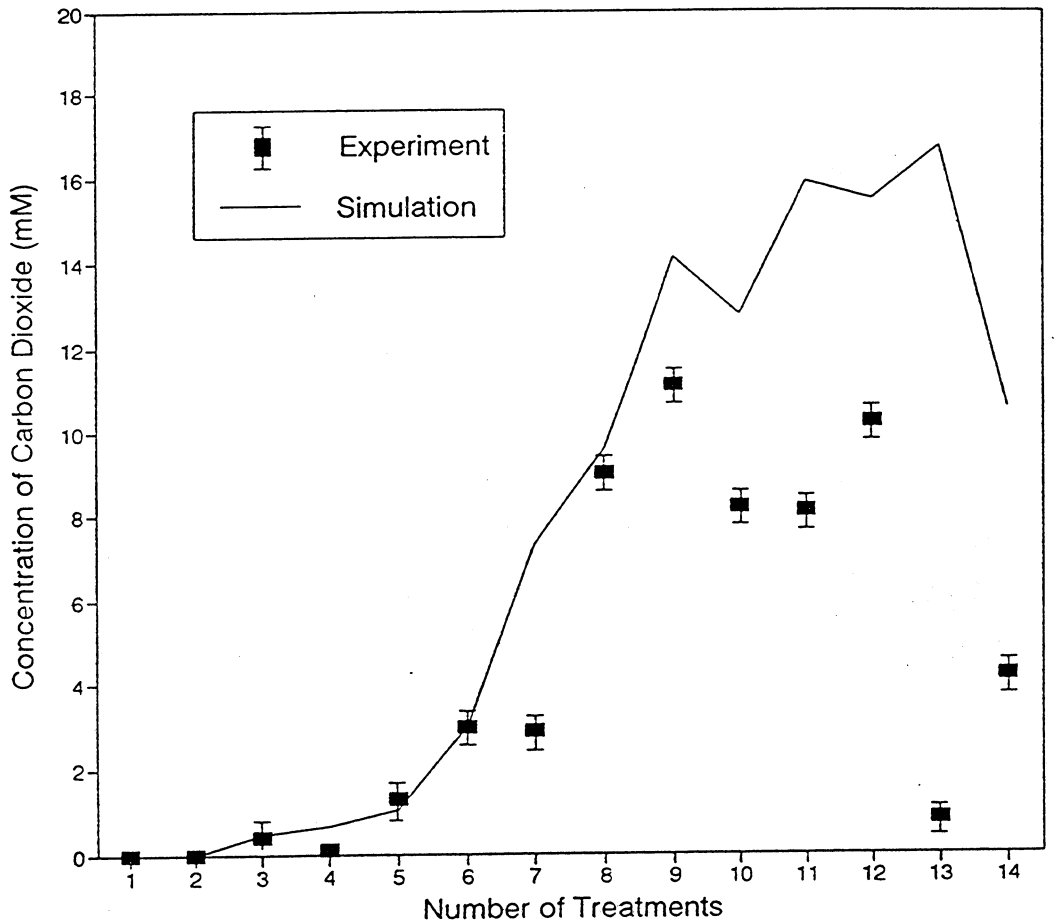

Figure 5.6 Production of CO_2 during MEOR processes in Core #6

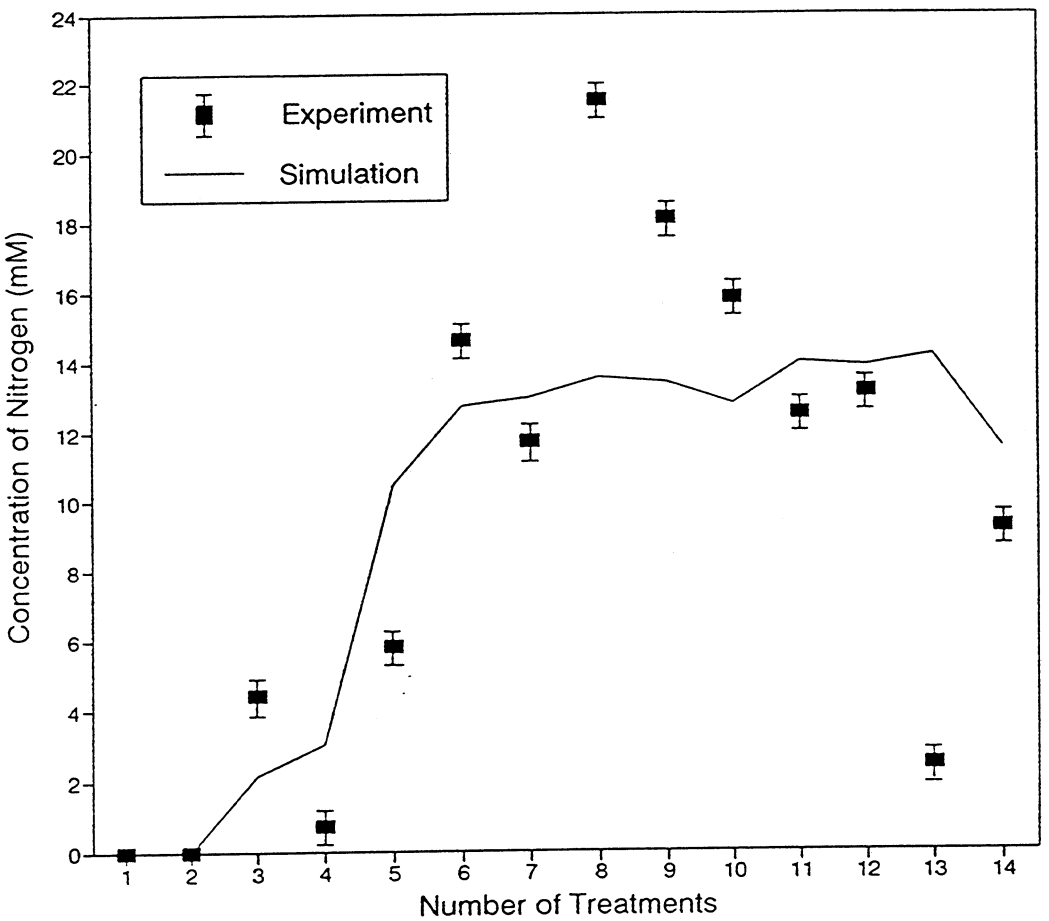

Figure 5.7 Production of N_2 during MEOR processes in Core #6

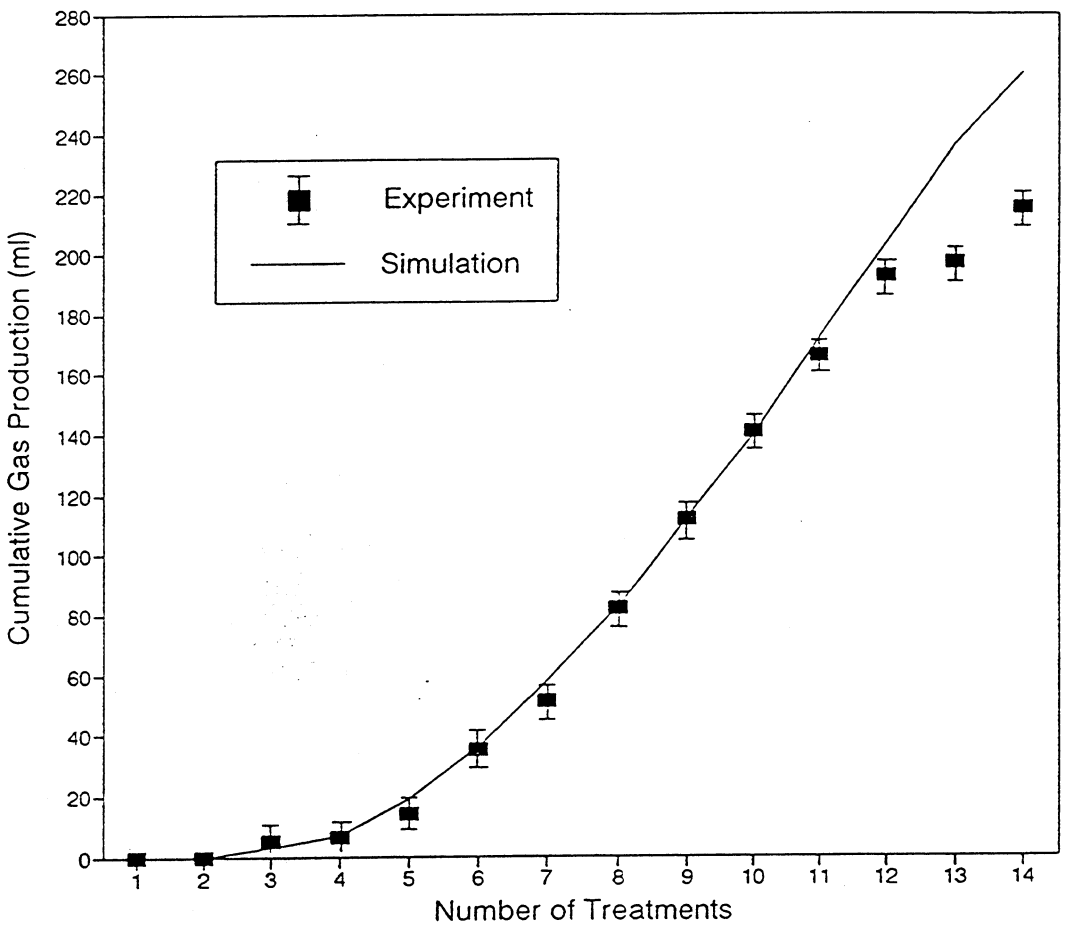

Figure 5.8 Cumulative production of total gases (CO_2 and N_2) during MEOR processes in Core #6

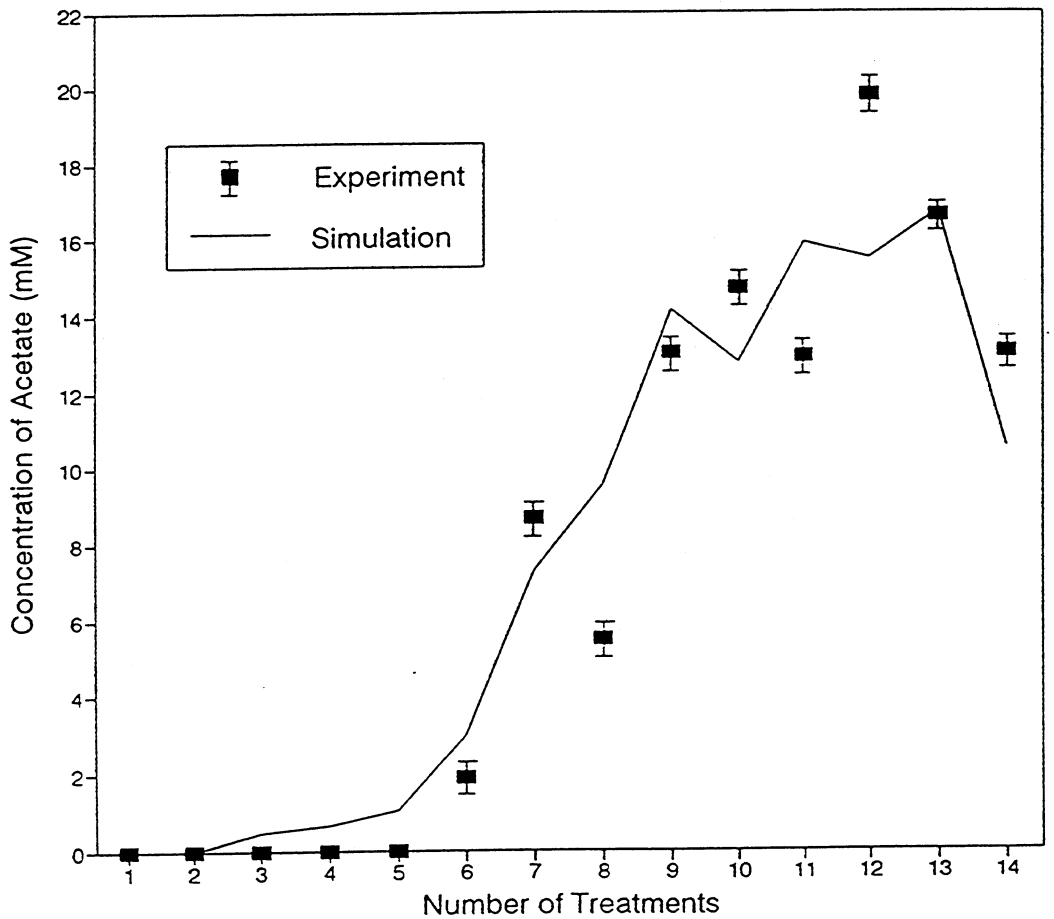

Figure 5.9 Production of acetate during MEOR processes in Core #6

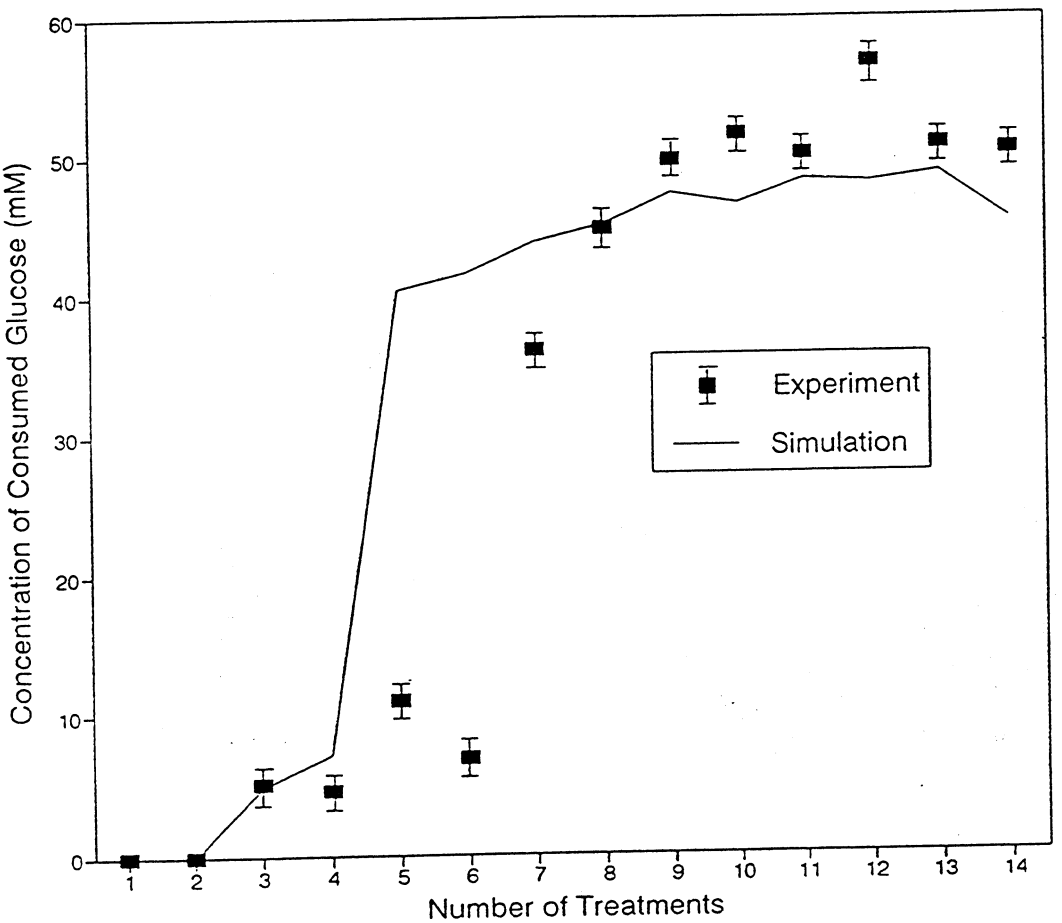

Figure 5.10 Consumption of glucose during MEOR processes in Core #6

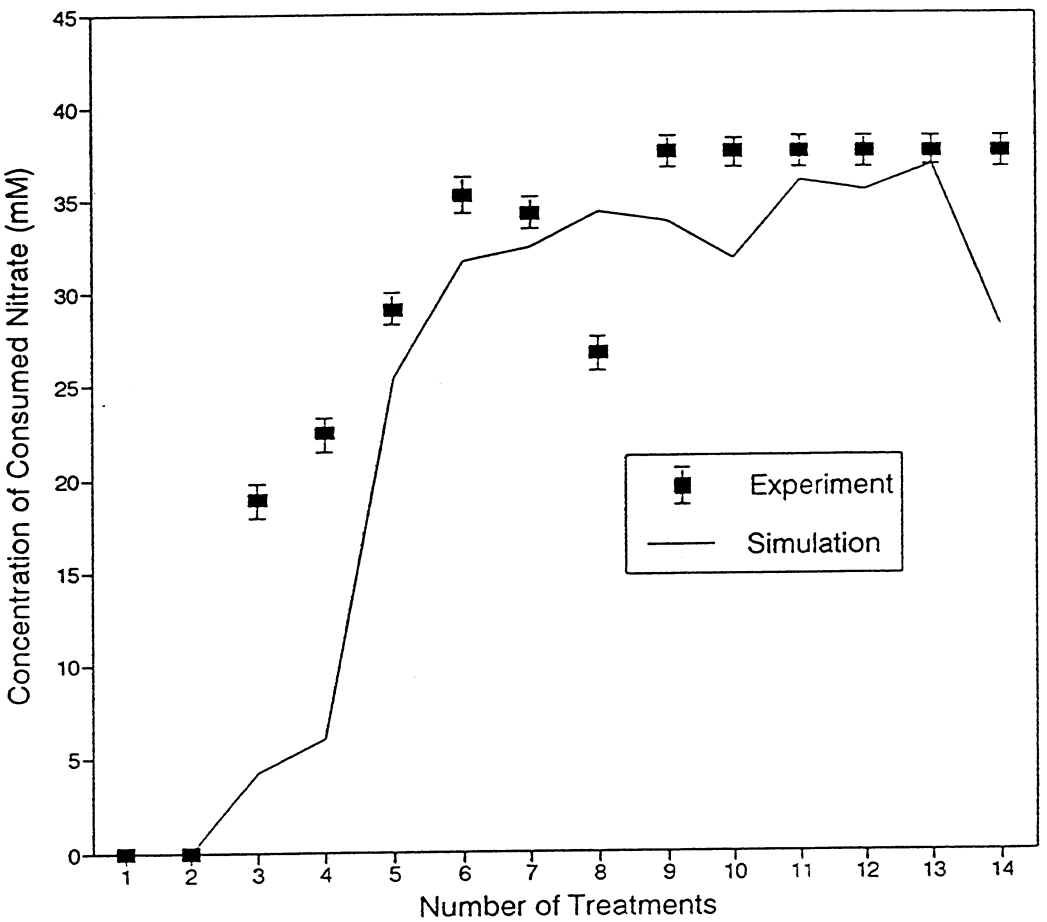

Figure 5.11 Consumption of nitrate during MEOR processes in Core #6

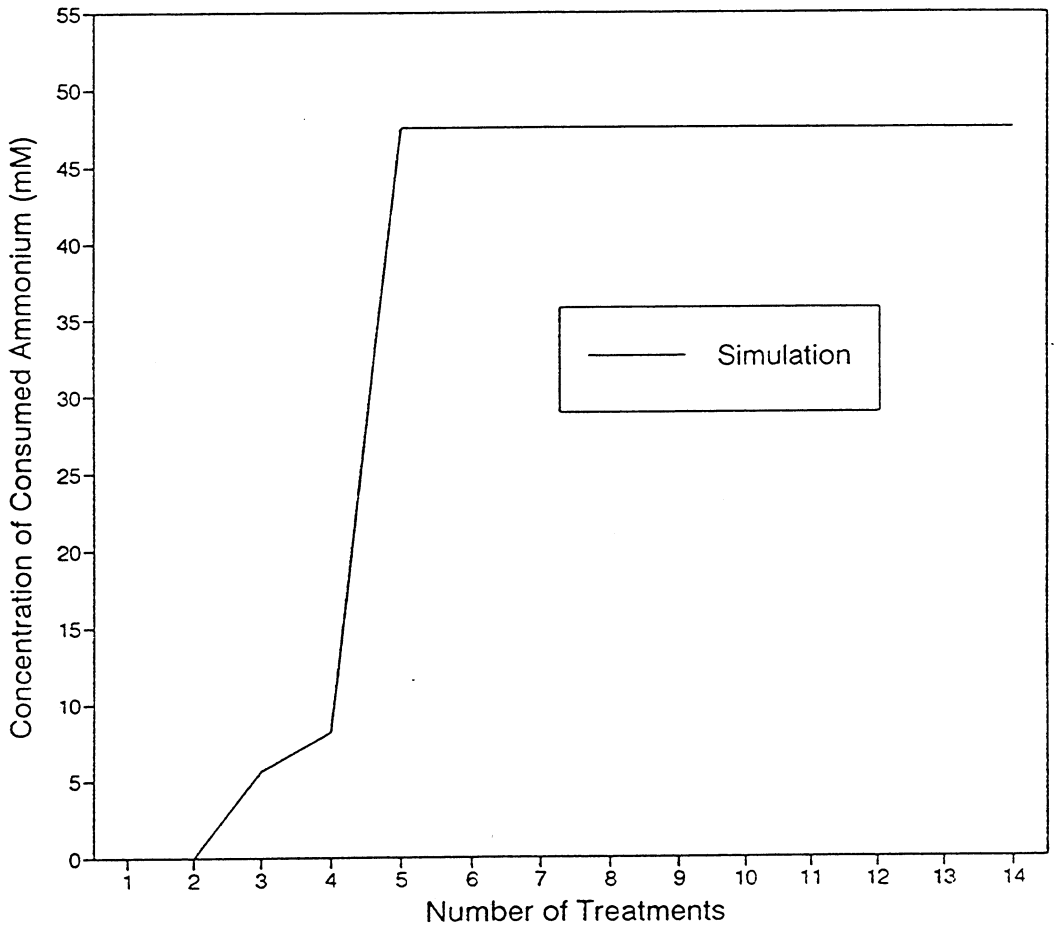

Figure 5.12 Consumption of ammonium during MEOR processes in Core #6

The simulator predicted consumption of glucose and nitrate at the end of the experiment close to that observed in the experiment (Figures 5.10 and 5.11) although there was some shift in treatment. Both simulation and experiment results show that large substrate consumption occurred following treatment 6, indicating significant growth and metabolism. However, after that treatment, the consumption rate of glucose (carbon source) stabilized. This suggests that microbial growth and metabolism may be limited by ammonium since ammonium is predicted to be completely utilized after treatment 5 (Figure 5.12).

5.8 Discussion

A model that can accurately predict biomass growth, end-product generation, and substrate consumption during a MEOR process in porous media was developed. The third-order upwinding convective differencing scheme effectively improved solutions for the convection-dispersion equation. The model was tested using experimental data and it appears that the model captured the essential features of the MEOR process. Sensitivity tests of the model showed that modeling of the MEOR process was sensitive to the stoichiometric parameters (yield coefficients) and the kinetic parameters (maximum specific growth, production, and consumption rates). This suggests that it will be important to find reasonable methods of estimating these parameters before using the model at field scale.

REFERENCES

Ames, W. F. 1977. Numerical methods for partial differential equations, 2nd ed., Academic Press, New York.

Bajpai, R. K. and Reuss, M. 1982. Coupling of mixing and microbial kinetic for evaluating the performance of bioreactors, Can. J. Chem. Eng., 60: 384-392.

Bu'lock, J. and Kristiansen, B. 1984. Basic Biotechnology, New York, pp. 75-131.

Cernansky, A. and Siroky, R. 1985. Deep-bed filtration on filament layers of particles polydispersed in liquids, International Chemical Engineering, 25 (2): 364-375.

Civan, F., Knapp, R. M., and Ohen, H. A. 1989. Alteration of permeability by fine particle processes, J. Pet. Sci, Eng., 3: 65-79.

de Marsily, G. 1972. Quantitative hydrogeology. Academic Press, New York, pp. 238-247.

Fanchi, J. R., Harpole, K. J., and Bujnowski, S. W. 1982. BOAST: A three-dimensional, three-phase black oil applied simulation tool (Version 1.1), Vol. 1: Technical description and Fortran code, Sept., Dept. of Energy DOE/BC/10033-3, US DOE Technical Information Center, Oak Ridge, Tennessee, 1982, 1-17.

Faust, A. S., Wenzel, L. A., Clump, C. W., Maus, L. and Anderson, L. B. 1960. Principles of unit operations. John Wiley and Sons, New York, pp. 567-563.

Fehlberg, E. 1969. Low-order classical Runge-Kutta formulas with stepwise control and their application to some heat transfer problems, National Aeronautics and Space Administration, Report No. NASA TR R-315.

Jenneman, G. E., Knapp, R. M., McInerney, M. J., Menzie, D. E., and Revus, D. E. 1985. Experimental studies of in-situ microbial enhanced oil recovery, Soc. Pet. Eng. J., 24: 33-37.

Knapp, R. M., Silfanus, N. J., McInerney, M. J., Menzie, D. E. and Chisholm, J. L. 1991. Mechanisms of microbial enhanced oil recovery in high salinity environments. AIChE Sym. Ser. 287, 87: 134-140.

Knapp, R. M., Civan, F., and McInerney, M. J. 1988. Modeling growth and transport of microorganisms in porous formations, pp. 676-679. In: R. Vichnevetsky, P. Borne, and J. Vignes, IMACS, Proceedings of 12th World Congress on Scientific Computation, Vol. 3, July 18-22, Paris, France.

Knapp, R. M., McInerney, M. J. and Menzie, D. E. 1990. Microbial Field Pilot Study, Annual Report, Nov. 22, 1988 - Oct. 31, 1989, U. S. Department of Energy, Contract No. DE-FG22-89BC14246.

Leonard, B. P. 1984. Third-order upwinding as a rational basis for computational fluid dynamics, pp. 106-120. In: J. Noye and C. Fletcher, Computational Techniques and Applications, CTAC-83.

Menzie, D. E., Dutta, S., Shadezadeli, R., and Malik, W. 1989. A method of measuring dispersivity and its use in slug size estimation in a miscible flooding process. J. Pet. Sci. Eng. 36: 35-45.

Raiders, R. A., McInerney, M. J., Revus, P. E., Torbati, A. M., Knapp, R. M., and Jenneman, G. E. 1986. Selectivity and depth of microbial plugging in Berea-sandstone cores. J. Indust. Microbiol. 1: 195-203.

Raiders, R. A., Knapp, R. M. and McInerney, M. J. 1989. Microbial selective plugging and enhanced oil recovery. J. Indust. Microbiol. 4: 215-230.

Reynolds, P. J., Sharma, P., Jenneman, G. E., and McInerney, M. J. 1989. Mechanisms of microbial movement in subsurface materials. Appl. Environ. Microbiol. 55: 2280-2286.

Weast, R. C. 1982. Handbook of Chemistry and Physics. CRC Press, Boca Raton, FL.

6. ACCOMPLISHMENTS

The following papers on various aspects of this project will be presented at national meetings.

1. **V.K. Bhupathiraju, P.K. Sharma, and R.M. Knapp.** 1991. Enhanced oil recovery: microbiological characterization of a hypersaline oil reservoir, Q59. (Presented at the 91st General Meeting of the American Society for Microbiology. Dallas, TX, May 5-9, 1991.)

2. **P.K. Sharma and M.J. McInerney.** 1991. Kinetics of microbial growth in unconsolidated porous media, Q63. (Presented at the 91st General Meeting of the American Society for Microbiology. Dallas, TX, May 5-9, 1991.)

3. **R.M. Knapp, X. Zhang and M.J. McInerney.** 1992. A mathematical model for microbially enhanced oil recovery process. To be presented at the SPE/DOE Eighth Symposium on Enhanced Oil Recovery. April 21-24, Tulsa, OK.

4. **P.K. Sharma.** 1992. Regulation of bacterial penetration by the geophysical environment. To be presented at the 92nd Annual Meeting of the American Society for Microbiology, May 26-30, New Orleans, LA.

*U.S.GPO:1992-661-026/60028